

Electronic Thesis and Dissertation Repository

2-8-2023 10:00 AM

Effect of process parameters on the mechanical properties of carbon fiber epoxy composites by wet compression molding

Saboora Ayatollahi, *The University of Western Ontario*

Supervisor: Prof. Hrymak, Andrew, *The University of Western Ontario*

A thesis submitted in partial fulfillment of the requirements for the Master of Engineering Science degree in Chemical and Biochemical Engineering

© Saboora Ayatollahi 2023

Follow this and additional works at: <https://ir.lib.uwo.ca/etd>

 Part of the [Polymer Science Commons](#)

Recommended Citation

Ayatollahi, Saboora, "Effect of process parameters on the mechanical properties of carbon fiber epoxy composites by wet compression molding" (2023). *Electronic Thesis and Dissertation Repository*. 9144. <https://ir.lib.uwo.ca/etd/9144>

This Dissertation/Thesis is brought to you for free and open access by Scholarship@Western. It has been accepted for inclusion in Electronic Thesis and Dissertation Repository by an authorized administrator of Scholarship@Western. For more information, please contact wlsadmin@uwo.ca.

Abstract

In recent years, due to growing environmental concerns, composite materials have emerged as a promising lightweight alternative for metals in structural applications in automobiles. Among composite manufacturing processes, Wet Compression Molding (WCM) is a new method of producing Carbon Fiber Reinforced Polymer (CFRP) components. For similar processes like RTM, operating conditions are always one of the factors that impact the mechanical performance of CFRP parts. Thus, this thesis aimed to investigate the effects of operating conditions, including resin temperature, mold temperature, resin set time, gap closure speed, and mold curing time on the mechanical property of the composite parts. In addition, the relationship between the initial resin application and the quality of the final parts was evaluated in this research.

Flat plaques of carbon-fiber composites in an epoxy matrix were fabricated using WCM equipment, and the flexural property (Young's Modulus) of the final parts were measured. Through statistical analysis, experimental results revealed that the part's mechanical property was significantly affected by the mold temperature, resin temperature, and resin set time. Moreover, at the higher level of the significant factors, the quality of the parts was lower, and the optical microscope test confirmed voids formation during the WCM process (air entrapment), which was the primary reason for the poor quality of the final parts. In addition, statistical results exhibited no correlation between the initial resin distribution and the mechanical property of the final parts.

Keywords

Wet compression molding, carbon fiber reinforced polymer, operating conditions, mechanical property, initial resin application, Young's Modulus, void, optical microscope

Summary for Lay Audience

Because of rising regulatory obligations worldwide, the automotive industry has focused on improving automobile fuel efficiency. As a result, the automotive industry began to prioritize weight reduction. Using materials with great strength and low density, such as polymer composites, to reduce the weight of a car is known as “lightweighting.” Wet compression molding (WCM) is a new method of producing Carbon Fiber Reinforced Polymer (CFRP) components in composite manufacturing processes. Since the WCM process is still in its early stages, there are no complete studies about how to improve it. So, the main goal of this study is to understand better which process factors have a significant effect on the WCM process and then investigate the relationship between process and material parameters and the mechanical properties of the composite.

The first part of this research aimed to understand how several operating conditions, such as mold temperature, resin temperature, resin set time, gap closure speed, mold curing time, and sampling area, impact the quality of carbon composite products produced by the wet compression technique. The influence of these process variables on the part quality was statistically investigated; the slope of the stress-strain curve measured by the flexural test was used to indicate the part quality at specific sampling locations. Experimental results showed that the mold temperature, resin temperature, and resin set time were significant variables for improvements in the mechanical property of the parts. In contrast, the effects of mold curing time and gap closure speed on the mechanical property appeared insignificant. In addition to that, it was found that at the higher level of the significant variables, the quality of the produced parts was lower, which was further investigated with an optical microscope test, and void (air entrapment) was observed.

The second part of this research studied the correlation between the initial resin application area and the final part's mechanical property to see if the initial resin distribution is a significant factor in determining part quality. According to the data, there were no statistically significant correlations between the initial resin distribution and the mechanical property of the final parts.

Acknowledgments

I would like to express my sincere gratitude to my supervisor, Professor Andrew Hrymak, for accepting me as his student and financially supporting me in my graduate program. I thank him for his patience and continuous support, advice, and motivation throughout this journey. Thanks for giving me this great opportunity and for being a fantastic role model in both academic and real life.

I would like to thank Gleb Meirson and Jen Sears for their constant support, help, and advice during my research.

I would like to thank Keith Rock, Rob Cosh, Steve Jones, and the rest of the Fraunhofer Innovation Platform for Composite Research team for their assistance with composite part manufacturing, testing equipment training, and general research support.

I would like to extend my special thanks to Dr. Mehdi Ghazimoradi for his guidance and assistance during my research.

I would like to thank Mr. Ivan Barker and Mr. Vahid Dehnavi at Surface Science Western for helping me with sample preparation and taking high-quality optical micrographs.

Thanks to my dear parents for encouraging me to pursue higher education and for their enduring love and teachings; you are my strength, biggest support, and motivation. Also, this work would not have been possible without the support of my friends, and I owe all of them my deepest thanks.

Lastly, I would like to dedicate this thesis to my older brother, Saber, whom I can always count on for his wise advice, nurturing love, and moral support. He was always there for me in the past two years, helped me when I needed it the most, and never let me feel away from home.

Table of Contents

Abstract	ii
Summary for Lay Audience	iii
Acknowledgments.....	iv
Table of Contents	v
List of Tables	ix
List of Figures	x
List of Appendices	xiv
List of Abbreviations	xv
Chapter 1	1
1 Introduction	1
1.1 Background information	2
1.2 Fast CoFRP processing	4
1.2.1 Resin Transfer Molding (RTM).....	5
1.2.1.1 High-Pressure Resin Transfer Molding (HP- RTM)	6
1.2.1.2 High-Pressure Injection Resin Transfer Molding (HP-IRTM)	7
1.2.1.3 Compression Resin Transfer Molding (CRTM).....	8
1.2.1.4 High-Pressure Compression Resin Transfer Molding (HP- CRTM)	9
1.2.2 Thesis composition	11
Chapter 2.....	12
2 Literature review	12
2.1 Wet Compression Molding (WCM) process	12
2.2 Process studies in Resin Transfer Molding (RTM) process	16
2.3 Motivation and Objective	19
Chapter 3.....	22

3	Experimental Methodology.....	22
3.1	Experimental procedures	22
3.1.1	Material reinforcement.....	22
3.1.2	Resin system	23
3.1.3	Processing parameters.....	24
3.1.4	Preform placement	25
3.1.5	Process description and plaque manufacturing.....	25
3.2	Mechanical testing	30
3.2.1	Plaque Screening.....	30
3.2.2	Mechanical testing coupons.....	35
3.2.3	Sample preparation	36
3.2.4	Three-point beam flexural test set-up	37
3.2.5	Flexural test results	38
3.2.5.1	Modulus of Elasticity	39
3.2.5.2	Flexural Strength (Ultimate Strength).....	40
3.2.5.3	Strain at Break	41
3.3	Optical Microscopy.....	41
3.4	Conclusion	43
	Chapter 4.....	44
4	Investigation of the effect of process parameters on the mechanical property of CFRP parts	44
4.1	Overview.....	44
4.2	Effect of sample thickness	44
4.3	Statistical Modeling Technique	45
4.3.1	Design of Experiment (DOE) - Factorial Design	45
4.4	Statistical Analysis results and discussions	46

4.4.1	ANOVA results.....	46
4.4.2	Normality test.....	49
4.4.3	Box-Cox transformation	52
4.4.4	ANOVA results of the transformed data	53
4.4.5	Pareto chart	54
4.4.6	Main effect plot.....	55
4.5	Optical Microscope (OM) results and discussion.....	58
4.6	Conclusion	64
Chapter 5	65
5	Effects of initial resin application area on the Mechanical Property of CFRP parts ...	65
5.1	Objective of this part of research	65
5.2	Analysis technique	65
5.3	Area coverage	65
5.3.1	Initial wetted (resin) area definition.....	65
5.3.2	Measurement of initial wetted (resin) area from captured videos	66
5.3.3	Targeted wetted (resin) area definition	69
5.3.4	Observation of area coverage measurement data.....	71
5.4	Area coverage per quadrant	73
5.4.1	Quadrant's definition	73
5.4.2	Initial wetted (resin) area per quadrant measurement.....	73
5.4.3	Targeted wetted (resin) area per quadrant measurement	74
5.4.4	Observation of quadrants measurement for area coverage data	75
5.5	Wetted vs. non-wetted regions.....	78
5.5.1	Definition	78
5.5.2	Observation of flexural data for wetted vs. non-wetted regions.....	79
5.6	Results and discussion	80

5.6.1 Investigate the data correlation for wetted regions	81
5.6.2 Investigate the data correlation for non-wetted regions.....	84
5.7 Conclusion	86
Chapter 6.....	87
6 Conclusion and recommendations	87
6.1 Conclusion	87
6.2 Recommendations for future work	88
References.....	90
List of Appendices	100
Curriculum Vitae	159

List of Tables

Table 3-1: Summary of Processing Parameters	24
Table 3-2: Preform properties	27
Table 3-3: Details of the specimens.....	42
Table 3-4: Grit size and polishing time.....	43
Table 4-1: Analysis of Variance Results for Response	48
Table 4-2: Analysis of Variance results after data transformation of Response.....	54
Table 4-3: Sample information for OM.....	59
Table 4-4: Viscosity of the resin system at different temperatures (Hexion, 2015).....	64

List of Figures

Figure 1-1: Classification of composites. Adopted from (Yang, 2019)	2
Figure 1-2: Reinforcement Classification of Composite Materials (Gorss, 2003)	4
Figure 1-3: Diagram of a simple RTM injection setup. Adopted From (Raja, 2005)	6
Figure 1-4: High-Pressure Resin Transfer Molding (HP-RTM) process steps. Adopted from (Vita, A. et al., 2019)	7
Figure 1-5: Resin injection sequence in the High Pressure - Injection RTM (HP-IRTM) process. Adopted from (Hatz, 2011).....	8
Figure 1-6: Schematic of the various steps in CRTM process. Adopted from (Bhat, P. et al., 2009)	9
Figure 1-7: Resin injection sequence in the High Pressure - Compression RTM (HP-CRTM) process. Adopted from (Chaudhari, R. et al., 2012)	10
Figure 2-1: WCM steps- (a) Direct process; (b) Indirect process. Adopted from (Poppe, 2021)	14
Figure 2-2: Investigated WCM parameters in this study	21
Figure 3-1: (a) Zoltek PX35-UD300 unidirectional non-crimp fabric with stitching and glass fiber sides indicated, (b-c) microstructure of fabric. Adopted from (Ghazimoradi, M. et al., 2022)	23
Figure 3-2: Manufacturing system of WC	26
Figure 3-3: Wet compression molding steps	26
Figure 3-4: Image of resin distribution nozzle (flat nozzle)	28
Figure 3-5: Image of mold cavity	28
Figure 3-6: WCM process in details	29

Figure 3-7: Example of large dry spot- Plaque number 1.....	32
Figure 3-8: Example of medium dry spot- Plaque number 23.....	32
Figure 3-9: Example of small dry spot- Plaque number 17	33
Figure 3-10: Example of shifted preform- Plaque number 21	34
Figure 3-11: Example of shifted preform- Plaque number 47	34
Figure 3-12: Specimens cutting diagram of flexural test.....	36
Figure 3-13: Three-point beam flexural test- Loading diagram (International, 2007)	37
Figure 3-14: Strain-Stress curve details	39
Figure 3-15: Validation specimen locations for OM analysis	42
Figure 4-1: Whisker and Box plot of sample thickness segregated by sampling area	45
Figure 4-2: Histogram of residuals	49
Figure 4-3: Normal probability plot (Q-Q plot) of residuals- the outliers shown in the above graph belong to 1- plaque number 3 and 2- plaque number 7	51
Figure 4-4: Normal probability plot (Q-Q plot) of residuals after removing outliers	51
Figure 4-5: Box-Cox transformation data with the Rounded Value (λ) of 0.5.....	53
Figure 4-6: Pareto chart of standardized effects ($\alpha=0.05$) for Response	55
Figure 4-7: Main effect plot for response	56
Figure 4-8: Microscopic images of different voids observed from carbon/epoxy composites fabricated using WCM.....	60
Figure 4-9: Optical micrographs of a specimen taken from plaque number 2 (resin temperature of 50 °C, mold temperature of 110 °C, and resin set time of 0 sec) and sampling area B - voids are noted by red arrows	61

Figure 4-10: Optical micrographs of a specimen taken from plaque number 2 (resin temperature of 50 °C, mold temperature of 110 °C, and resin set time of 0 sec), and sampling area E - voids are noted by red arrows.....	61
Figure 4-11: Optical micrographs of a specimen taken from plaque number 9 (resin temperature of 70 °C, mold temperature of 130 °C, and resin ret time of 40 sec), and sampling area B - voids are noted by red arrows	62
Figure 4-12: Optical micrographs of a specimen taken from plaque number 9 (resin temperature of 70 °C, mold temperature of 130 °C, and resin ret time of 40 sec), and sampling area E - voids are noted by red arrows.....	62
Figure 5-1: Camera configuration.....	66
Figure 5-2: Camera view	67
Figure 5-3: Image Extraction reference points	68
Figure 5-4: Thresholding method for initial area measurement	69
Figure 5-5: Schematic of the targeted resin area - the dimension of the flat nozzle is provided in Figure 3-4: Image of resin distribution nozzle (flat nozzle)	70
Figure 5-6: Whiskers and Box plot for total initial and targeted resin area.....	72
Figure 5-7: Thresholding method for measuring initial wetted area per quadrant	73
Figure 5-8: Targeted resin area per quadrant	74
Figure 5-9: Whiskers and Box plot for initial and targeted wetted area - UL: Upper Left, UR: Upper Right, LR: Lower Right, LL: Lower Left	76
Figure 5-10: Whiskers and Box plot for initial and targeted wetted area in right and left side	77
Figure 5-11: Wetted and Non-wetted (dry) sampling areas on an extracted frame	79

Figure 5-12: Flexural Modulus of wetted (sampling area A and C) vs. non-wetted (sampling area B, D, and E) regions	80
Figure 5-13: Correlation between initial wetted area per quadrant and Flexural Modulus of Sample Area A.....	82
Figure 5-14: Correlation between initial wetted area per quadrant and Flexural Modulus of Sample Area C	83
Figure 5-15: Correlation between initial wetted area per quadrant and Flexural Modulus of Sample Area B	84
Figure 5-16: Correlation between initial wetted area per quadrant and Flexural Modulus of Sample Area D.....	85
Figure 5-17: Correlation between initial wetted area per quadrant and Flexural Modulus of Sample Area E	86

List of Appendices

Appendix 1: ZOLTEK™ PX35 unidirectional fabric data sheet	100
Appendix 2: EPIKOTE™ Resin TRAC 06170 resin data sheet	102
Appendix 3: Experimental test matrix	107
Appendix 4: A developed spreadsheet for the plaques screening.....	109
Appendix 5: Flexural properties of produced plaques-sampling area A	111
Appendix 6: Flexural properties of produced plaques-sampling area B.....	120
Appendix 7: The initial wetted area measurements (units cm ²)	157
Appendix 8: The targeted wetted area measurements (units cm ²).....	158

List of Abbreviations

WCM- Wet Compression Molding

RTM- Resin Transfer Molding

HP-RTM – High Pressure-Resin Transfer Molding

COFRP- Continuous Fiber Reinforced Polymers

NCF- Non-Crimped Fabric

UD-NCF- Unidirectional Non-Crimped Fabric

CFRP- Carbon Fiber Reinforced Polymer

ANOVA- Analysis of Variance

ASTM – American Society for Testing and Materials

IMR – Internal Mold Release

SMC- Sheet Molding Compounds

ISO- International Organization for Standardization

LCM- Liquid Composite Molding

CRTM- Compression Resin Transfer Molding

HP-RTM- High-Pressure Resin Transfer Molding

HP-IRTM- High-Pressure Injection Resin Transfer Molding

HP-CRTM- High-Pressure Compression Resin Transfer Molding

DOE- Design of Experiment

OM- Optical Microscope

Chapter 1

1 Introduction

Composites have recently received widespread acceptance as a suitable alternative to traditional metallic Materials of Construction (MoC). Composites are used in various industries, from energy to sports and entertainment. Transportation is one industry where composites are in high demand (Suratkar, 2022).

Composites for structural applications in lightweight automobiles have also gained popularity in the last decade. The primary driving force behind the shift from steel and aluminum (traditional choices for automobile components) to lightweight composites is increasing legislative pressure on Original Equipment Automobile Manufacturers (OEMs) worldwide to dramatically reduce carbon dioxide and greenhouse gas emissions from passenger cars (lightweight, heavy impact), as an increasing number of countries continue to pledge carbon neutrality by the second half of the twenty-first century. According to reports, a 10% reduction in vehicle weight improves passenger car fuel economy by 6–8% and electric vehicle fuel economy by 10%, hence helping to reduce emissions (Carbon Neutrality Goals by Country, 2021).

Consequently, the automobile industry's usage of lightweight materials has seen a substantial increase in recent years. Continuous fiber-reinforced polymers (also known as CoFRP) offer the most significant opportunity for lightweight construction among composite materials due to their greater potential for reducing mass than metals, such as high-strength steel and aluminum while maintaining desirable mechanical properties (Lutsey, 2010).

1.1 Background information

As illustrated in Figure 1-1, composite materials can be widely categorized based on the type of matrix and reinforcement materials used (Yang, 2019). The materials are classified based on the chemical nature of the matrix material, i.e., whether the matrix is polymer, metal, or ceramic. The composites are further classified based on the geometry (if the reinforcing phase is primarily fibers, particles, etc.), size (length of the fibers, the diameter of particles, etc.), and arrangement of the reinforcing phase (if the fibers are randomly dispersed, if the reinforcing phase is present as a stack of aligned continuous fibers, etc.). Even though the broad classification in Figure 1-1 covers a wide range of materials, the discussion in this study will concentrate on "continuous fiber reinforced polymer composites."

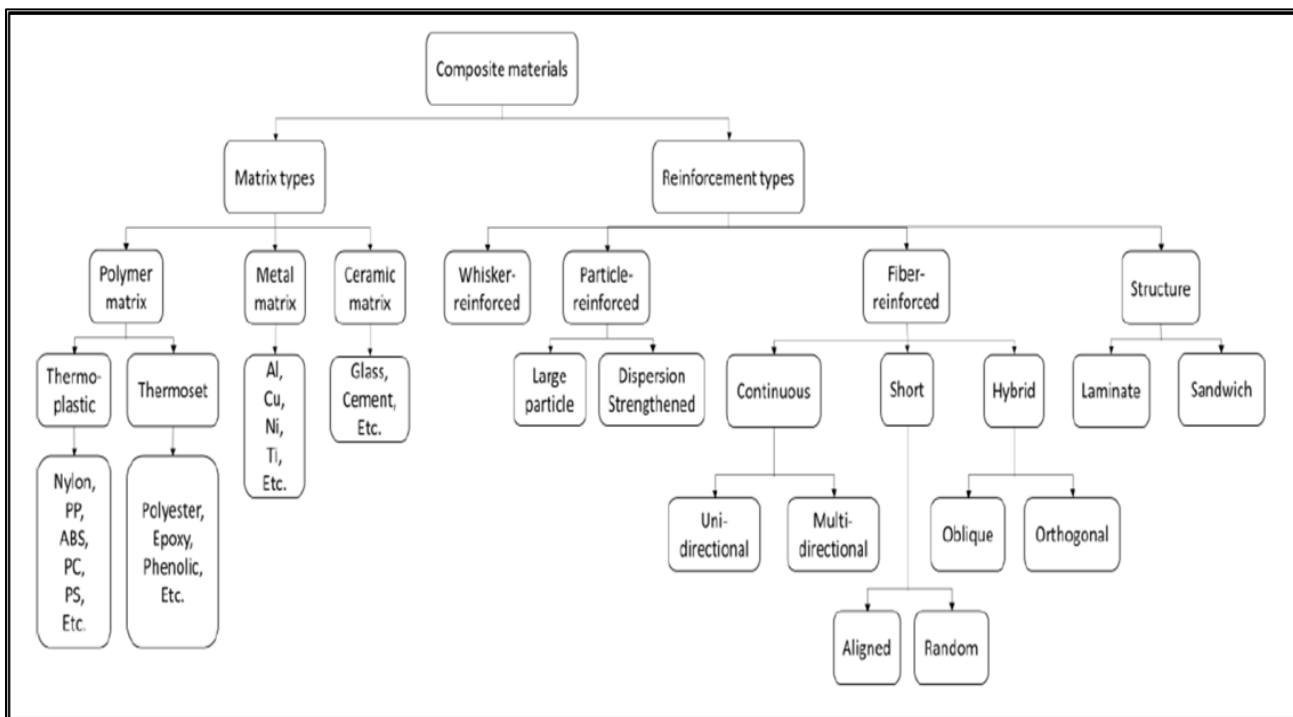


Figure 1-1: Classification of composites. Adopted from (Yang, 2019)

Polymer Matrix: Based on the intermolecular interactions between the polymer chains, polymer matrices are classified as thermosets or thermoplastics (Yang, 2019). Thermoset goes through a curing process in which a cross-linking chemical reaction occurs during vitrification. The shape of the thermoset material cannot be modified once it has been cured. Unlike thermosets, thermoplastics do not cure, and their form changes purely due to physical phase change. This characteristic allows thermoplastic to be recyclable but also makes processing more difficult. Thermosets and thermoplastics both have advantages and disadvantages (Chang, 2021).

Thermosets provide greater temperature resistance and dimensional stability. They have a low viscosity, which makes thermosets easier to process. They are less expensive and have a better aesthetic appearance, however, as previously said, they cannot be remolded. On the other hand, thermoplastics have a broader opportunity for recycling and more property tunability, but they are more expensive than thermosets (Thermoplastics Vs. Thermoset, 2017).

Reinforcements: Like other reinforcing polymers, CoFRP offers high tensile stiffness. Various reinforcements, such as natural fibers (such as wool, hemp, or banana), organic fibers (such as polyethylene, aramid, or carbon), or in-organic fiber (such as glass), are used according to the desired application (Poppe, 2021). In this study, continuous Carbon Fiber Reinforced Polymers for high-performance applications is the main topic.

CoFRPs are divided into dry and pre-impregnated textiles. For shell-like structures, woven fabrics, and non-crimped fabrics (NCF) are the most common types of dry engineered textiles (Gereke, T. et al., 2013). When it comes to the production of high-performance FRP composite structures employing liquid resin molding techniques, warp stitched unidirectional nonwoven carbon fibers are particularly appealing (Trejo et al., 2020; Ghazimoradi, M. et al., 2021; Ghazimoradi, M. et al., 2022). The focus of this work is on the non-crimped fabrics (UD-NCFs).

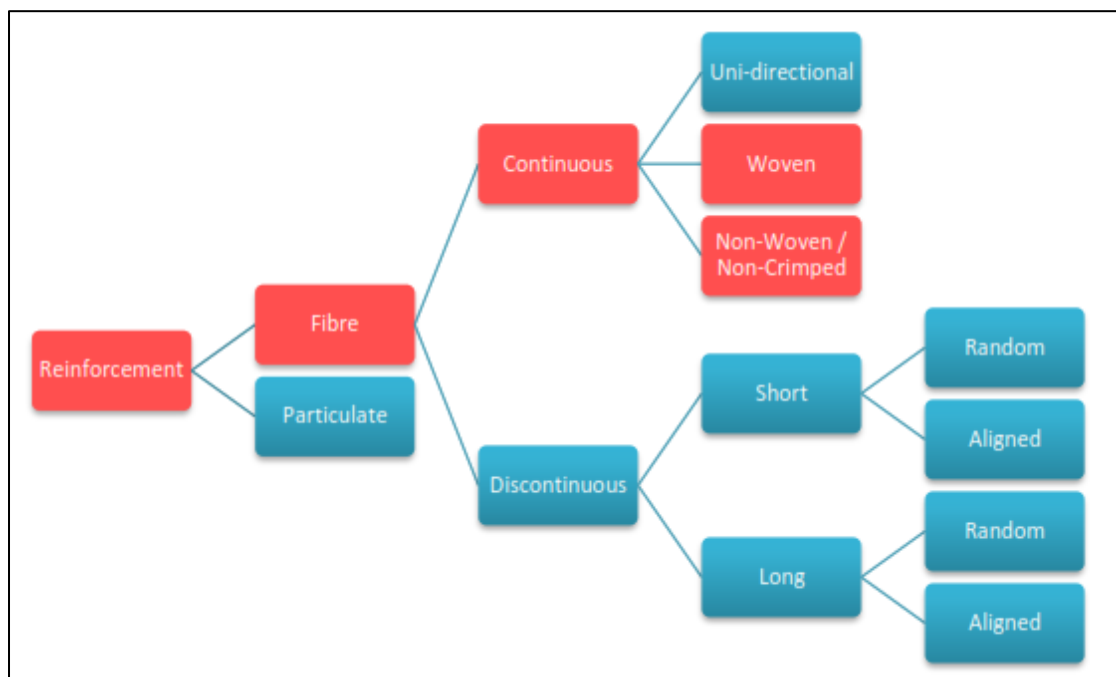


Figure 1-2: Reinforcement Classification of Composite Materials (Gorss, 2003)

1.2 Fast CoFRP processing

When cycle times are maintained to less than three minutes, as is required for mass manufacturing of automobiles, three techniques are applicable and economically relevant for Continuous fiber reinforced polymers (CoFRP). Resin Transfer molding (RTM) and Wet Compression Molding (WCM) procedures that use polymers (thermoset based CoFRPs) that cure quickly (Poppe, 2021) and thermoforming techniques that use thermoplastic organosheets or tape laminates (Henning, F. et al., 2019). Other well-established methods of liquid moldings, such as Vacuum-assisted Resin Injection (VARI), cannot reach comparable processing timeframes because of their long infiltration paths and a significant number of manual process steps (Rudd, C. D. et al., 1997; Ermanni, P. et al., 2011). In this thesis, the focus is on Wet Compression Molding (WCM) and the related literature review of this process provided in Chapter 2. Short descriptions of Resin Transfer

Molding (RTM) and their variants are provided in this chapter as elements of these processes are incorporated in WCM.

1.2.1 Resin Transfer Molding (RTM)

The conventional RTM process is an in-mold resin-injection process that has been in the industry for many decades (Ermanni, P. et al., 2011). Considerable time and effort have been invested researching and developing this method for mass production. (Henning, F. et al., 2019; Ermanni, P. et al., 2011; Seuffert, J. et al., 2020). Equipment for handling and dosing extremely reactive resins is required to meet manufacturing standards (Bernath, A. et al., 2016).

Resin Transfer Molding (RTM) is one of the most efficient, attractive, and economical processes for high-performance composite materials with low-cost manufacturing. In the process, a thermoset thermally activated resin is injected at low pressures (<700 kPa) into a closed mold cavity containing a pre-placed fiber preform or a stack of fiber mats of reinforcing material in the shape of the desired part. The resin flows into the mold cavity to occupy the empty spaces between the fibers. The mold is usually heated to initiate a curing reaction, an exothermic resin polymerization phenomenon that cross-links the resin and results in a composite structure. A step-by-step diagram of the RTM process is shown in Figure 1-3. This process has been improved through automation and better control over the past years. RTM's ability to produce a wide variety of shapes at a moderate cost makes it a very attractive process (Raja, 2005).

RTM has become an interesting method for producing high-quality fiber reinforced composite parts because of its capabilities such as reasonable-priced process equipment, excellent control of mechanical properties, closed mold process, low filling pressure, incorporation of metal inserts and attachments, possibility of producing large and complex parts, and low labor cost (Potter, 1999; Advani, S. G, 1994; Chen, S.C. et al., 2000).

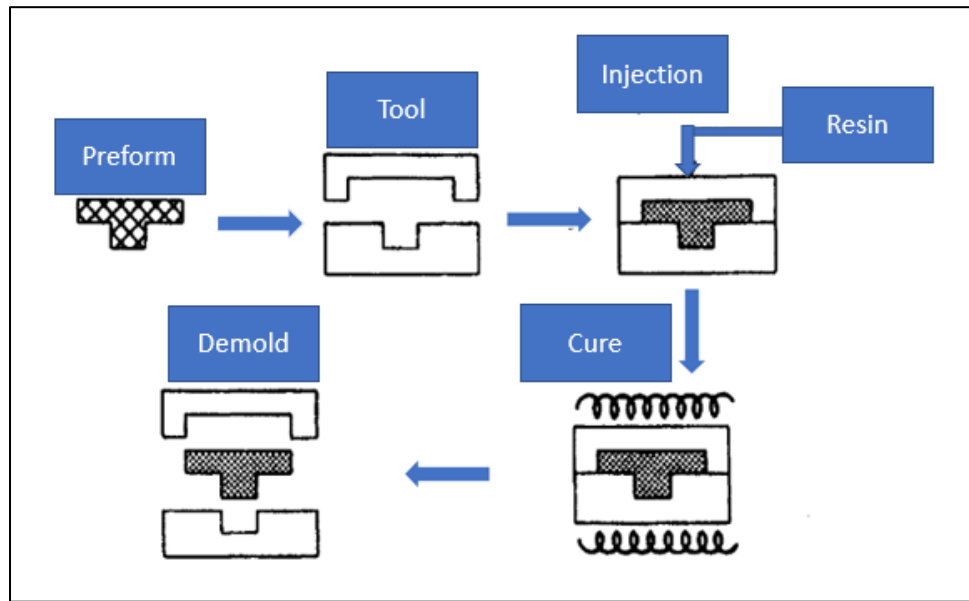


Figure 1-3: Diagram of a simple RTM injection setup. Adopted From (Raja, 2005)

1.2.1.1 High-Pressure Resin Transfer Molding (HP- RTM)

The next generation of RTM technology is high-pressure Resin Transfer Molding (HP-RTM). Faster cycle times can be achieved by increasing the injection pressure in the mixing head and mold (Lettau). High pressures are used to achieve high fiber content of up to 70%. The primary drawbacks of HP-RTM are mostly associated with high tooling costs and the potential shifting of dry fibers caused by high pressure. The latter affects the part's mechanical performance (Vita, A. et al., 2019).

The composite component is placed in the mold to begin the process. The resin is then pumped into a partially opened mold. When the injection is finished, the mold is closed, causing the resin to be evenly distributed throughout the face of the mold and reinforcement material. Air can escape through the mold venting located away from the injection locations. The vents can also be utilized to draw a vacuum, which improves the quality of the laminate. Different steps of the HP-RTM process are shown in Figure 1-4.

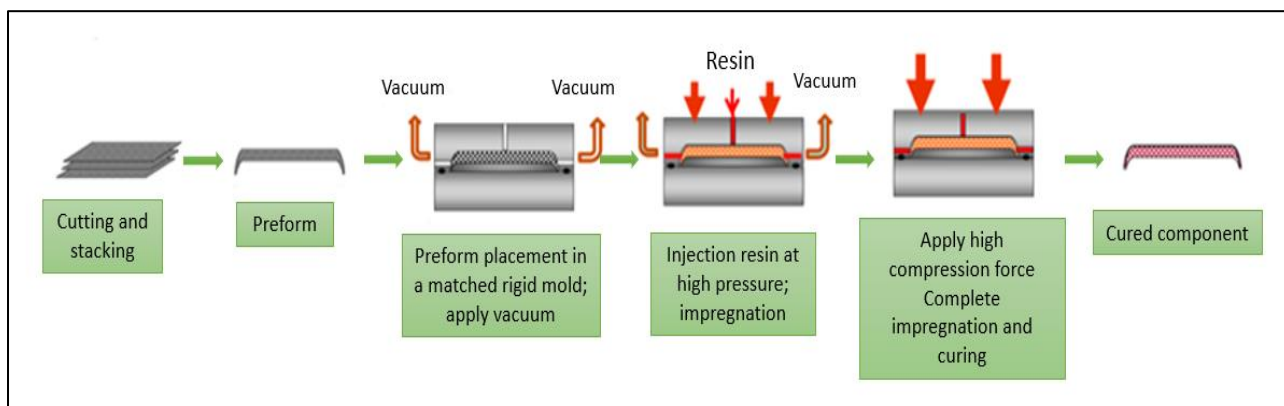


Figure 1-4: High-Pressure Resin Transfer Molding (HP-RTM) process steps.

Adopted from (Vita, A. et al., 2019)

1.2.1.2 High-Pressure Injection Resin Transfer Molding (HP-IRTM)

In the RTM process, low-pressure mixing and dosing equipment is used to process resins. In the HP-RTM process, however, High-Pressure RTM equipment is used to mix and dose resins. In the HP-IRTM process, the preform is put into the mold cavity just like in the classic RTM process. Then, the mold is closed to compact the preform to the final part thickness. After the mold is closed, the mixture of resin and hardener is injected into the cavity quickly. The high throughput rate results in fast filling of the cavity, and hence the resin injection time can be reduced significantly. This process variation makes it possible to use resins with higher reactivity because the resin can be injected into the cavity in less time. After the resin curing reaction is completed, the part can be demolded (Graf, M. et al., 2010). The main process steps of the HP-IRTM cycle are shown in Figure 1-5.

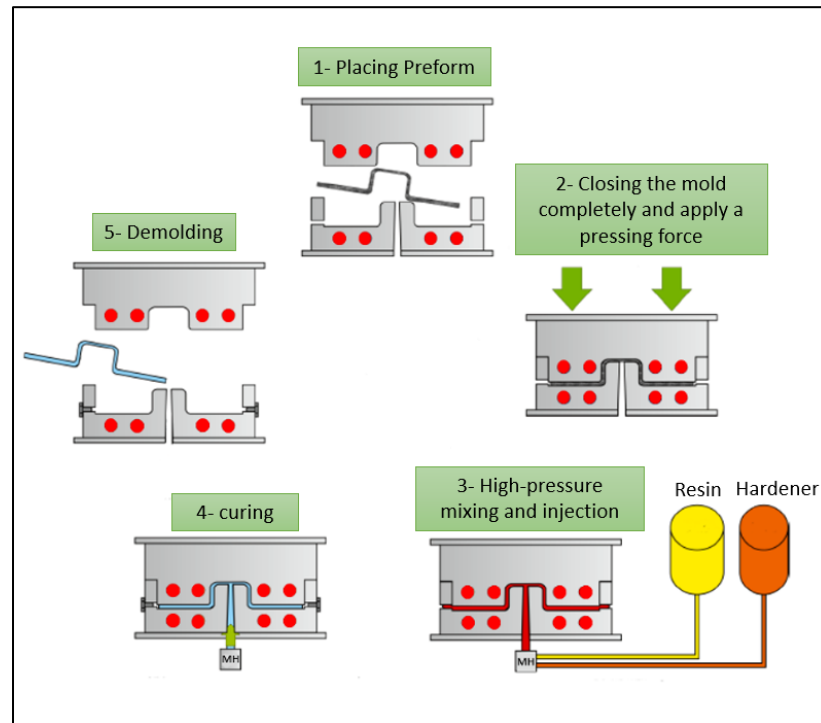


Figure 1-5: Resin injection sequence in the High Pressure - Injection RTM (HP-IRTM) process. Adopted from (Hatz, 2011)

1.2.1.3 Compression Resin Transfer Molding (CRTM)

The compression Resin Transfer Molding (CRTM) process is being investigated as an advanced composites net shape manufacturing process for high-volume manufacturing parts. The net-shaped preform is placed in a mold cavity during this process. In contrast to Resin Transfer Molding (RTM), the mold is not completely closed. The top mold platen is instead lowered to create a small gap between the mold platen walls and the fiber preform. Resin is supplied into this gap via the injection gates and flows smoothly over the preform and may also partially impregnate the preform. Once the required quantity of resin is injected into the gap, and the gate is closed, the mold platen moves down to finish the mold and squeeze the resin into the preform, which also undergoes compaction to achieve the desired volume fractions. Once the resin has fully cured, the mold can be opened, and the

part can be de-molded. In Figure 1-6, a diagram shows the different steps of the CRTM process (Simacek, P. et al., 2005).

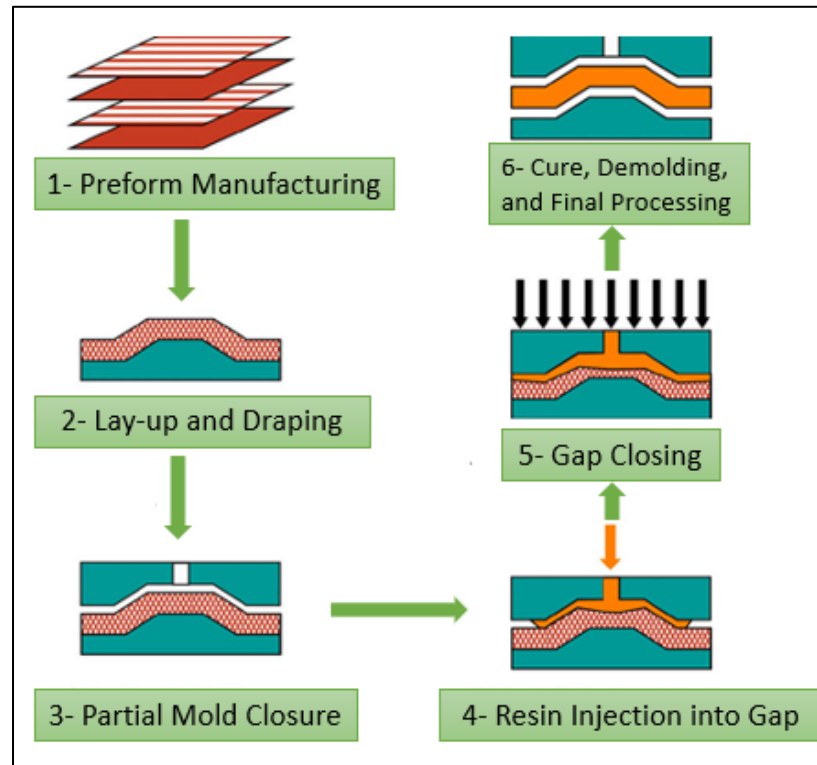


Figure 1-6: Schematic of the various steps in CRTM process. Adopted from (Bhat, P. et al., 2009)

1.2.1.4 High-Pressure Compression Resin Transfer Molding (HP-CRTM)

The HP-CRTM process combines Resin Transfer Molding (RTM) and compression molding. During this process, the preform is placed into the mold cavity, and then the mold is partially closed to create a small gap between the mold surface and the fiber preform. The resin is injected into the gap, flows easily over the preform, and may partially

impregnate the preform. After the desired amount of resin is injected into the gap, the mold is fully closed. It exerts intense compression pressure on the resin within the preform. The part can be demolded after the resin has cured (Simacek, P. et al., 2008). Figure 1-7 illustrates each HP-CRTM process step.

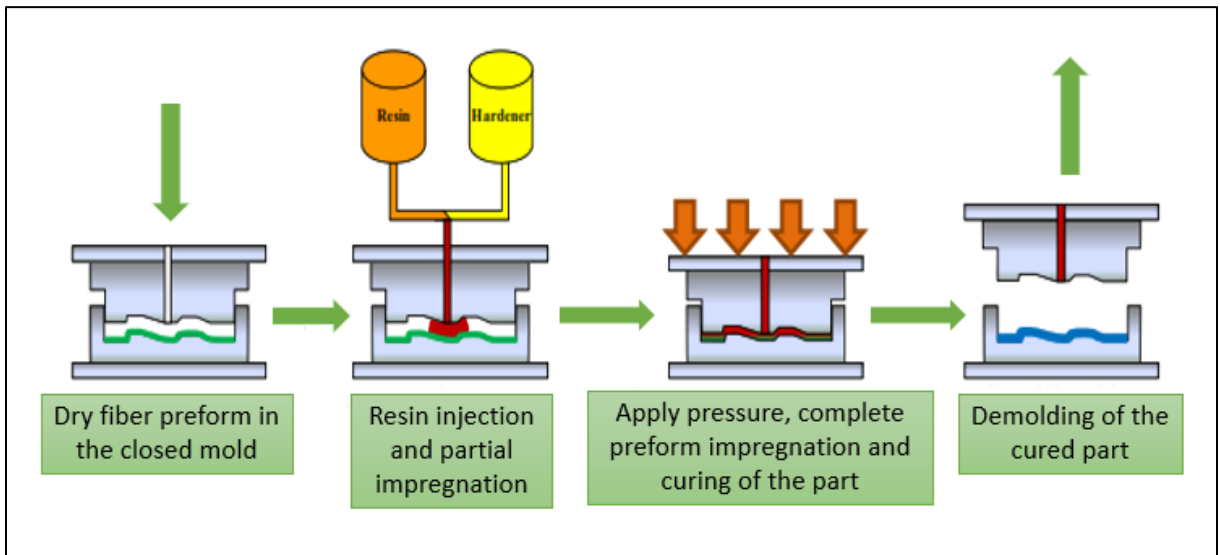


Figure 1-7: Resin injection sequence in the High Pressure - Compression RTM (HP-CRTM) process. Adopted from (Chaudhari, R. et al., 2012)

1.2.2 Thesis composition

This thesis is divided into six chapters:

Chapter 1-Introduction. This chapter covers the background of the research topic which includes a short description of composite materials, specifically Continuous Fiber Reinforced Polymers (CFRP) and their importance in the automobile industry. Short explanations of Resin Transfer Molding (RTM), and the various types of RTM are provided in this chapter.

Chapter 2- Literature Review. This chapter reviews the relevant literature and background information for the Wet Compression Molding (WCM) process. The motivation and the objectives of the research are also discussed.

Chapter 3- Experimental Methodology. This chapter presents in detail the specifics of the examined material system, the experimental procedures of this project and explains the mechanical testing methodology protocols and standards.

Chapter 4- This chapter provides the statistical approach to investigate the effect of process parameters on the final mechanical property of CFRP produced parts. Following that, the significant and insignificant variables will be identified based on the statistical design results.

Chapter 5- This chapter covers the method used to examine the effect of initial resin distribution on the final mechanical property of the CFRP produced parts.

Chapter 6- Conclusions and recommendations. This chapter contains both the conclusions and some recommendations for future work.

Chapter 2

2 Literature review

This chapter provides some existing studies for the resin transfer molding technique, its variants, and the wet compression molding process, then compares the benefits and disadvantages of both techniques. Next, reviewing existing literature will outline techniques for analyzing the mechanical properties of continuous fiber-reinforced composites.

2.1 Wet Compression Molding (WCM) process

The technique of Wet Compression Molding (WCM), also known as liquid compression molding (LCM), is a relatively new manufacturing technique developed due to the recent requirements in the automotive industry. WCM uses continuous dry reinforcements and liquid resins as raw materials, like other composite molding methods such as Resin Transfer Molding (RTM) (imould, 2019). For two reasons, Wet Compression Molding is significantly faster than RTM. First, there is no injection step; the resin can be applied to the preform directly out of the mold, reducing mold occupation time. Second, because the preform is impregnated perpendicular to the fiber, lower-latency resins can be employed, resulting in a shorter cure time. Wet Compression Molding techniques often offer comparable or higher volumetric fiber reinforcement content but higher voids than HP-RTM. This results in decreased mechanical performance and lower part quality. These drawbacks are caused by a lack of hydrostatic pressure on the resin during and after mold closure (Gardiner, 2016).

Using the WCM process provides an opportunity to reduce operational expenses while preserving product quality. Because the WCM method allows for using fast-cure resin systems, it has considerable cost and cycle time advantages over RTM technologies. In comparison to RTM, the forming pressures are substantially lower (FRIMO, n.d.). According to the 2015 SPE ACCE paper (Karcher, M.D. et al., 2015), Wet Compression

Molding offers lower material cost and higher production capacity than autoclave or inline prepreg.

WCM combines the advantages of RTM, such as its high-quality surface finish and good dimensional tolerances (Rosenberg, P. et al., 2014, May; Simacek, P. et al., 2008), with the quicker production rates of Compression RTM (CRTM) (Simacek, P. et al., 2008) and High-Pressure Resin Transfer Molding (HP-RTM) (Rosenberg, P. et al., 2014, May; Baskaran, M. et al., 2014, June). In 1948, Molded Fiber Glass (Molded Fiber Glass Companies, n.d.), a business based in the United States, was the first to employ the WCM process for volume manufacturing. The BMW Group is utilizing WCM to create various Carbon Fiber Reinforced Plastic (CFRP) parts for its i3 and i8 vehicles (Gardiner, 2016). The elimination of a separate preforming phase of the reinforcing medium is the primary factor that makes the WCM process a more cost-effective alternative to the RTM process for medium- to high-volume production (Gardiner, 2016).

The primary steps of WCM include the application of resin to the preform outside the mold and then compression molding to shape and cure the part which frees up the mold related equipment for shorter cycle times and speeds up resin impregnation in contrast to the injection procedure that is necessary for Resin Transfer Molding (RTM) (Gardiner, 2016). It is possible to differentiate between two distinct process versions, as shown in Figure 2-1.

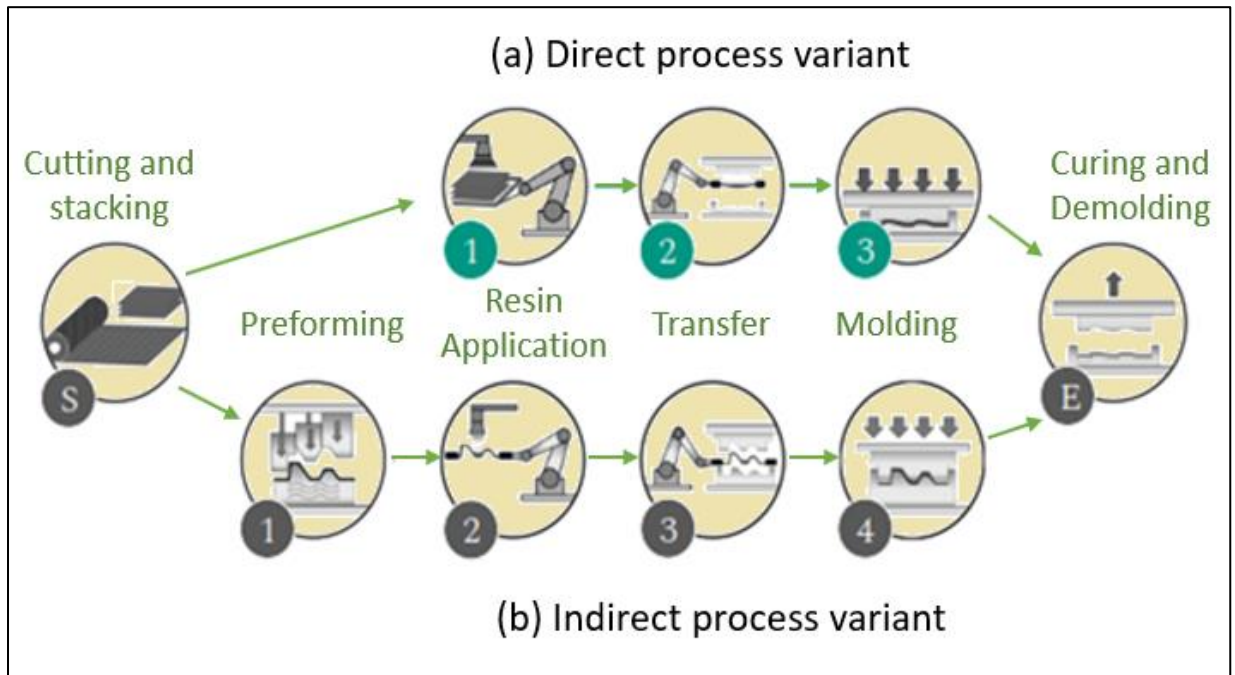


Figure 2-1: WCM steps- (a) Direct process; (b) Indirect process. Adopted from (Poppe, 2021)

Beginning with the direct process variation (refer to Figure 2.1(a)), individual fabric layers are cut (S), stacked (1), and a broad slit nozzle is used to apply resin on the fabrics (2). The resin begins to spread into the fibrous stack, and then the stack that has been partially infiltrated is put into the mold. Infiltration and the forming of the textile take place simultaneously during the third and most important stage (3) (Han, K. et al., 1998). Therefore, in contrast to RTM, injection does not come at a later stage in the manufacturing process after shaping in a closed mold. The stack is infiltrated prior to molding to a significant extent, which contributes to the achievement of thickness-dominated flow progression and short infiltration lengths. This leads to relatively low cavity pressures and lower tooling costs, which makes WCM more appealing in comparison to standard liquid composite molding methods such as RTM/CRTM processes (Bergmann, J. et al., 2016).

An additional preforming stage is included in the indirect process option (see Figure 2-1(b)) (1). The resin is placed on top of the stack, which has already been constructed and formed (2). The molding phase (4) is nearly identical to the compression step in the CRTM method. The direct WCM variant is economically more advantageous but also more complex to model. However, the indirect method can reduce cycle times to as little as two to three minutes (Henning, F. et al., 2019; Bergmann, J. et al., 2016).

Previous research in WCM has focused on the experimental assessment of important process factors, improved tooling techniques or the influence of process parameters on structural performance. Bergmann et al. (2016) have established relationships between component quality and process boundary conditions such as stack weight, mold temperature, resin volume, infiltration time, and molding sequence. They examine the part surface for characteristics such as wrinkles, undulations, and dry areas to determine the quality of the component. The overlapping effects on part quality that have been discussed make it challenging to do a process analysis based on physical principles.

Bockelmann (Bockelmann, 2017) used fluorescence photography to examine the through-thickness infiltration that occurred during the molding process. Using this information, he presents a new tooling and infiltration concept based on a spatially dispersed resin carrier frame. This integrated processing, also known as CIP, can be utilized to generate highly uniform infiltration outcomes inside the stack. Additionally, the process resilience is increased because of a closely controlled fluid progression. In addition to this, he provides a Life Cycle Assessment (LCA) that contrasts the conventional RTM with the WCM (both with and without the suggested CIP). Because WCM applications have shorter cycle times and lower cavity pressures, they have a lesser impact on energy consumption, energy prices, and the environment. This makes WCM process more favorable than conventional RTM. Both decrease the necessary number of pressing pressures and dwell times, which ultimately results in smaller and less energy and capital-intensive piece of processing equipment.

Muthuvel, B. et al., (2020) conducted an experiment to compare the two variants of the WCM process (see Figure 2.1) by applying it to the manufacturing of a complex sled-shaped demonstrator part with each WCM variant. Not only did the direct method cut down on processing time, but the quality of infiltration through dry spots was also better for simultaneous infiltration. This results from an earlier infiltration of critical areas before significant deformations take place inside the mold. The results directly indicate the importance of coupled draping and infiltration.

Lee et al. (2021) has provided an investigation on the compressive-strength-after-impact of non-crimped textiles that were produced by the WCM technique. They have demonstrated that a satisfactory mechanical impact performance could be obtained by achieving a low void content which could be realized in the material.

2.2 Process studies in Resin Transfer Molding (RTM) process

Throughout recent years, researchers have focused their attention on investigating the effects of the process variables on the mechanical properties of different types of Resin Transfer Molding process (RTM). Some of the studies are presented below.

Chang et al. (2006) examined how process variables affected the quality of compression resin transfer molded epoxy (the Ciba-Geigy epoxy resin-Araldite LY564 and Hardener HY2954) /glass fiber mat products. The influence of mold temperature on the mechanical properties of RTM parts was found to be less significant when compared to vacuum level, injection pressure, and resin temperature when pre-heated mold temperatures of 25, 50, and 75 °C were chosen. Chang et al. (2006) also studied the impact of initial resin temperature using three different temperature levels: 25, 32, and 40 °C. They demonstrated that using higher resin temperatures effectively reduces resin viscosity and thereby improves resin penetration into reinforcing interstices. This would therefore minimize the total void content and improve part quality.

Kaynak et al. (2008) examined the effects of mold temperature, application of vacuum at resin exits ports, and initial resin temperature on the mechanical properties of epoxy matrix (The matrix material used is a mixture of a special low viscosity epoxy resin -Araldite LY5052- and hardener -Araldite HY5052) / woven glass fiber reinforced composite specimens produced by Resin Transfer Molding process (RTM). For this purpose, six mold temperatures (25, 40, 60, 80, 100, and 120 °C), two initial resin temperatures (15 and 28 °C), and vacuum (0.03 bar) and without vacuum (1 bar) conditions were utilized. Specimens were characterized by ultrasonic C-scan inspection, mechanical tests (tensile, flexural, and impact), thermal analyses (ignition loss and TGA) and scanning electron microscopy. It was observed that mechanical properties of the specimens produced at a mold temperature of 60 °C with the application of vacuum and initial resin temperature of 28 °C proved to result in the highest properties (e.g., 16, 26, and 43% higher tensile strength, flexural strength, and Charpy impact toughness, respectively, compared to the lowest values attained with mold temperatures other than 60 °C while other variables are kept constant). It has been shown that application of vacuum contributes to the final mechanical properties of the produced composites by lowering the percentage of ‘voids. In fact, without the application of vacuum, the deterioration in mechanical properties can be as high as 26% loss in Charpy impact toughness and 5% losses in tensile and flexural strength. Additionally, lowering the initial resin temperature is shown to alter mechanical properties (e.g., 14, 12, and 18% losses in tensile strength, flexural strength, and Charpy impact toughness, respectively, when the initial resin temperature is decreased from 28 to 15 °C) (Kaynak, C. et al., 2008).

Han et al. (2018) used cavity pressure and temperature sensor monitoring to determine the connection between outputs and the quality of the final component. Carbon fiber sheets with an epoxy resin (KER- 9610, Kumho Petrochemical) and hardener (KCA 9610, Kumho Petrochemical) were used for this experiment. Selected process parameters such as the mold gap size, maximum pressing force, void location, curing time, and injection volume have been examined, and the mechanical performance has been established with tensile testing (ASTM D-3039) and flexural testing (ASTM D-790). As an illustration, the

research made use of an injection pressure of 120 –130 bar, pressurization of 1200 and 1800 kN, and a mold temperature of 114 °C for different preform layers consisting of between six and eleven sheets of carbon fiber.

In another study, the researchers investigated and compared the results of two different molding techniques, namely High-Pressure Injection Resin Transfer Molding (HP-IRTM) and High-Pressure Compression Resin Transfer Molding (HP-CRTM) (Rosenberg, P. et al., 2014, May). The study helped researchers gain a better knowledge of the correlation between selected process parameters such as mold gap size and maximum applied press force on the mold cavity pressure profile and resulting carbon fiber reinforced composites properties. The mold temperature, duration of vacuum application, mixing pressure, amount of resin used (an epoxy resin from Sika AG with the trade name Biresin CR 170 and amine hardener with the trade name Biresin CH 150-3 was used in this research), rate of resin injection, and curing time were all held consistent throughout the process. The initial rate of resin injection was 40 g/s, and the mixing head pressure was set at 120 bar. The temperature of the hardener was 25 °C, the resin temperature was 80 °C, and the temperature of the mold was 125 °C. Following the injection of the resin in the cavity of the mold in the amount of 710 g, the mixing head was then closed, and the pressing force was increased to 5000 KN within 6 seconds. After compression there was a drying time for the resin of three minutes, and then the laminate was demolded. The results of mechanical testing showed that these parameters had a negligible effect on the mechanical qualities of the laminate. When the first two experiments are compared to one another, it becomes clear that additional research must be conducted to determine whether cyclic loading or a stricter variation on the process parameters is necessary.

Swentek et al. (2015) investigated glass and carbon fibers using two different matrix materials, namely epoxy (Hexion Epikote 05475/05443) and polyurethane (Huntsman RIMLINE SK 97014). The press force during injection, the pressing force during cure, and the injection rate were the main process parameters that were evaluated. In this investigation, injection flow rates of 20, 40, and 60 g/s were employed. The part's nominal

thickness was fixed at 2.3 millimeters, and the fiber volume fraction was determined to be 60%. The compression force during injection was varied between 500-5000 KN, while the compression force during cure was varied between 1000-5000 KN. Prior to injection, the temperature of the resin was increased to 50 ° C. (for epoxy) or 60 ° C (for polyurethane), while the temperatures of the hardener and isocyanate were set at 28 ° C. and 30 ° C, respectively. Injection pressure was 120 bar, injection mass was 710 grams, and the cure time was 300 seconds. The mold temperature for epoxy was 95 °C, while the mold temperature for polyurethane was 120 °C. The research team carried out three separate tests in which they altered either the injection rate, the compression force during injection, or the compression force during cure. The tensile test was conducted according to ISO 527-4, and the flexure tests were carried out according to ISO 14125. Both tests were part of the mechanical evaluation. The incineration method described in ISO 7822 was utilized for the purpose of measuring the fiber volume fraction, and ISO 14130 was utilized for the purpose of calculating the interlaminar shear strength measurements.

According to the findings of this investigation, the compression forces during injection and cure do not impart significant effects on the processed panels. Despite this, increasing the injection flow rate results in an improvement in the elimination of entrapped air during the fiber impregnation process, which leads to an increase in the composite's strength and stiffness. The improvement is minor, and it is only to the extent that the air is extracted, as there were no additional gains at greater flow rates.

2.3 Motivation and Objective

As discussed earlier, RTM (HP- RTM) is a breakthrough technique in and of itself, but WCM has already caught the interest of European Original Equipment Manufacturers (OEMs) (Gardiner, 2016). The WCM technique is distinguished by its ability to cure one part in the mold while the resin for another part is added to the fabric. Because the resin injection does not occur inside a hot mold, higher temperatures and shorter cure cycles can be achieved without the material curing before the part is filled. These advantages significantly reduce the cycle time to a three-minute benchmark; thus, they are suitable for

use in the automotive industry. This method can help to reduce costs compared to the RTM without compromising the quality of the final product. Understanding relevant process variables, their connections, and their influence on part quality form the foundation of an economical method. Therefore, this project aimed to determine the critical input parameters for the WCM process and investigate their impacts on the quality of the final parts.

In order to fulfill project objectives, a Design of Experiments (DoE) matrix was developed to minimize the number of experiments required to perform the statistical data analysis. In the DoE matrix, the operating conditions and their levels were adopted based on the comprehensive literature review above and based on the literature review and the industrial experience of the collaborators Jennifer Sears, Ph.D. candidate, University of Windsor, and Dr. Gleb Meirson, research engineer at Fraunhofer Innovation Platform for Composite Research.

The overall objective of this project is to investigate the correlation between process parameters and the composite mechanical property (Chapter 4). In addition, this research aims to evaluate the correlation between the local mechanical property of carbon fiber-produced plaques and the initial resin application at different locations in the produced parts (Chapter 5).

The detailed objectives of this research are as follows:

- Estimate the relationship of the local mechanical property (measured Young's modulus) to the input parameters including process operating conditions, and the initial resin application.

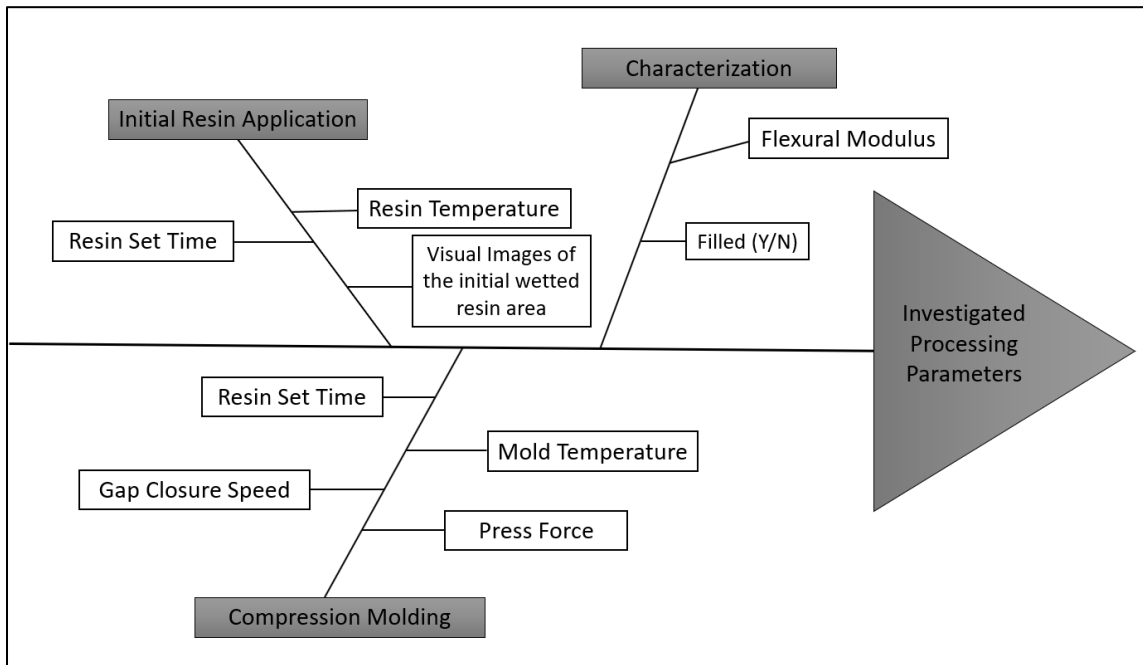


Figure 2-2: Investigated WCM parameters in this study

Chapter 3

3 Experimental Methodology

3.1 Experimental procedures

This chapter describes the experimental procedures, an overview of the material system explored in this study and an explanation of the techniques used for the manufacturing process. Mechanical testing protocols, preparation of samples, and appropriate experimental methods for performing the mechanical testing according to American Society for Testing and Materials (ASTM) standards are also provided.

3.1.1 Material reinforcement

The material used in this project is a non-crimped fabric which contains Panex PX35-UD300 supplied by Zoltek Corp (Corporation, n.d.) as shown in Figure 3-1. The PX35 UD300 heavy tow reinforcement fabric contains straight tows, containing 50,000 continuous carbon filaments each, stitched with polyester in a tricot knitting pattern in the tow direction. The reinforcement fabric consisted of supporting glass yarns oriented perpendicular to the tows. The reinforcement properties are provided in Appendix 1.

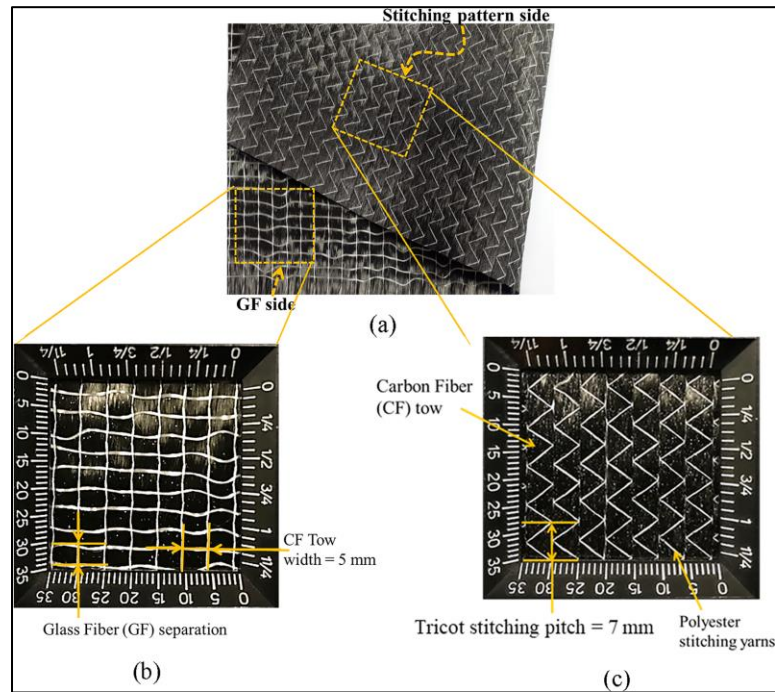


Figure 3-1: (a) Zoltek PX35-UD300 unidirectional non-crimp fabric with stitching and glass fiber sides indicated, (b-c) microstructure of fabric. Adopted from (Ghazimoradi, M. et al., 2022)

3.1.2 Resin system

In this project, the resin system has a curing time of 5 minutes provided by Hexion Inc (Hexion, 2015). EPIKOTETM Resin TRAC 06170 is employed as a medium viscosity epoxy resin; EPIKURETM Curing Agent TRAC 06170 is a low viscosity, amine hardener; and the HELOXYTM Additive TRAC 06805 is a silicone-and wax-free internal mold release (IMT) agent. The resin: hardener: mold release mixing ratio is 100:24:1.2 for all experiments. Key properties of the resin system are provided in Appendix 2.

3.1.3 Processing parameters

The parameters investigated in this study are the resin temperature, mold temperature, resin set time, gap closure speed (for the last 2mm of gap), press force, and mold curing time. See Table 3-1 for the details of process parameters (factors) and the selected Design of Experiments levels for each factor. Appendix 3 provides the processing conditions for each produced plaque.

Table 3-1: Summary of Processing Parameters

Investigated process parameters	Unit	Values
Resin temperature	°C	50-60-70
Mold temperature	°C	110-130
Resin set time	sec	0-20-40
Mold curing time	sec	120-300
Press force	KN	3000
Gap closure speed	mm/sec	1-2-3

3.1.4 Preform placement

In the experiments, the preform is placed into the frame of a 6-axis robot end of the arm tool (provided by the Fraunhofer Institute for Chemical Technology in Germany).

3.1.5 Process description and plaque manufacturing

In this experimental design, 48 flats plaques incorporating the Panex PX35-UD300 carbon fiber preforms, are manufactured with dimensions of 900 mm × 550 mm (length × width) and an average thickness of 1.20 mm using Wet Compression Molding process (WCM) at the Fraunhofer Innovation Platform for Composites Research (FIP) at Western University. An overall view of the WCM manufacturing system is indicated in Figure 3-2.

The indirect WCM technique is employed (as explained in Figure 2-1 in Chapter 2) as shown in Figure 3-3.

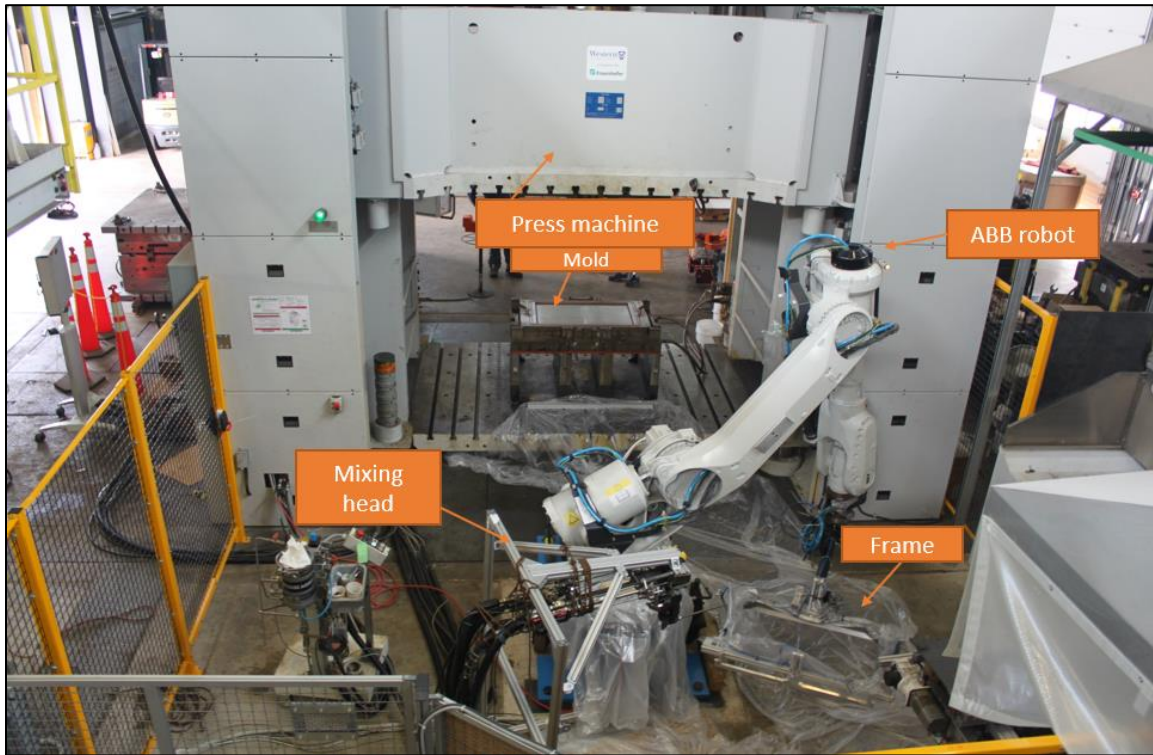


Figure 3-2: Manufacturing system of WC

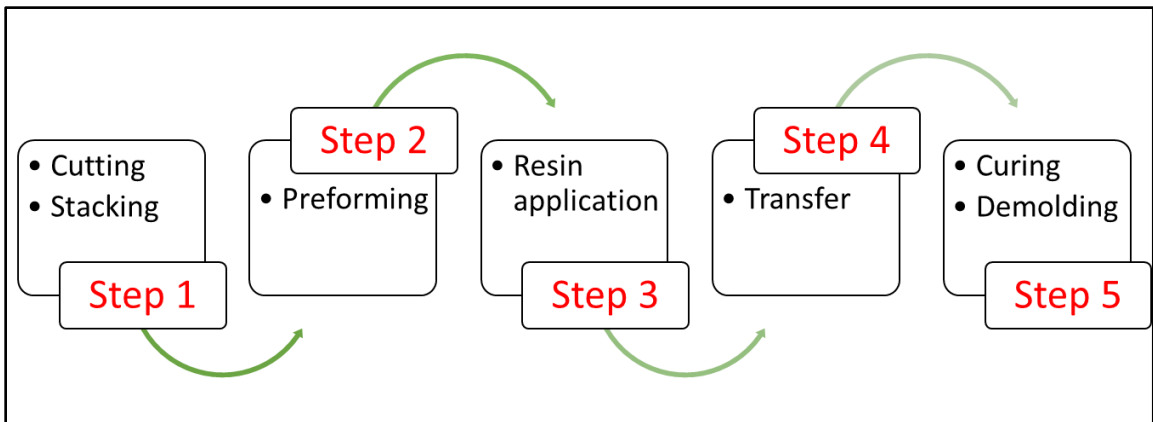


Figure 3-3: Wet compression molding steps

Four layers of fabrics with two multi-directional stacking sequences (0/90/0/90) are cut for each part and stacked together. In the second step, the stacked mats with binder are preformed. The binder reaction initiation is done in the press machine at 500 KN pressure at 120 °C for 10 minutes (preform properties are summarized in Table 3-2). The third and fourth steps involve applying and spreading resin and transporting the preform into the mold. A total of 500-gram shot mixture of resin, hardener, and internal mold release (IMR) with the injection rate of 50 g/s is applied to the preform. Resin is continually pumped into the mixing head and flows onto the surface of fabric through the distribution nozzle, which is attached to the mixing head. Dimensions and image of the flat nozzle is shown in Figure 3-4. After the resin pouring process, the robot transfers the resin-applied preform into the mold, as shown in Figure 3-5. Then the press machine closed the two mold halves with a press force of 3000 KN.

WCM process for steps 3 and 4 are automated (using an ABB robot) and completed in seventy (70) seconds. The timing for each sequence step is provided in Figure 3-6.

Table 3-2: Preform properties

Preform Properties	
Areal Wight	200 gr/m ²
Initial Thickness	0.76 mm

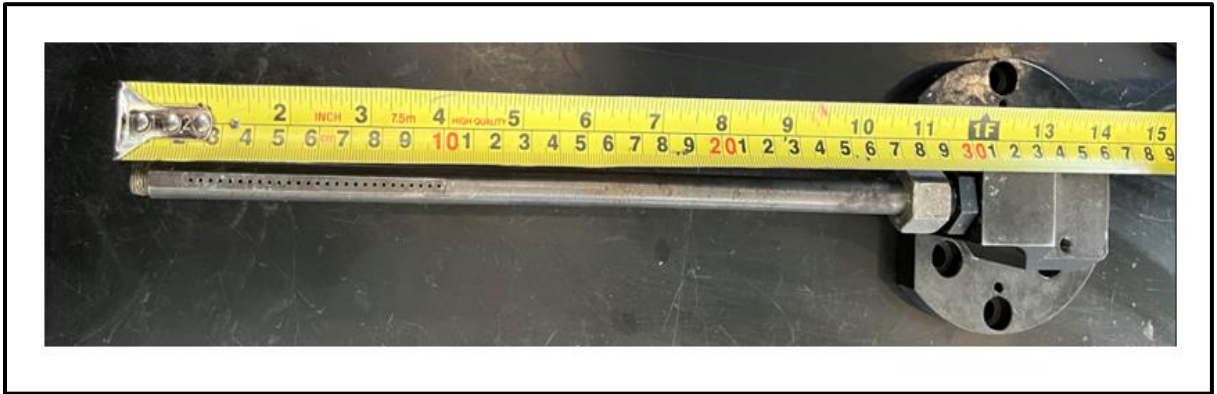


Figure 3-4: Image of resin distribution nozzle (flat nozzle)

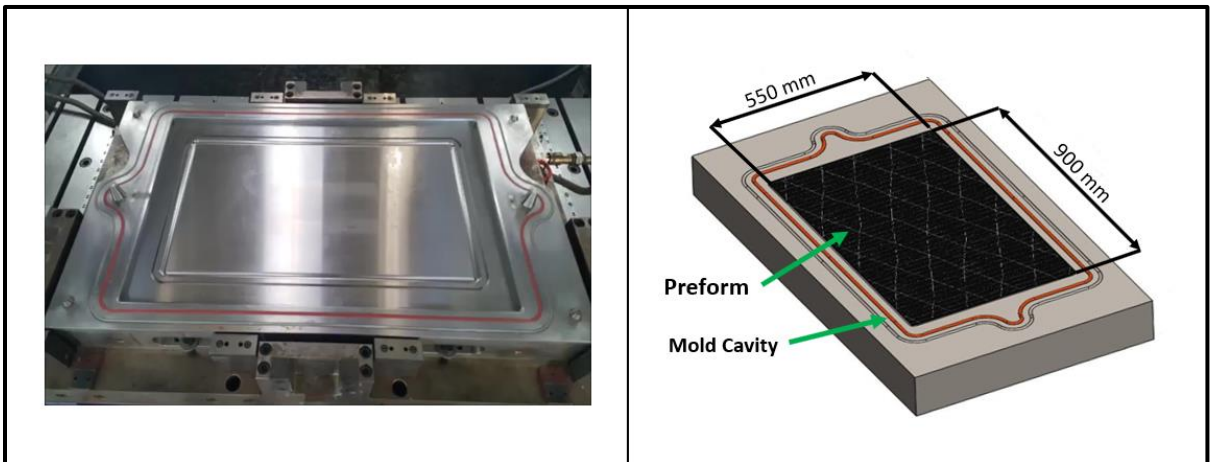


Figure 3-5: Image of mold cavity

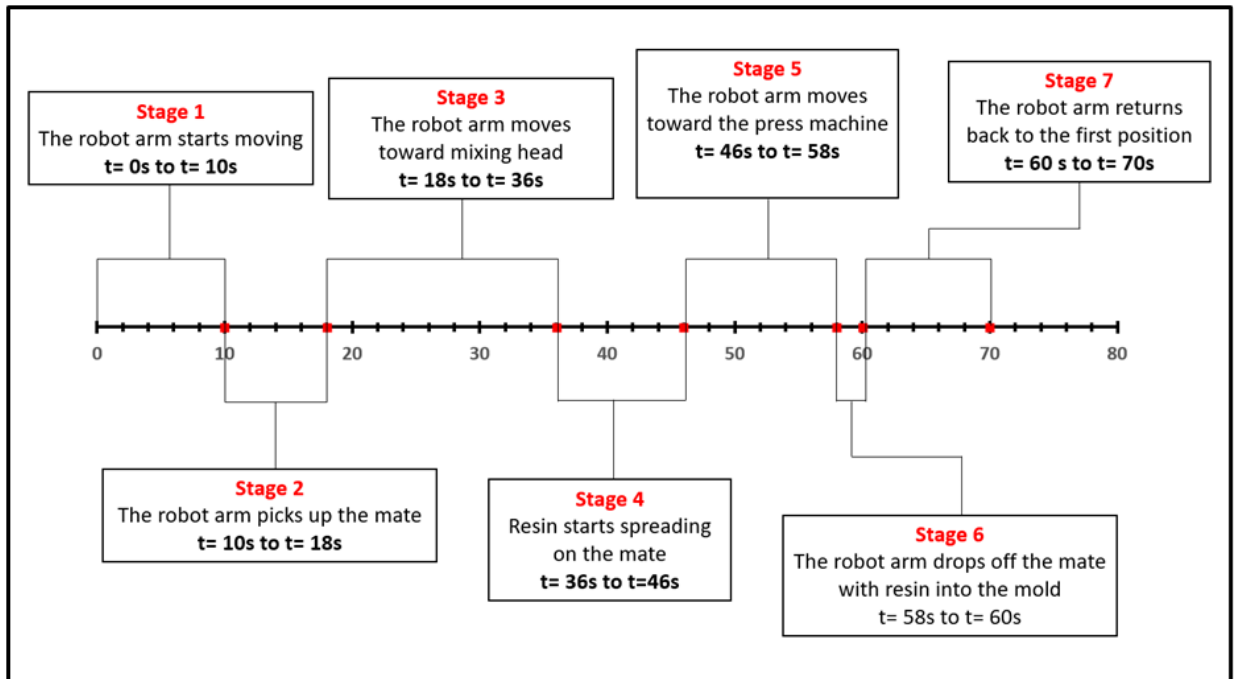


Figure 3-6: WCM process in details

3.2 Mechanical testing

3.2.1 Plaque Screening

The plaques are examined and classified based on their appearance (visual observations) before being subjected to any kind of mechanical testing as summarized in Appendix 4. Acceptable plaques without visual defects are then subjected to the mechanical (flexural) testing protocol. The investigated observed defects for plaque rejection with short descriptions are presented below.

➤ **Dry spots:**

A dry spot is a zone that has not yet been impregnated by the macroscopic resin flow but has been reached by the resin flow front (Lawrence, J. M. et al., 2009). In other words, dry spots are unsaturated preform areas within WCM parts. This sort of void is observable even with the eye, as shown in Figures 3-7, 3-8, and 3-9.

Dry spots usually appear when a large volume of air is entrapped by the resin during the infusion process. There are several causes for the development of large unsaturated zones, or dry spots, within WCM sections. For instance, they may emerge when impregnation causes the resin to begin curing prematurely, locally slowing down, or blocking subsequent resin flow. Dry spots can also result from the well-known race tracking phenomenon, channeling effects due to high permeability regions, and converging flows produced by improperly positioned input ports (Lawrence, J. M. et al., 2002; LeBel, F. et al., 2014; Naik, N. K. et al., 2014).

Before resin flow, permeability with a constant fiber volume fraction is expected to be constant throughout the molds. However, several reasons, including inadequate preform preparation, misplacement or shifting of the preform in the molds, unintentional inclusion of foreign material, and preform natural planar density variation, can result in significant variations in the permeability distribution. In the channeling phenomena, local variations in permeability have an impact on the resin's flow patterns, leading the resin to flow

initially through high permeability zones and resulting in the creation of dry places (Lee, D. H. et al., 2006; Villière, M. et al., 2015).

In several investigations, it was aimed at preventing all preventable permeability differences, such as inclusions and misalignments, by carefully positioning the preform. When preform heterogeneities cannot be avoided, active and passive flow control can be used to correct the flow after race tracking is recognized to ensure proper preform wetting. This is done before designing scenario-based solutions (Carlone, P. et al., 2015; Demirci et al., 1995; Sozer, E. M. et al., 2000).

In order to steer the resin through the preform and prevent the formation of dry spots, a number of researchers (Demirci et al., 1995; Nielsen, D. et al., 2001) used artificial neural networks trained with process simulation data to make real-time decisions about the proper injection parameters. During the LCM process, Lawrence et al. (2002) controlled the resin flow online using sensors and actuators. Disturbances in the planned flow propagation were found by tracking the fluid flow using installed sensors. To ensure successful mold filling, the disturbed flow front was next guided towards exit vents using auxiliary control gates. To avoid the establishment of dry spots, other researchers suggested an automated simulation/control strategy (Lee, D. H. et al., 2006). The authors demonstrated how altering the injection pressure of auxiliary gates can improve control of the resin front. Johnson et al. (2006) even suggested employing localized induction heating to lower the resin's viscosity and guarantee the absence of dry spots in low-permeability areas. Yet, these dynamically managed, scenario-based solutions frequently call for expensive tooling, the installation of tough sensors, and flow control hardware that is meant to be integrated with the injection equipment.

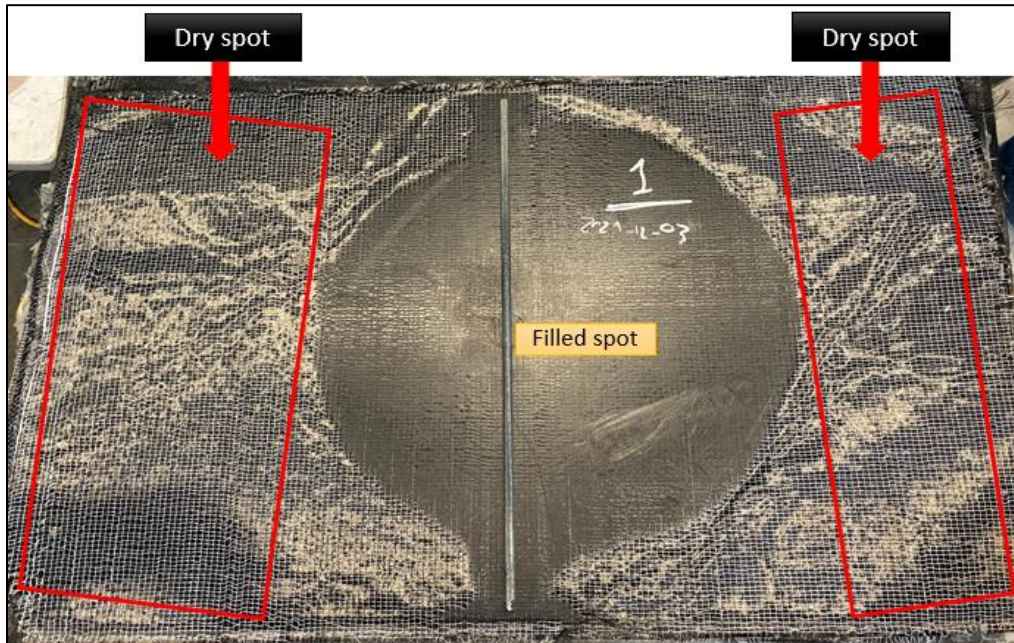


Figure 3-7: Example of large dry spot- Plaque number 1

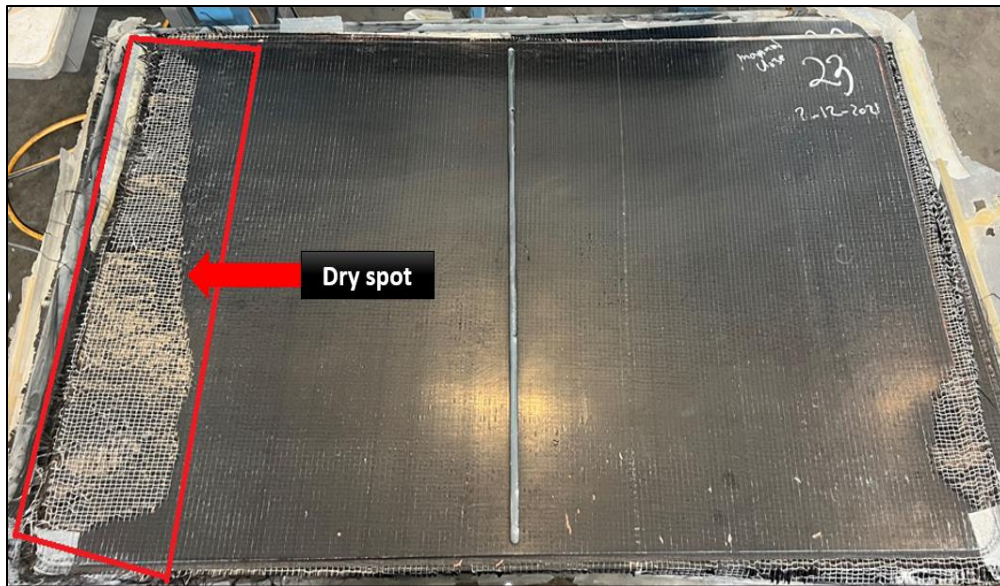


Figure 3-8: Example of medium dry spot- Plaque number 23

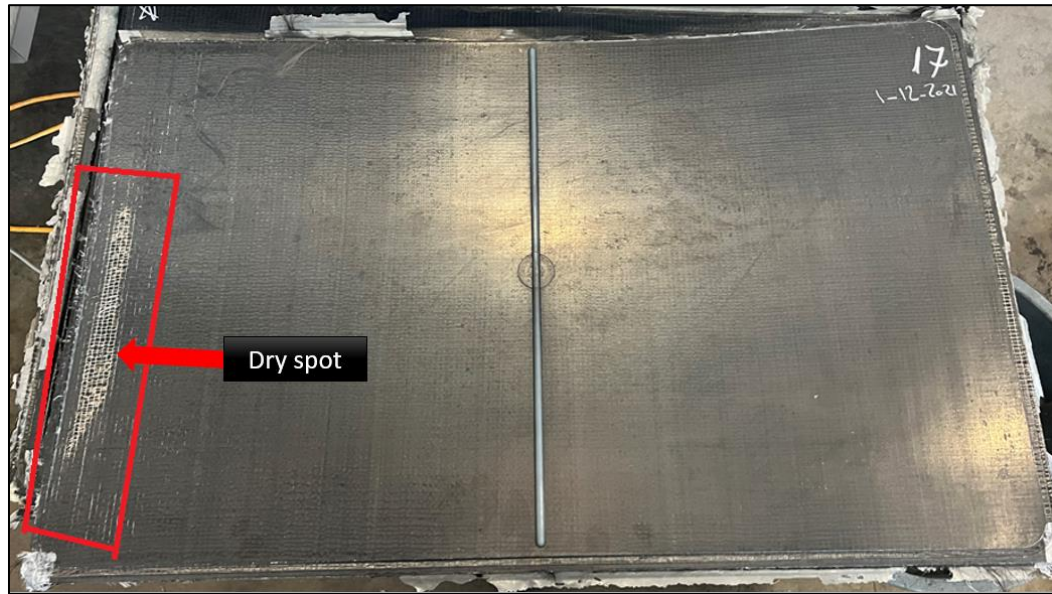


Figure 3-9: Example of small dry spot- Plaque number 17

➤ **Shifted preforms:**

In some cases, the resin flow could move the preform out of place, which depends on WCM process parameters: resin viscosity, flow front velocity, injection pressure, and fiber volume fraction (Gereke, T. et al., 2013). However, it has been noted that the primary cause of shifted preform in WCM is the incorrect positioning of the preform in the mold cavity prior to resin injection, which results in a significant scatter from the intended fiber orientation (Altmann, A. et al., 2016; Khan, Z. M. et al., 2016; Li, Y. et al., 2016). Examples of shifted preforms are provided in Figures 3-10 and 3-11.

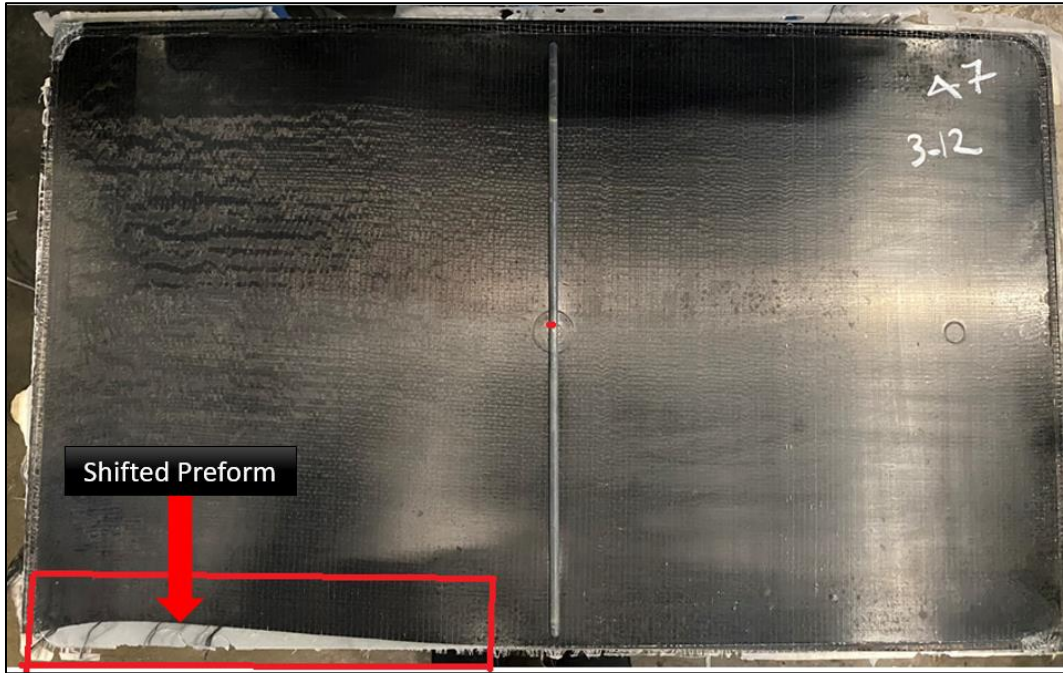


Figure 3-10: Example of shifted preform- Plaque number 21

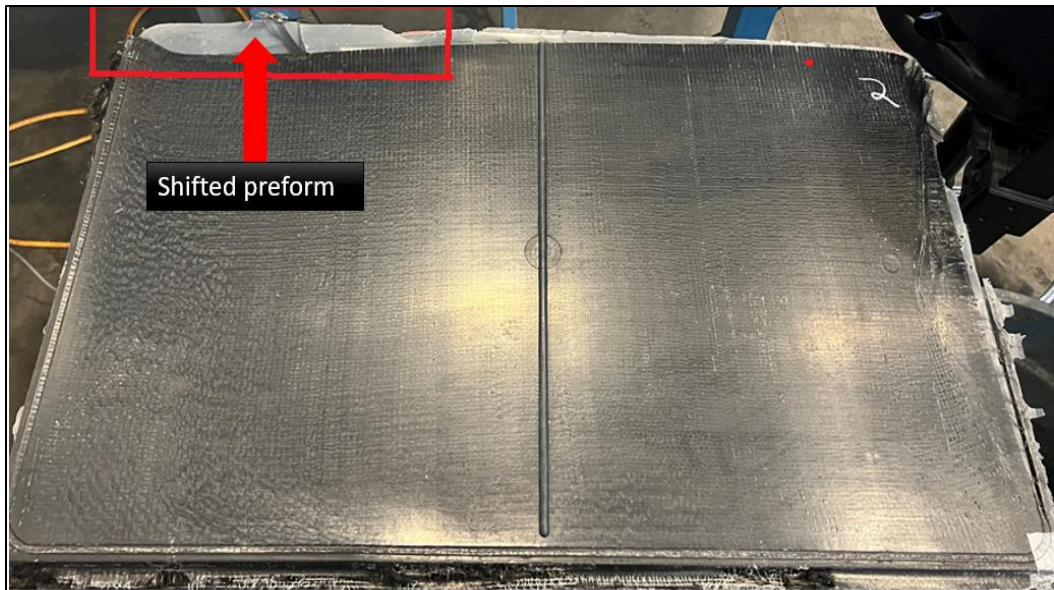


Figure 3-11: Example of shifted preform- Plaque number 47

3.2.2 Mechanical testing coupons

In this section, test coupon samples are selected from the acceptable plaques to conduct mechanical testing. Ideally, the test samples must be obtained in varying directions in relation to the flow direction (e.g., 0° , 45° , and 90°) to evaluate the anisotropic mechanical properties of the parts.

However, due to the size limitation of the produced plaque and the sampling plaques, taking samples in all directions from each plaque was not possible. Hence, specimens were only taken from one loading direction in relation to the flow direction (0°). Of course, samples taken in a different direction will show different properties, but since the fabric stacking sequences contain 0° and 90° directions (0/90/0/90), sampling in one or two directions is not expected to generate significantly different results. Due to time constraints, only the flexural test (ASTM D7264) (International, 2007) is conducted on the plaques.

Five different sampling areas (coupons) of interest are selected for the mechanical flexural test based on the initially wet and non-wetted (dry) regions. As shown in Figure 3-12, coupons from sampling areas A and C are chosen as initially wetted (resin) areas, while the coupons from sampling areas B, D, and E, are selected from the initially dry areas. The reason for this selection is to determine if there is a difference between the flexural properties of the locations where the resin was initially applied (sampling areas A and C) and the locations without any initially resin application (sampling areas B, D, and E). The results of the analysis are presented in Chapters 4 and 5.

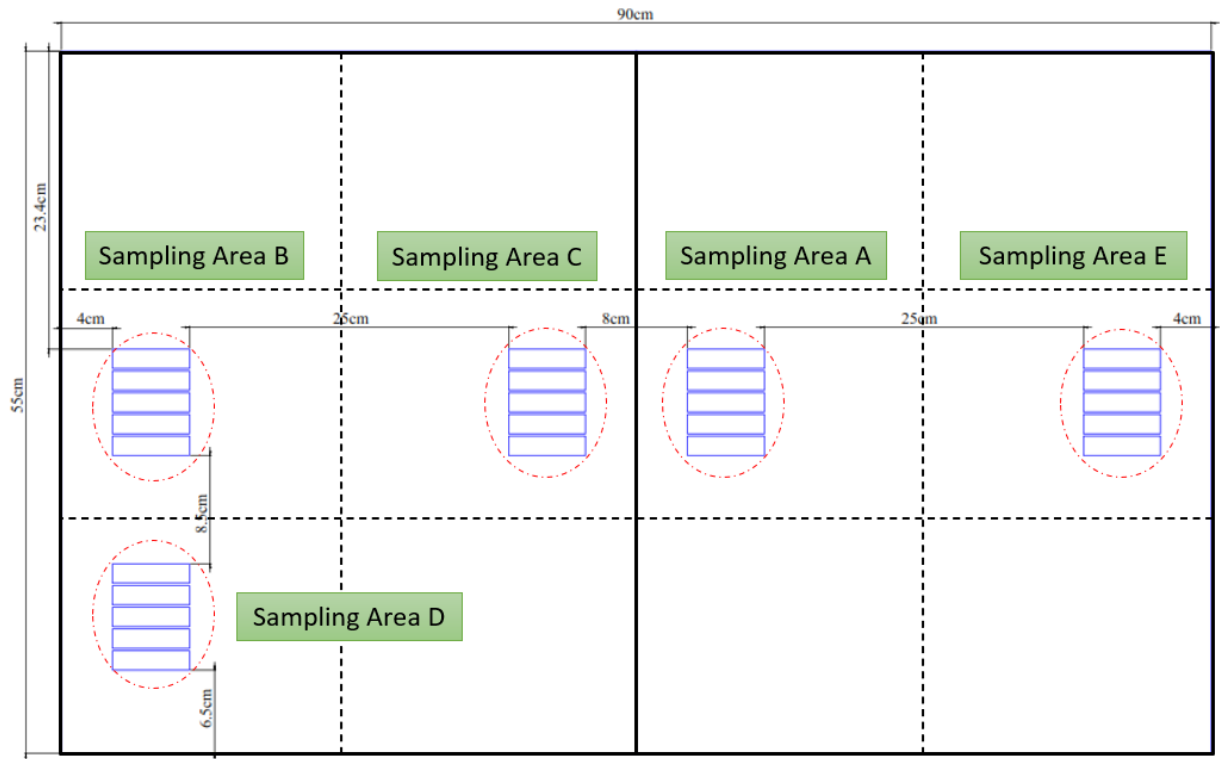


Figure 3-12: Specimens cutting diagram of flexural test

3.2.3 Sample preparation

A bandsaw and waterjet cutting machine are used to acquire flexure samples taken from five different sampling areas of each part. Flexure specimen dimensions are in accordance with ASTM 7264 (International, 2007) sample dimensions: 13 mm in width and 46 mm in length. The thickness is measured by a caliper at the center of each sample. Samples have a thickness ranging from 1.05 mm to 1.40 mm.

3.2.4 Three-point beam flexural test set-up

Flexural testing involves placing a specimen on two supports and applying a load, three-point bending has one loading point, which is shown in Figure 3-13. The ASTM D7264 (International, 2007) three-point bending method is utilized to conduct evaluations of the flexural stiffness and strength characteristics of polymer matrix composites.

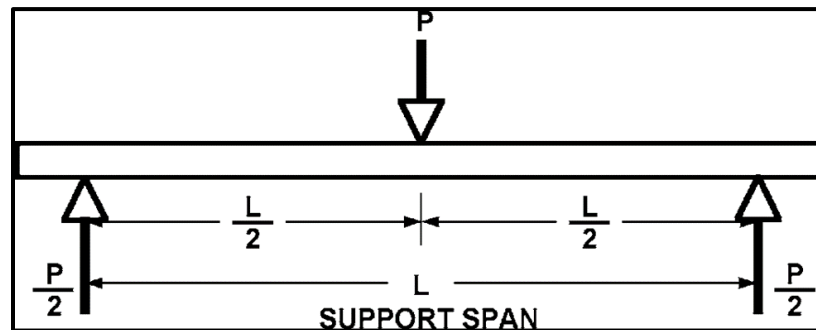


Figure 3-13: Three-point beam flexural test- Loading diagram (International, 2007)

An MTS Criterion Model 45 at the Fraunhofer Innovation Platform for Composites Research (FIP) is used to conduct the flexure test. The bearing radius of the samples is 3 millimeters, and the loading rate during the test is 1 millimeter per minute at room temperature. The span length of the samples is varied according to the sample thickness. The average thickness of each set of specimens is measured; then, using the standard support span-to-thickness ratio of 32:1, the span length was calculated (International, 2007). The sample orientation is such that the top face of the plaque faced upwards in the flexural test.

3.2.5 Flexural test results

The three-point beam flexural test provides the Flexural Modulus of Elasticity (Young's Modulus), Flexural Strength, and Strain at Break. The Stress-Strain curve with details of the three key parameters of the flexural test is illustrated in Figure 3-14, and calculation of each parameter is presented below. The three key values from the flexural tests are calculated using an Excel Macro, which was developed in the Fraunhofer Innovation Platform for Composites Research.

The Young's Modulus data, from the initial linear slope of the stress-strain diagram, represents the mechanical property of the parts and was only used in statistical analysis (Chapters 4 and 5). The main reason was that for some specimens, the break did not happen during the test because some specimens thickness was much higher than the average thickness for the Sample Area, resulting in a required larger span size (in Section 3.2.4, the span size determination was explained). Hence, this made Strength and Strain at Break data less reliable, and they were excluded from statistical analysis.

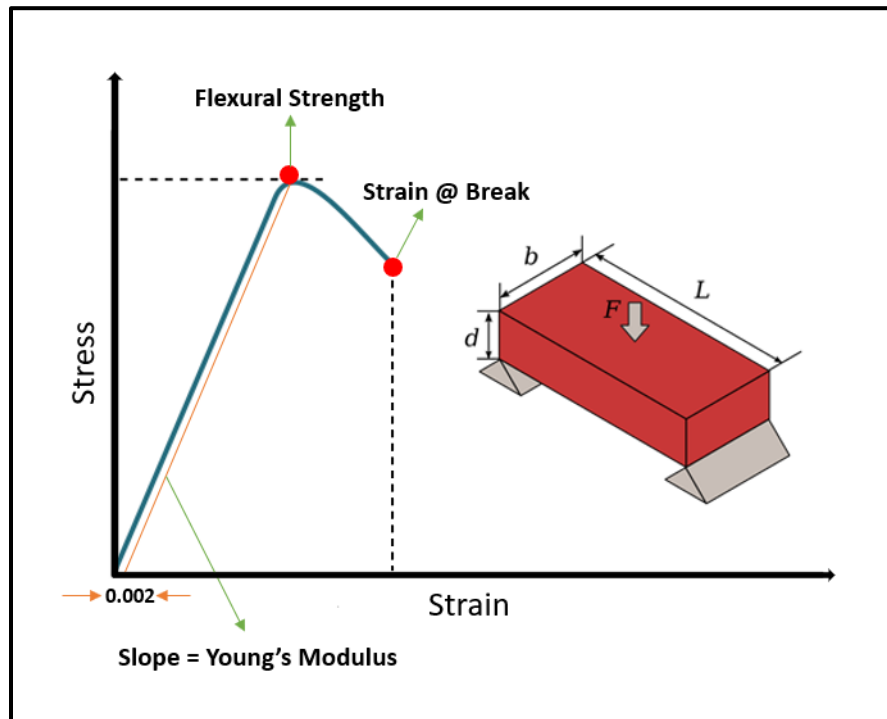


Figure 3-14: Strain-Stress curve details

3.2.5.1 Modulus of Elasticity

The Modulus of Elasticity, also known as Young's Modulus, is the slope of the stress-strain curve within the elastic range, which is the range of material behavior where the sample will return to its original dimensions following deformation. A higher Young's modulus indicates that the material requires more stress to produce the same strain or a greater force to produce the change in length. In line with the ASTM D7264 (International, 2007), the recommended strain range for calculating the flexural chord modulus is 0.002, with a start point of 0.001 and an endpoint of 0.003. Therefore, the Young's modulus is calculated based on the start and end point of strain. The related equation is provided as equation (1).

$$E_f^{chord} = \frac{\Delta\sigma}{\Delta\varepsilon} \quad \text{Eq (1)}$$

Where:

E_f^{chord} = flexural chord modulus of elasticity, MPa [psi]

$\Delta\sigma$ = difference in flexural stress between the two selected strain points, MPa [psi]

$\Delta\varepsilon$ = difference between the two selected strain points (Nominally 0.002)

3.2.5.2 Flexural Strength (Ultimate Strength)

Flexural Strength is the highest stress at the outer surface that corresponds to the peak applied force before failure and calculated in accordance with equation 2 (International, 2007).

$$\sigma = \frac{3PL}{2bh^2} \quad \text{Eq (2)}$$

Where:

σ = stress at the outer surface at mid-span, MPa [psi],

P = applied force, N [lbf],

L = support span, mm [in.],

b = width of beam, mm [in.],

h = thickness of beam, mm [in.].

3.2.5.3 Strain at Break

The maximum strain at the outer surface also occurs at mid-span and calculated as follows (International, 2007).

$$\varepsilon = \frac{6\delta h}{L^2} \quad \text{Eq (3)}$$

Where:

ε = maximum strain at the outer surface, mm/mm [in./in.],

δ = mid-span deflection, mm [in.],

L = support span, mm [in.],

h = thickness of beam, mm [in.].

The calculations for the three parameters of the flexural test were carried out for each sample, and the results are provided in Appendices 6-10.

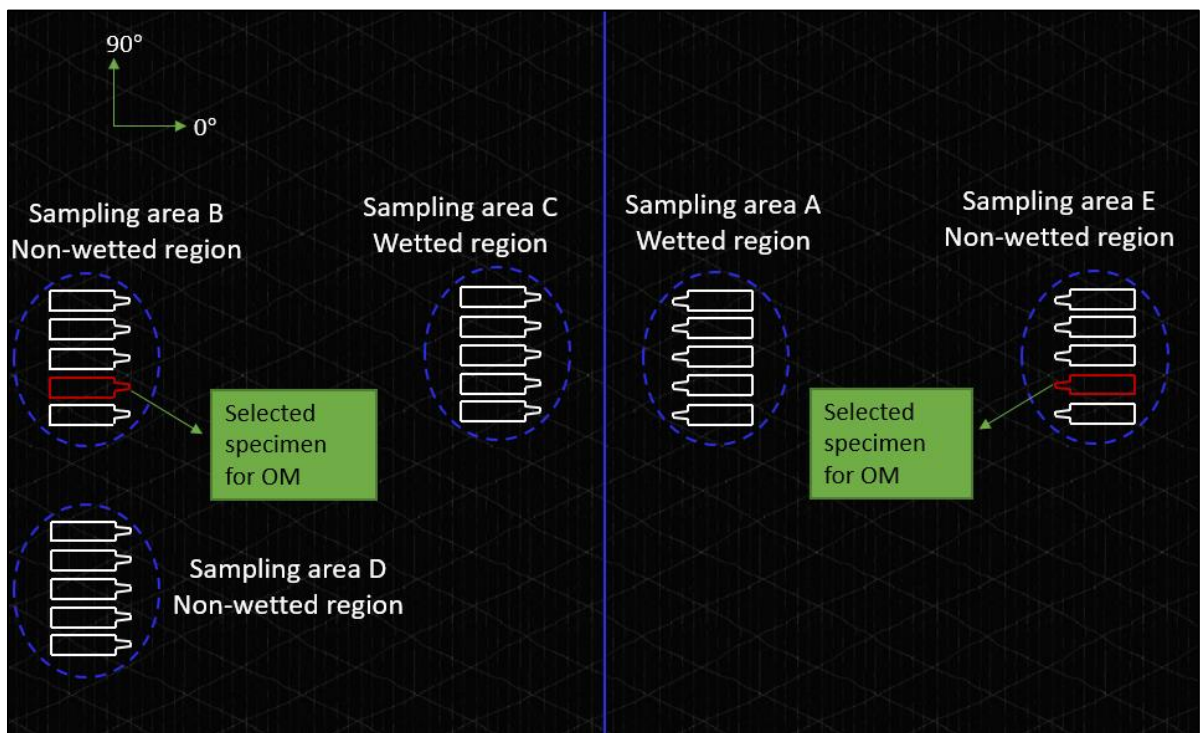
3.3 Optical Microscopy

Optical Microscopy (OM) is a well-established and commonly used technology for investigating the microstructures of materials and is employed here to investigate microvoids in the samples. This approach delivers high-resolution morphological information regarding a cross-section's void size, shape, distribution, and content. Optical microscopy is a destructive procedure from a two-dimensional cross-section of the material rather than its bulk (Farhang, 2014; Kedari, V. R. et al., 2011; Fanni, 2020).

Four flexural test specimens are used to perform the OM test. Table 3-3 shows information about the chosen samples, including plaque number and sampling area. Also, the specimen selection is consistent for the OM test, and the fourth specimen from each sampling area is taken, which is illustrated in Figure 3-15, and the selected specimens are shown in red.

Table 3-3: Details of the specimens

Specimen	Plaque number	Sampling area
1	2	B
2	2	E
3	9	B
4	9	E

**Figure 3-15: Validation specimen locations for OM analysis**

The OM sample is prepared by first mounting the samples in 20 ml epoxy in mounting rings. After removing the cured specimen from the mounting ring, the excess parts are trimmed off one face using a diamond wire saw and then manually ground with grit papers at 250 RPM. The grit size and levels and the polishing time are listed in Table 3-4. A final

cleaning stage is carried out using liquid-soap to remove dust from polishing. After the sample preparation, the cross-section of the sample is imaged at 100x magnification with VHX Keyence 6000 at Surface Science Western.

Table 3-4: Grit size and polishing time

Grit size	Median grit size (μm)	Polishing time (s)
P180	78	30
P320	46.2	30
P600	25.8	30
P1200	15.3	30
P2400	8.4	180
P4000	5	180

3.4 Conclusion

This chapter covers the material systems investigated in this work (fabric and resin systems) and explains the manufacturing techniques employed in this project (wet compression molding). The procedures for conducting mechanical testing, sample locations on the plaque tool and preparation, and suitable experimental techniques following ASTM standards are also discussed in this chapter. In the last part, the optical microscopy technique for void formation, including sample preparation and investigation with a microscope, was discovered.

Chapter 4

4 Investigation of the effect of process parameters on the mechanical property of CFRP parts

4.1 Overview

A statistical analysis method is employed to investigate the effect of operating conditions on the quality of CFRP products (measured as Young's Modulus of flexural test). Minitab® statistical software version 19.2020.1 (Minitab, 2019) is used to perform a variety of statistical analyses on the experimental data at a 95% confidence level, including a pareto chart, main effect plot, analysis of variance (ANOVA), and normal probability plot of residuals (Montgomery et al., 2010). The effects of the operating factors (independent variables) on the Young's Modulus of the flexural test (response variable) are analyzed using the analysis of variance (ANOVA), and the significance of the main effect factor order on the response is investigated using pareto charts. Validation of model adequacy is achieved through a comparison of experimental and predicted data using a normal probability plot of residuals.

4.2 Effect of sample thickness

As mentioned in Chapter 3.2.3, the thickness varies per specimen and has been presented using Whisker and Box plot in Figure 4-1. The reason for varying thickness per sampling area is not apparent, so the effect of thickness was not considered in our statistical analysis.

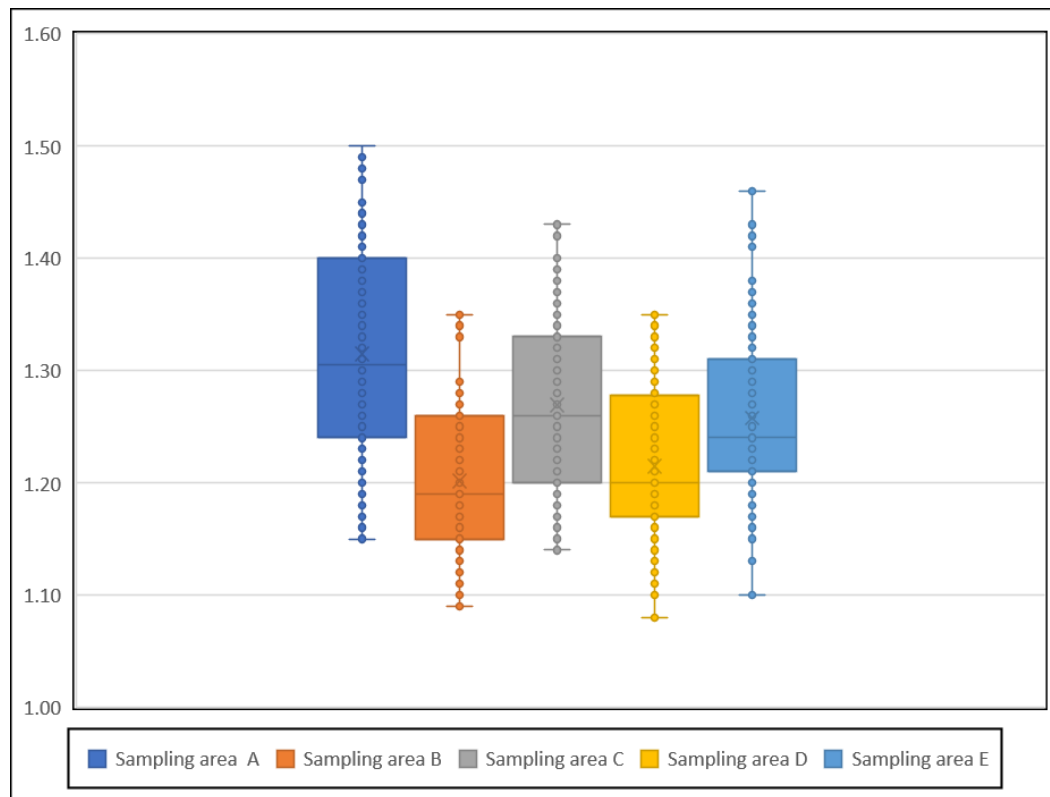


Figure 4-1: Whisker and Box plot of sample thickness segregated by sampling area

4.3 Statistical Modeling Technique

4.3.1 Design of Experiment (DOE) - Factorial Design

Factorial design is a well-known practical method that helps determine which apparent variables are the most important and how they affect the process (Shih et al., 1997). It is typically conducted when the effect of multiple factors on a single measurable response is of interest, and in such experiments, no factor is regarded as statistically insignificant. (Milton, J. S. et al., 1995). Factorial designs are more efficient than one-factor-at-a-time experiments. Finally, factorial designs allow for analysis at different levels for each factor (Montgomery, 2001). The type of statistical analysis employed to analyze factorial design results is analysis of variance (ANOVA).

The operating condition parameters (i.e., mold temperature, resin temperature, resin set time, gap closure speed, mold curing time) were used as input factors. The Young's Modulus of the flexural test, measured at the different sampling areas of the final CFRP parts, is selected as the response variable to be used in Minitab® statistical software. Sampling areas including A, B, C, D, and E were also utilized as categorical input factors.

As discussed in Chapter 3, mechanical testing is conducted on 28 acceptable plaques, and each plaque had five sampling areas, and from each sampling area, five specimens are taken. However, it should be noted that among all acceptable plaques, one plaque (number 29) had missing video recordings (required for analysis in Chapter 5), and to be consistent for analysis in both chapters 4 and 5, the data points of this plaque are removed from the analysis. Therefore, the total number of data points used in the analyses is 675 ($27 \times 5 \times 5$).

4.4 Statistical Analysis results and discussions

4.4.1 ANOVA results

P-Values at a 95% confidence level ($\alpha = 0.05$) for each factor from the ANOVA table are utilized to establish which factors are statistically significant. This means that if P-Values are found to be less than 0.05, those factors are significant.

Table 4-1 shows the Minitab® output for the ANOVA analysis of the results. As shown in Table 4-1, factors including resin temperature, mold temperature, resin set time, and sampling areas are found to have a significant effect in the model with the P-Values of 0.012, 0.000, 0.035, and 0.000 respectively. On the other hand, the effect of gap closure speed and mold curing time are found to be insignificant at 95% confidence level with P-Values of 0.78, and 0.68 respectively. Only the main effect (1st order term) of these factors is analyzed because statistical analysis of interactions between factors requires a significantly larger amount of data (i.e., more trials).

Definitions for the Analysis of Variance table are provided below (Minitab, 2019):

DF: The amount of information in data is shown by the total degrees of freedom (DF). This information is used in the analysis to estimate the values of population parameters that are not known. The number of observations in the sample determines the total DF. The DF of a term shows how much information that term uses. Increasing the sample size provides more information about the population, which increases the total DF.

Seq SS: Sequential sums of squares serve as metrics of variance for different model components. The sequential sums of squares are dependent on the order in which the terms are entered into the model, as contrasted to the adjusted sums of squares. Minitab divides the sequential sums of squares into various components that describe the variation resulting from various sources in the Analysis of Variance table.

Contribution: Contribution shows the percentage of the total sequential sums of squares that each source in the Analysis of Variance table contributes to Seq SS.

Adj SS: Adjusted sums of squares show how different parts of the model vary from one another. The adjusted sums of squares are the same no matter what order the predictors are in the model. In the Analysis of Variance table, Minitab divides the sums of squares into different parts that describe the differences that come from different sources.

Adj MS: Adjusted mean squares measure how much variation a term or model explains, assuming that all other terms are in the model, no matter what order they were entered. The adjusted mean squares are different from the adjusted sums of squares because they consider the degrees of freedom.

F-Value: A term's association with the response can be tested using the F-value. For each of the independent variables, an F-static is calculated using the F-distribution.

P-value: The P-value is a measure of how much evidence there is against the null hypothesis. Less likely outcomes make the evidence against the null hypothesis stronger.

Table 4-1: Analysis of Variance Results for Response

Source	DF	Seq SS	Contribution	Adj SS	Adj MS	F-Value	P-Value
Model	11	993553283	29.28%	993553283	90323026	24.96	0.000
Linear	11	993553283	29.28%	993553283	90323026	24.96	0.000
Resin temperature	2	161854274	4.77%	32071964	16035982	4.43	0.012
Mold temperature	1	413456189	12.19%	92489803	92489803	25.56	0.000
Resin set time	1	17587304	0.52%	16210887	16210887	4.48	0.035
Mold curing time	1	715332	0.02%	617065	617065	0.17	0.68
Gap closure speed	2	1994505	0.06%	1991744	995872	0.28	0.76
Sampling area	4	397945679	11.73%	397945679	99486420	27.49	0.000
Error	663	2399178422	70.72%	2399178422	3618670		
Lack-of-Fit	49	375799653	11.08%	375799653	7669381	2.33	0.000
Pure Error	614	2023378769	59.64%	2023378769	3295405		
Total	674	3392731706	100.00%				

Minitab® also provides the histogram of residuals to show the distribution of the residuals for all observations data. The residual for each observation represents the difference between the expected and actual values of y (the dependent variable). The histogram of the residuals is used to determine whether the data are skewed or include outliers and can be used to verify the assumption that the residuals are normally distributed and hence the correctness of the model. A long tail on one side may indicate a skewed distribution. If one or two bars are far from the others, those points may be outliers. If a histogram plot of residuals is roughly bell-shaped then the normality assumption can be accepted (Montgomery, 2001).

As shown in Figure 4-2, the histogram plot is skewed to one side. From this preliminary observation it became evident that the assumption of normality distribution is not satisfied due to skewed distribution and outliers. This is further discussed and investigated in the following section.

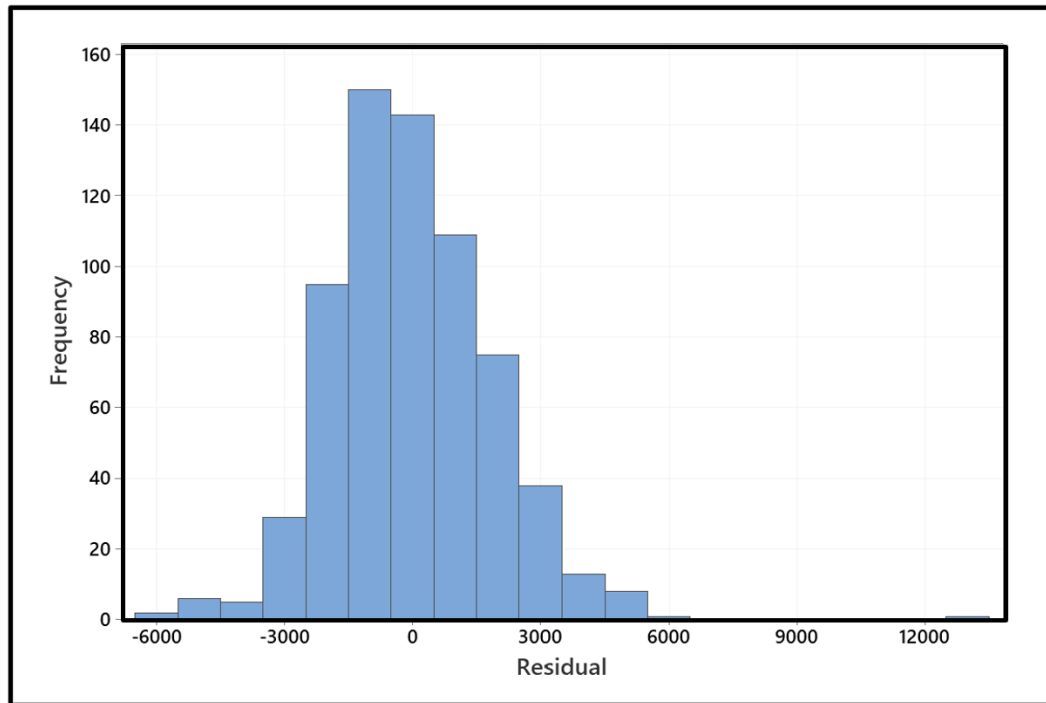


Figure 4-2: Histogram of residuals

4.4.2 Normality test

A normality test is commonly used to determine whether the data used in the study has a normal distribution. Many statistical procedures, such as correlation, regression, t-tests, and ANOVA, are based on normal data distribution (Ghasemi, A. et al., 2012).

One of the assumptions of ANOVA test is that the data should be normally distributed. The normality test generates a normal probability plot and conducts a hypothesis test to assess whether the observations follow a normal distribution or not. If the P-Value of the test is greater than the set significance level of $\alpha = 0.05$, it fails to reject the null hypothesis (that the data follow a normal distribution). Thus, this may require a transformation of the data if the error term is not normally distributed.

As noted in the previous section, to accept or reject the method employed in this statistical approach, the normality test of residuals is carried out using MINITAB®. The test generates a normal probability plot (or Q-Q plot) and conducts a hypothesis test to assess whether the observations follow a normal distribution or not. Figure 4-3 indicates the results of the normality test based on Anderson-Darling method (Öztuna, D. et al., 2006). Looking at the Q-Q plot revealed that the residual data are not in a straight line and the plot includes two outliers. In addition to that, in this test, the P-Value was less than 0.005 (less than significance level of $\alpha = 0.05$), based on which it can be concluded that the residuals do not follow a normal distribution. Hence, the data needs to be transformed and reanalyzed.

As mentioned, two outlier data points are visually observable in the Q-Q plot (Figure 4-3). The two outlier data points belong to 1- plaque number 7, sampling area A, specimen/coupon number 3, with the response value (Young's Modulus) of 19000 MPa, and 2- plaque number 3, sampling area D, specimen 1, with the response value of 26000 MPa. The very high Young's Modulus of those specimen could be due to testing/instrument errors as the other four coupons (that are obtained from the same plaque and section as the coupon with high Response value) show a much lower response average with small deviations from that mean. However, one should note that five specimens are taken from each sampling area in each plaque, and it is not possible to rerun the test because of the breakage of specimen during testing. To check whether the non-normality of data is because of those outliers or not, they are removed from the data point, then the analysis is rerun, and the residual values are checked with the normality test. Figure 4-4 shows a new normal probability plot without the two outliers. It is observable that the data is still not normal, and the P-Value is less than 0.005; thus, they need to be normalized.

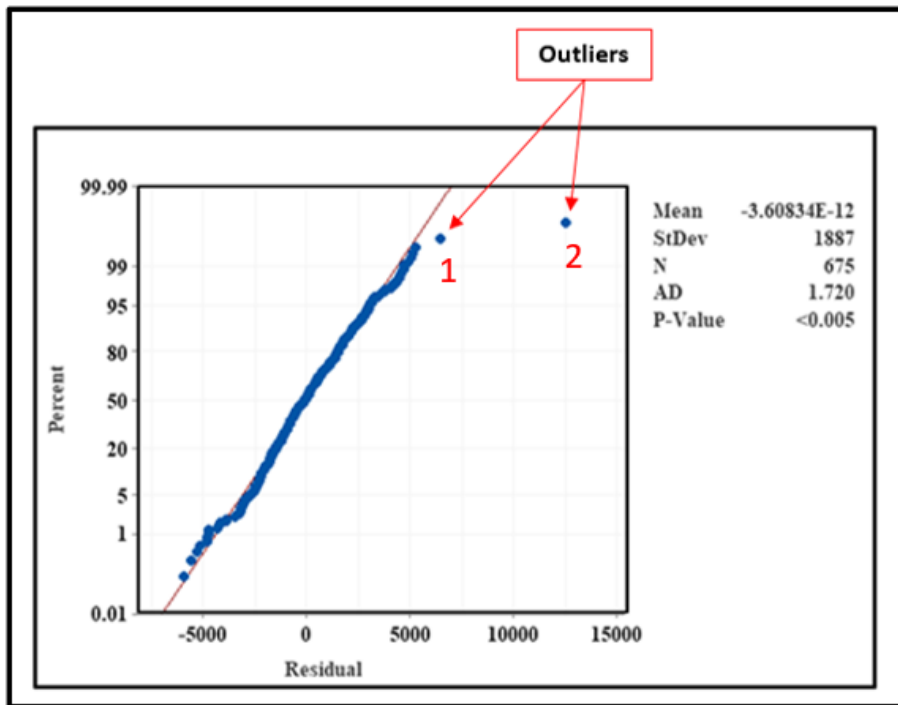


Figure 4-3: Normal probability plot (Q-Q plot) of residuals- the outliers shown in the above graph belong to 1- plaque number 3 and 2- plaque number 7

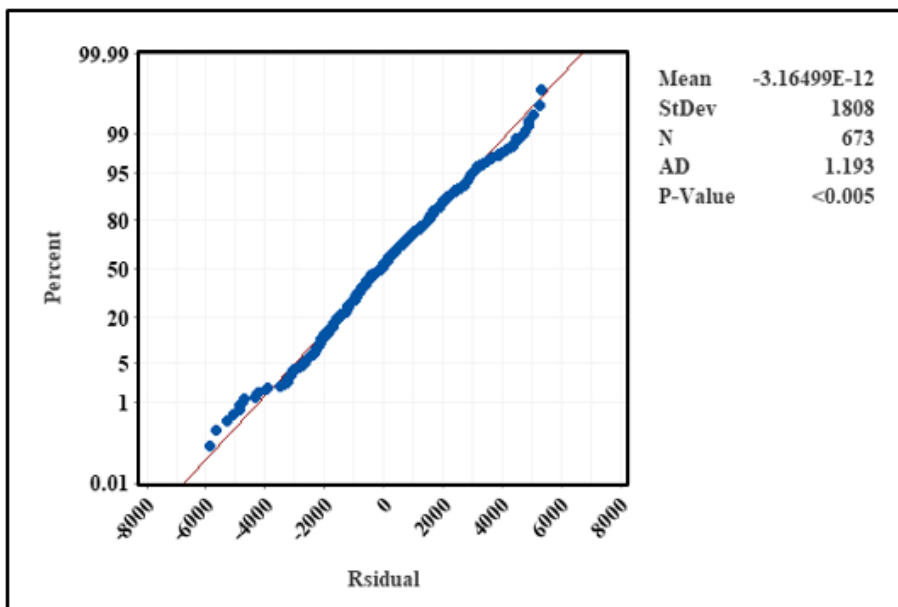


Figure 4-4: Normal probability plot (Q-Q plot) of residuals after removing outliers

4.4.3 Box-Cox transformation

When the model does not pass the normality test, data transformation is typically used to make data appear to closely match the assumptions of a statistical inference model or to improve the interpretability or appearance of graphs. One of the corrective operations that could help in the normalization of data is the Box-Cox power transformation that was developed by statisticians George Box and David Cox (Box et al., 1964). This procedure is used to identify an appropriate exponent (λ) to use to transform data into a normal shape.

The formula of the Box Cox transformation is:

$$\left\{ \begin{array}{l} y = \frac{x^{\lambda}-1}{\lambda} \text{ where } \lambda \neq 0 \\ y = \ln(x) \text{ where } \lambda = 0 \end{array} \right.$$

Where:

y is the transformation result

X is the variable under transformation

λ is the transformation parameter

The Lambda value (λ) specifies the power to which all data should be raised. The Box-Cox power transformation searches from Lambda = -5 to Lambda = +5 until the best value is obtained.

MINITAB® offers Box-Cox transformation with an optimal λ that minimizes the model SSE (sum of squared error). This transformation is employed on the response data (Young's Modulus). In this case, the minimum value is 0.35, and the transformation's rounded value is 0.5, which means the square root of the response will be used as the new response value.

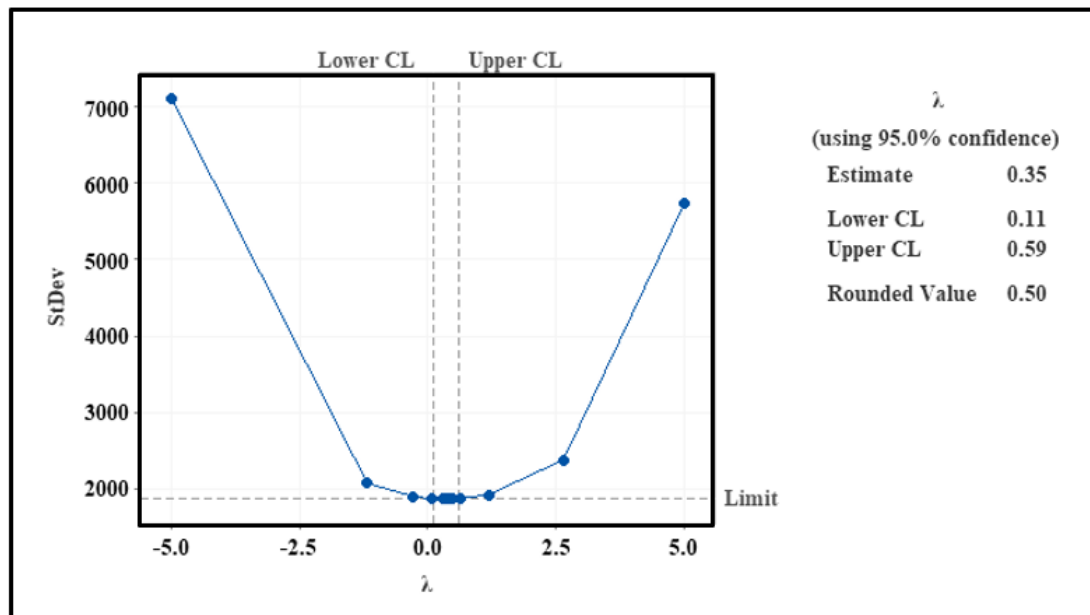


Figure 4-5: Box-Cox transformation data with the Rounded Value (λ) of 0.5

4.4.4 ANOVA results of the transformed data

After the data transformation, ANOVA is performed on the transformed data (Section 4.4.1) and the results are summarized in Table 4-2. Resin temperature, mold temperature, resin set time, and sampling area are all determined to be significant with P-Values of 0.012, 0.001, 0.018, and 0.000, respectively. In contrast, at the 95% confidence level, the P-Values for gap closure speed and mold curing time are 0.78 and 0.68, indicating that these factors have no significant influence on the model. It should be noted that the same

conclusion is reached using the data before the Box-Cox transformation. This indicates that the significant factors are still the same, but the P-Values are different.

Table 4-2: Analysis of Variance results after data transformation of Response

Source	DF	Seq SS	Contribution	Adj SS	Adj MS	F-Value	P-Value
Model	11	20535.4	29.94%	20535.4	1866.85	25.76	0.000
Linear	11	20535.4	29.94%	20535.4	1866.85	25.76	0.000
Resin temperature	2	3267.5	4.76%	651.5	325.73	4.49	0.012
Mold temperature	1	8397.9	12.24%	1752.8	1752.75	24.18	0.001
Resin set time	1	465.1	0.68%	406.7	406.74	5.61	0.018
Mold curing time	1	8.7	0.01%	7.5	7.53	0.1	0.747
Gap closure speed	2	46.3	0.07%	46.2	23.09	0.32	0.727
Sampling area	4	8349.9	12.17%	8349.9	2087.48	28.8	0.000
Error	663	48050.4	70.06%	48050.4	72.47		
Lack-of-Fit	49	8400.6	12.25%	8400.6	171.44	2.65	0
Pure Error	614	39649.8	57.81%	39649.8	64.58		
Total	674	68585.8	100.00%				

4.4.5 Pareto chart

The pareto chart is used to estimate the extent and significance of the effects and displays the absolute values of the standardized impacts from largest to smallest. A reference line is also included in the graph to illustrate which effects are statistically significant. The significance level (denoted by α) determines the reference line for statistical significance.

As shown in Figure 4-5, horizontal bars that represent four factors (sampling area, mold temperature, resin temperature, and resin set time) are all crossing the reference line meaning these factors are statistically significant at the 0.05 level with the current model terms. On the other hand, two factors (mold curing time and gap closure speed respectively) are insignificant for the investigated response since they are below the reference line. As

indicated from the pareto chart result in Figure 4-6, factors including sampling area and mold temperature are the most influential factors. This supports the findings in Section 4.4.4

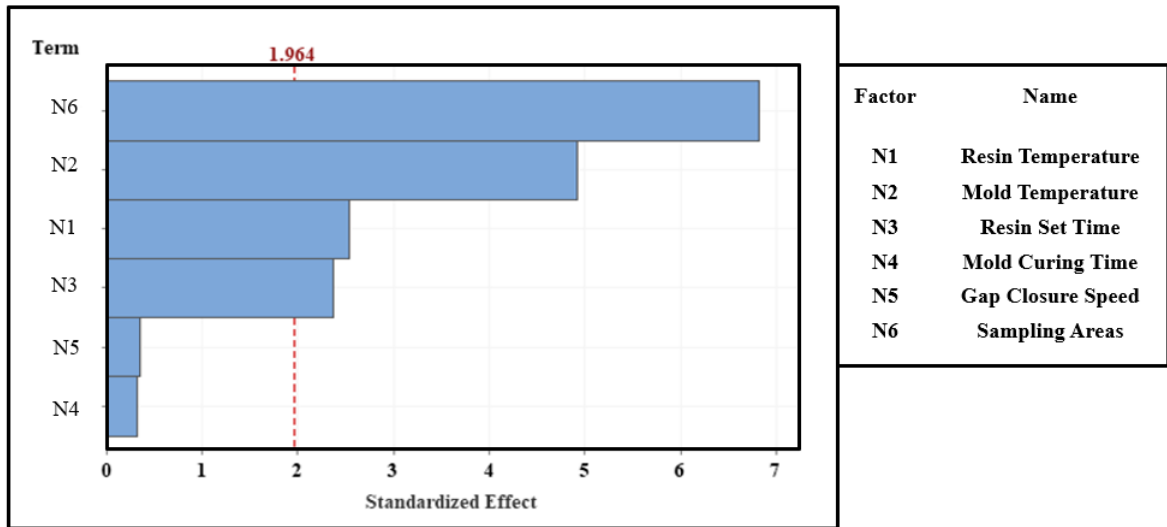


Figure 4-6: Pareto chart of standardized effects ($\alpha=0.05$) for Response

4.4.6 Main effect plot

The main effect plot is used to examine differences between level means for one or more factors. The main objective of the plot is to visualize changes in the means to determine the most influential factors. The mean response for each factor level within a categorical variable are plotted and are connected via a line. The statistical significance of a factor is directly related to the slope of the main effect line, i.e., the steeper the slope of the line, the greater the magnitude of the main effect. A reference line is also drawn at the overall (grand) mean of response (Flexural Modulus).

Among all the main effect lines presented in Figure 4-7, the greatest slope is observed for the factors sampling area, mold temperature, resin temperature, and resin set time. Hence,

they are the most influential factors among the selected variables, which is also supported by the results of the pareto chart (Figure 4-6) and the ANOVA (Table 4-2). The least significant main effects are the mold curing time and gap closure speed factors.

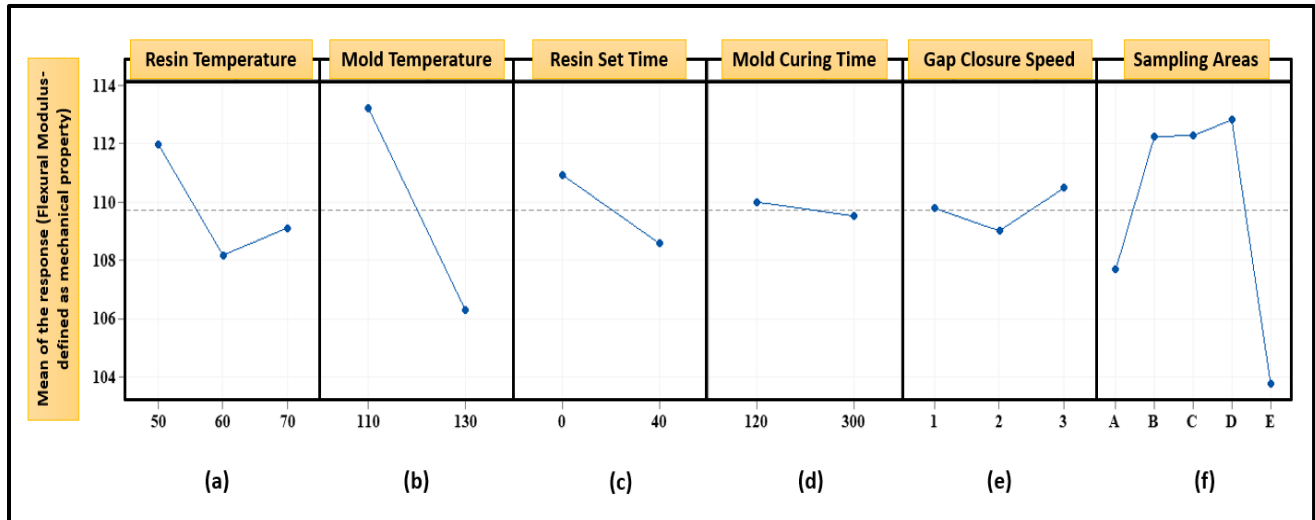


Figure 4-7: Main effect plot for response

It can be seen from Figure 4-7 (a) that the mean of response is 112 MPa with a resin temperature of 50 °C; however, the mean of Flexural Modulus decreases with increasing the resin temperature to 60 °C and reaches around 108 MPa. At 70 °C resin temperature, the mean of response increases and comes to 109 MPa. It can be concluded that the highest mechanical property is obtained at 50 °C resin temperature. Among the three variations of resin temperatures, the highest response value was obtained at the lowest temperature. The increase (in response value) from 60 to 70 °C is opposite to the movement from 50 to 60 °C. More tests at a temperature less than 50 °C and above 70 °C are required to understand where the maximum response can be obtained.

According to Figure 4-7 (b), the mean of response exhibits a decreasing trend from 110 °C to 130 °C mold temperature; this means that the parts produced under the condition of 110 °C mold temperature have around 10% higher values than those of the parts produced using 130 °C mold temperature.

According to Figure 4-7 (c), the mean of response changes significantly with increasing resin set time. As reported in this Figure, there is a decrease of 2.25% in the mechanical property when the resin set time goes from 0 to 40 sec. In other words, the highest mechanical property is achieved with the 0 s resin set time.

As shown in Figure 4-7 (f), the mean of response for sampling areas B, C, and D yields around 113 MPa; however, this value for sampling areas A and E is around 108 and 103 MPa, respectively. In other words, sampling areas B, C, and D have the best mechanical property. On the other hand, sampling Areas A and E revealed the worst ones.

In summary, from the main factor charts, higher mechanical property (the value of response) of the final parts is achieved at the lower resin temperature, mold temperature, and resin set time, with values of 50 °C, 110 °C , 0 s, respectively. The results for the sampling areas revealed that a higher mechanical property is achieved at sampling areas B, C, and D, compared to sampling areas A and E, that yield a lower mechanical property.

Lastly, looking at Figure 4-7, it is obvious that the trend for the factors with more than two levels, including resin temperature, gap closure speed, and sampling area, is non-monotonic meaning that they do not show either decreasing (non-increasing) or an increasing (non-decreasing) pattern.

4.5 Optical Microscope (OM) results and discussion

As discussed in the previous sections, three process parameters, including resin temperature, mold temperature, and resin set time, affected the mechanical property of the parts. In addition, it was seen in the main effect plot (Figure 4-7) that by increasing the level of the process factors, the mechanical property of the parts degraded. Voids are always potential failure spots and produce a discontinuity in the material characteristics of CFRP, lowering its mechanical performance. Air entrapment in the resin system during formulation, moisture absorption in storage or processing, and improper tow placement in molding are all potential causes of void formation (Mehdikhani, M. et al., 2019; Svensson, N. et al., 1998). Several research studies investigated the effects of voids on the mechanical property of CFRP (Xueshu et al., 2016; de Almeida, S. F. M., et al., 1994; Olivier et al., 1995; Suhot, M. A. et al., 2014; Liu, L. et al., 2005; Ghiorse, S. R., 1993).

In this project, the existence of voids is investigated with the use of optical microscopy (OM). The OM test is conducted on two plaques produced at different operating conditions, plaque numbers 2 and 9 (see Table 4-3 for more details). Plaque number 2 is selected because it is manufactured at the lowest level of the significant process factors and showed the highest mechanical property. Plaque number 9 is chosen because it is produced using the highest level of the significant process factors and exhibited the lowest mechanical property. OM is used to qualitatively assess if voids exist for the two plaques in the sampling area. This study does not determine how and why process parameters contribute to the formation of voids.

Also, it should be noted that OM analysis is not performed on all specimens belonging to a particular plaque identified by its plaque number; only two specimens from two different sampling areas, B and E (the chosen specimens shown in Figure 3-15: Validation specimen locations for OM analysis) are taken from each plaque. The reason for selecting sampling areas B and E was that they are located symmetrically in the geometry with a higher mechanical property in sampling area B and a lower value in sampling area E. (see Figure

4-7 f). The OM examination results are shown in Figures 4-7 to 4-10 for plaque numbers 2 and 9.

Table 4-3: Sample information for OM

Plaque number	Sampling area	Operating condition			Young's Modulus for coupon 4	Average Young's Modulus
		Mold temperature	Resin temperature	Resin set time		
2	B	110	50	0	12886	13189
2	E	110	50	0	11331	10829
9	B	130	70	40	11871	11030
9	E	130	70	40	9627	9406

Intra-tow voids refer to spaces that become trapped inside of fiber tows. Void spaces created between fiber tows are known as inter-tow voids. Figure 4-8 shows some examples of such voids within composites manufactured by the WCM process. Nonetheless, it is considered that the main source of void formation in WCM is air entrapped by the non-uniform flow of the resin front (Leclerc, J. S. et al., 2008).

Injection of resin into a dry preform results in two micro flows: a viscous flow through the spaces between the fiber tows or preform layers, and a capillary flow consisting of local penetration of the resin into fiber tows. During mould filling, these two micro flows occur simultaneously and compete with one another, leading to void creation. When the viscous flow is faster, voids will appear inside the fibre tows. Air is trapped between fiber bundles or preform layers when capillary flow directs the impregnation. Traditional methods for reducing void occurrence focus on finding the judicious selections between preform architectural permeability and resin viscosity to optimize resin flow (Hamidi et al., 2017).

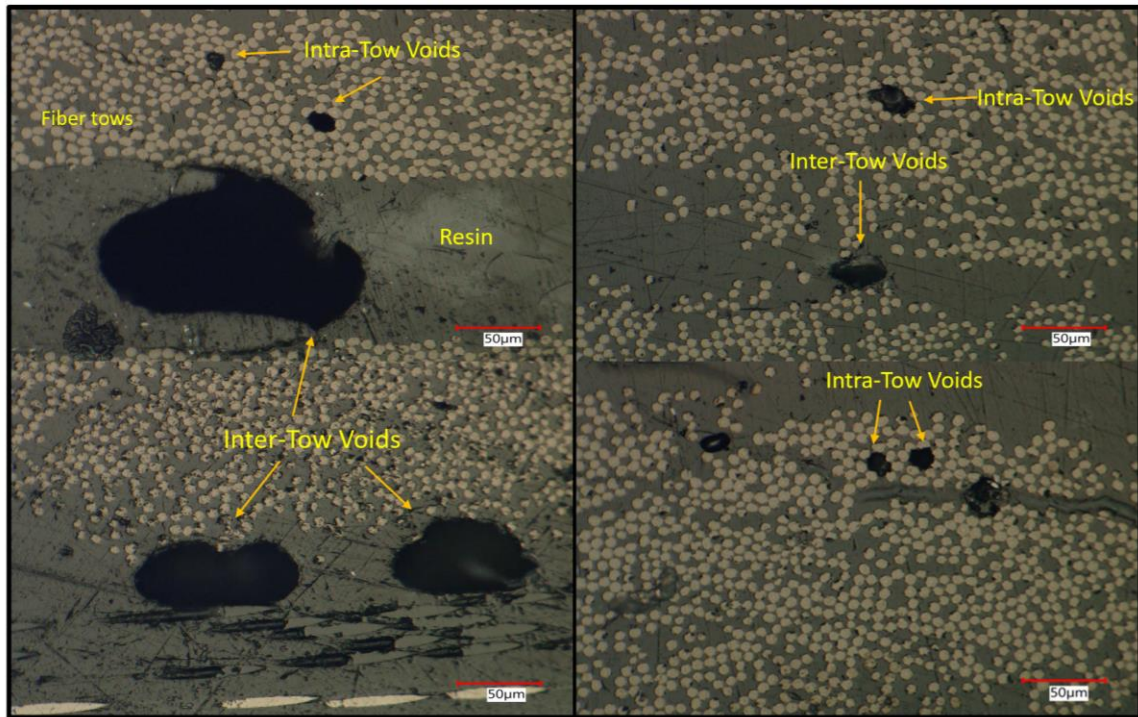


Figure 4-8: Microscopic images of different voids observed from carbon/epoxy composites fabricated using WCM

From the OM results in Figures 4-9 and 4-10 with Figures 4-11 and 4-12, fewer voids can be seen in plaque number 2 in comparison with plaque number 9 in both sampling areas B and E. Thus, it could be concluded that the lower mechanical property of the parts is due to the higher void contents. From these results voids have a negative effect on the flexural modulus as expected. It is also evident that the number of voids in sampling area E for the two plaques (9 and 2) is much more than in sampling area B, which is a reason for the lower mechanical property in sampling area E compared to sampling area B. However, it is not clear (and not expected) why the mechanical property (or void formation) is not symmetrical with respect to the part's geometry. This asymmetry is discussed further in Chapter 5. It can also observe more voids between the tows (Inter-Tow voids) than inside the tows (Intra-Tow voids).

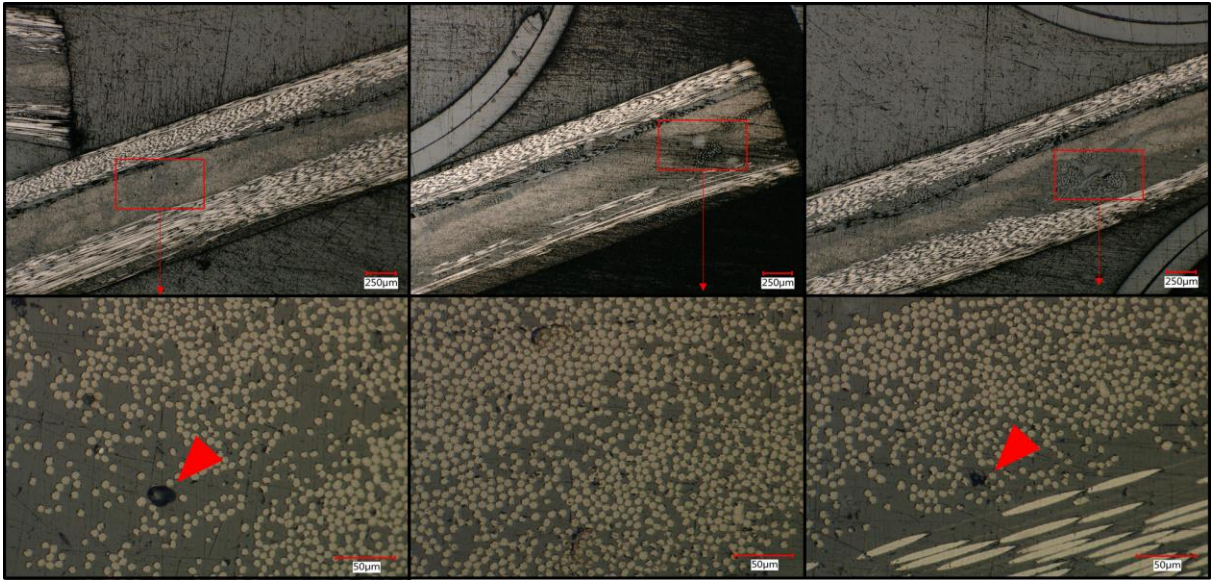


Figure 4-9: Optical micrographs of a specimen taken from plaque number 2 (resin temperature of 50 °C, mold temperature of 110 °C, and resin set time of 0 sec) and sampling area B - voids are noted by red arrows

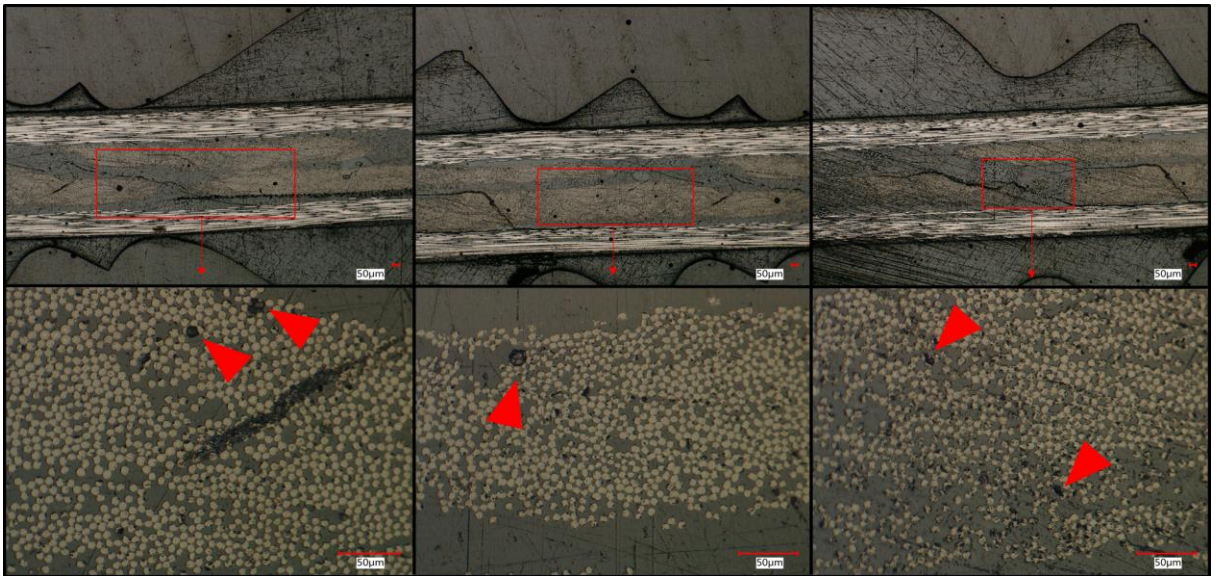


Figure 4-10: Optical micrographs of a specimen taken from plaque number 2 (resin temperature of 50 °C, mold temperature of 110 °C, and resin set time of 0 sec), and sampling area E - voids are noted by red arrows

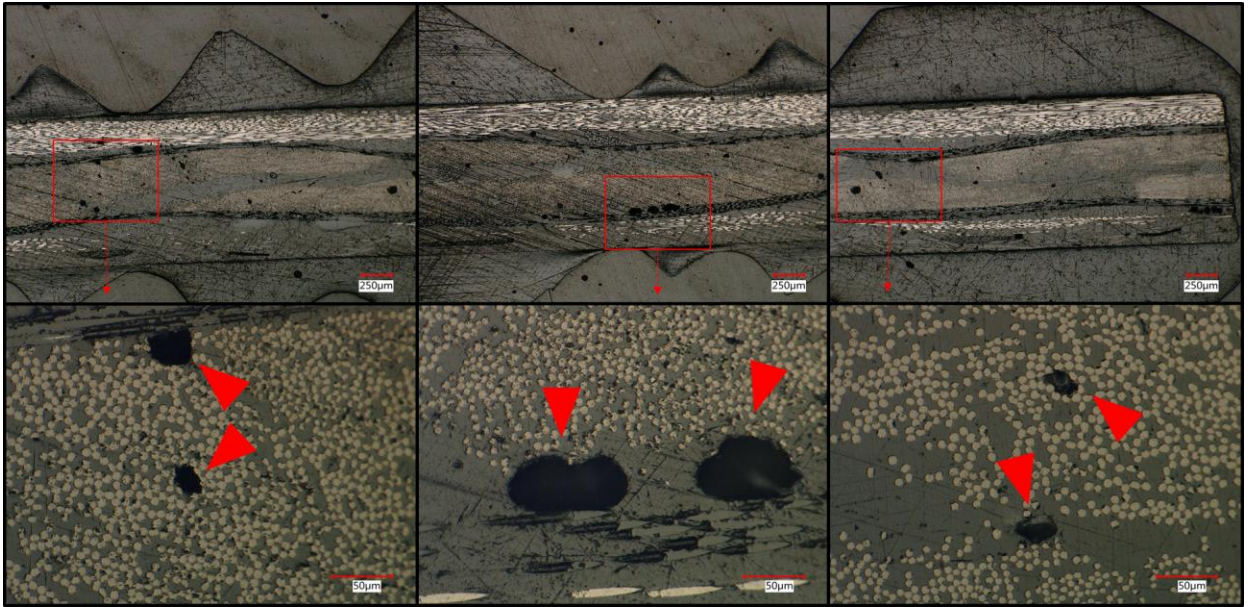


Figure 4-11: Optical micrographs of a specimen taken from plaque number 9 (resin temperature of 70 °C, mold temperature of 130 °C, and resin ret time of 40 sec), and sampling area B - voids are noted by red arrows

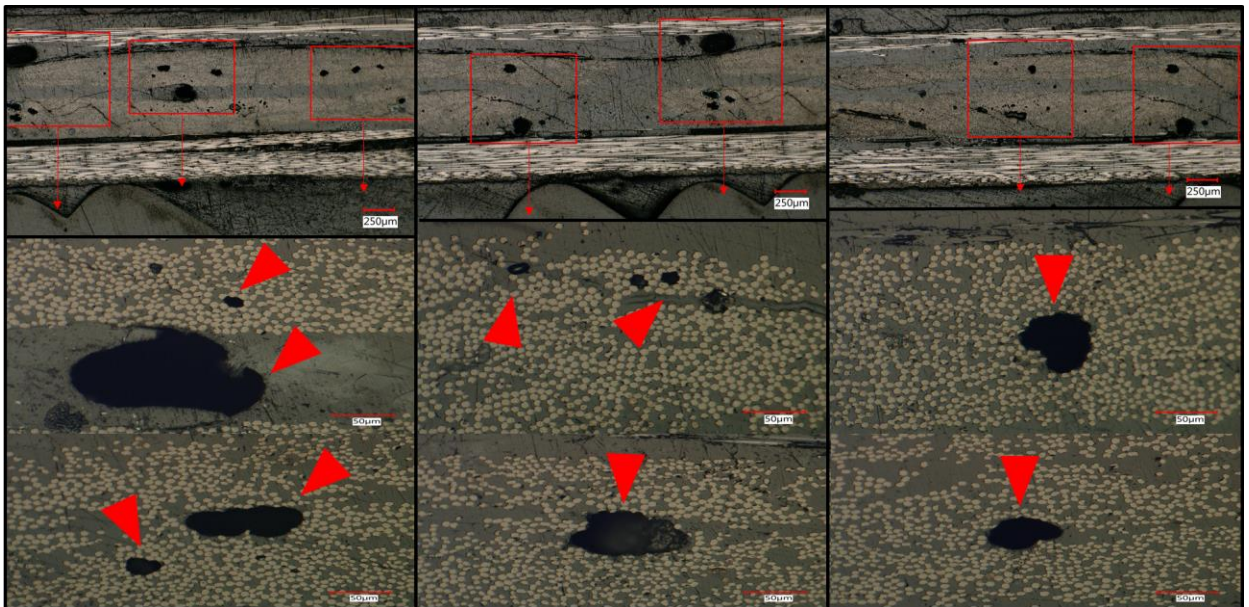


Figure 4-12: Optical micrographs of a specimen taken from plaque number 9 (resin temperature of 70 °C, mold temperature of 130 °C, and resin ret time of 40 sec), and sampling area E - voids are noted by red arrows

It is known that during manufacturing, the processing parameters simultaneously impact voids distribution, location, shape, and size. Each of these parameters has different influences on the mechanical property (flexural property) of CFRP products. Mold temperature and resin temperature contribute to determine the viscosity of the resin, Table 4-4 provides the resin viscosities (Hexion, 2015), and thus drives the flow velocity of the resin in the preform. This velocity is critical in the mechanism that causes voids to occur during the filling of preforms. The flow visualization studies performed by Molnar et al. (1989) and Patel et al. (1993) showed that at high flow rates, the micro-flow in the fiber tows is provided by the macro-flow between the fiber tows; however, at low flow rates, the findings are opposite. When the resin meets a fiber tow, it tends to flow around it due to the viscous forces, which leads the flow front to dominate over the capillary action into the fiber tows. The entrapment of air in the fiber tows (voids) is demonstrated to be caused by the early impregnation of the sites between the fiber tows compared to the sites within the tows (Damani, S. G. et al., 1990).

At low flow rates, the micro-flow front within the tows is shown to lead the macro-flow front around the tows due to capillary action in the fiber tows. This flow condition is known to prevent the creation of micro-voids. When a low resin flow rate is combined with a mold temperature higher than room temperature, the resulting lowered resin viscosity (before significant reaction) has been observed to improve micro-flow, favoring fiber wetting, and reducing total void content (Patel, N. et al. , 1993). This mechanism of void formation can explain the lower mechanical property observed in this study as the mold temperature increased. An increase in the resin temperature presents a similar effect to increased mold temperatures in that decreased resin viscosity may promote increased void content, as proposed by Patel et al. (1993).

Table 4-4: Viscosity of the resin system at different temperatures (Hexion, 2015)

Temperature (°C)	Value (mPas)
80	41 ± 10
100	19 ± 10
110	15 ± 5
120	11 ± 5

4.6 Conclusion

In this chapter, a statistical analysis method is employed to investigate the effect of operating conditions on the quality of CFRP products (measured response is the Young's Modulus of the flexural test). Statistical results revealed that mold temperature, resin temperature, and resin set time significantly influence the mechanical property of the carbon fiber/ epoxy parts. However, gap closure speed and mold curing time did not significantly affect the mechanical property of the plaques. At the lowest level of mold temperature (110 °C), resin temperature (50 °C), and resin set time (0 s), the mechanical property of the parts was higher; however, at the higher level of the factors, the quality of the parts was lower. The poor quality of the plaques was checked using an optical microscope. Optical micrographs indicated that voids (air entrapment) were observed, which was the primary reason for the low part's performance.

Chapter 5

5 Effects of initial resin application area on the Mechanical Property of CFRP parts

5.1 Objective of this part of research

In the previous chapter, it was found that the mechanical property of the produced part is not symmetrical and varies over different sampling areas (i.e., sampling areas E and A have lower mechanical property than sampling areas B, C, and D). This is shown by statistical analysis of the results in Chapter 4, as shown in Figure 4-7 and Section 4.4.6. The asymmetry in the mechanical property might be due to the initial non-symmetrical resin distribution. Therefore, this part of the research investigates the correlation between the effects of initial resin application area on the local mechanical property (Flexural Modulus) of final CFRP parts.

5.2 Analysis technique

In this analysis technique, three key features of the initial resin application are identified and selected to enable us to perform a quantitative analysis. These features include total initial resin area coverage, targeted resin area, and area coverage per quadrant. Their definitions and the methods of measurements are as follows.

5.3 Area coverage

5.3.1 Initial wetted (resin) area definition

When the resin is applied to the surface of the preform, it covers an area called the initial wetted (resin) area. These areas may have different shapes and sizes depending on the resin application protocol.

5.3.2 Measurement of initial wetted (resin) area from captured videos

A high-resolution Canon EOS M200 DSLR camera (24 Megapixels) is utilized to capture the wetted resin application pattern across the fabric surface. To get a wide view of the resin impregnation pattern under the mixing head and to have the final shape of the resin distribution pattern before the preform goes inside the press, the camera is installed on the crane. The crane is fixed to the ceiling and did not move during the trials. The configuration of the camera is illustrated in Figures 5-1 and 5-2.

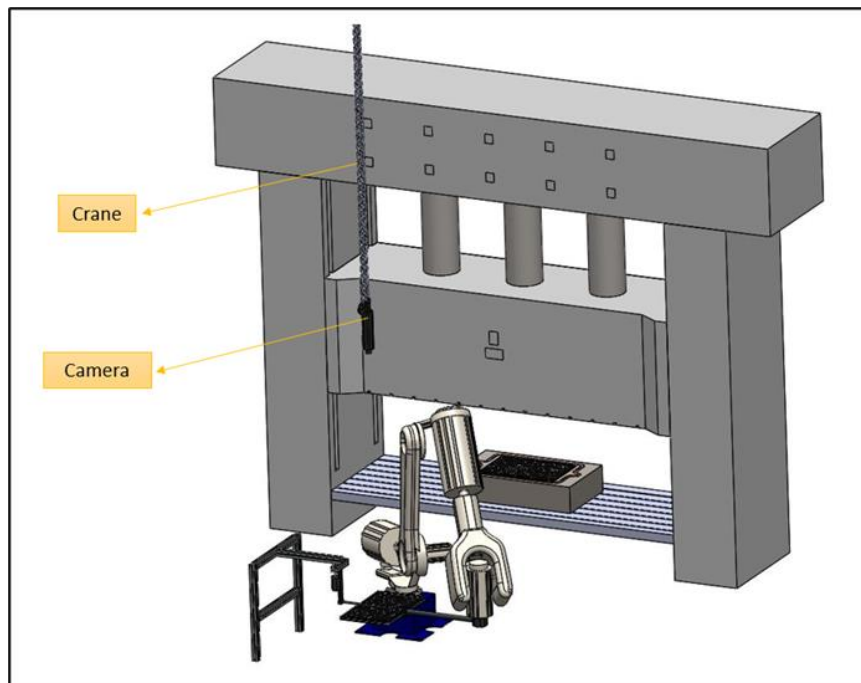


Figure 5-1: Camera configuration

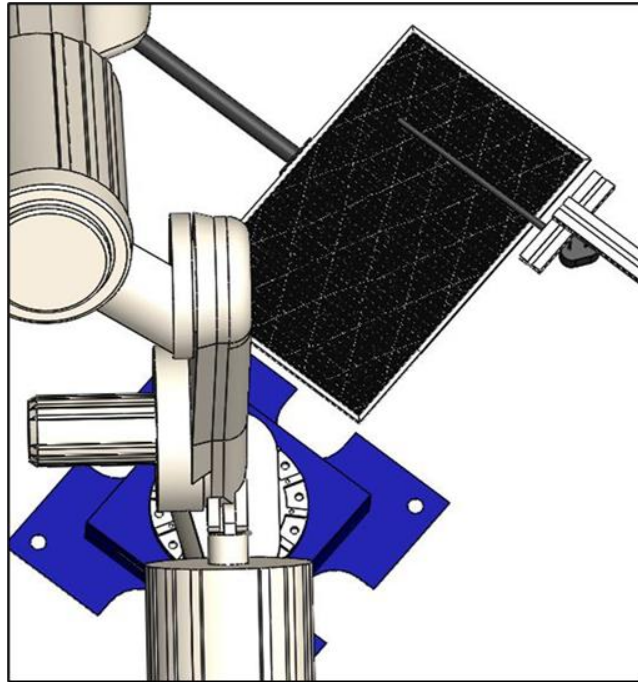


Figure 5-2: Camera view

The resin dispersion is captured by video in each trial. Afterwards, the videos are converted into individual frames to calculate the wetted area. Extracted frame positioning are made consistent from one trial to the next by using the center line on the top of the robot arm as a reference, as shown in Figure 5-3, at the time when the angle between the end of the arm tool and the metal frame is 42 degrees in a frame. AutoCAD software is utilized to determine the angle between the reference line and the metal frame.

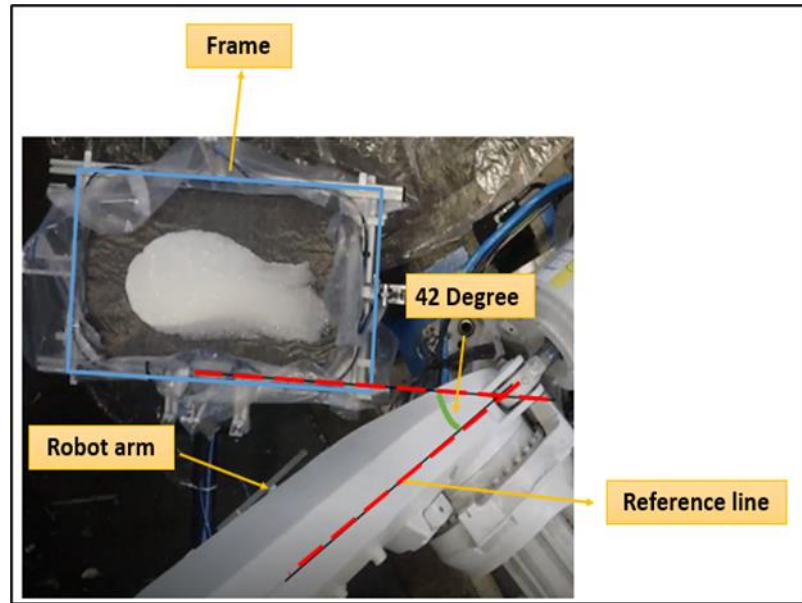


Figure 5-3: Image Extraction reference points

After frame extraction, the scalar vector graphics file is converted into a 2D vectorized image to determine the wetted versus non-wetted pixel areas. The thresholding method in the Background Subtraction algorithm in MATLAB is employed to generate a binary image. An example of original and binary images is shown in Figure 5-4. The area of the initial resin application is calculated based on the number of white pixels for each binarized image. Finally, the area in number of pixels were converted to initial wetted area (cm^2).

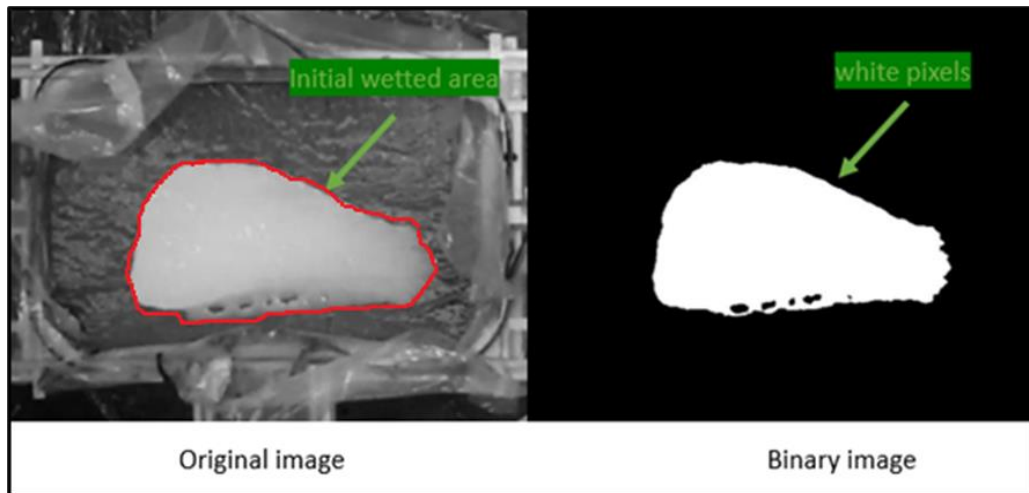


Figure 5-4: Thresholding method for initial area measurement

5.3.3 Targeted wetted (resin) area definition

The targeted wetted (resin) area is defined as the expected area on the preform on which resin is supposed to be applied (see Figure 5-5). This expectation is set through a program that controls the robot and positions it to pre-determined coordinates.

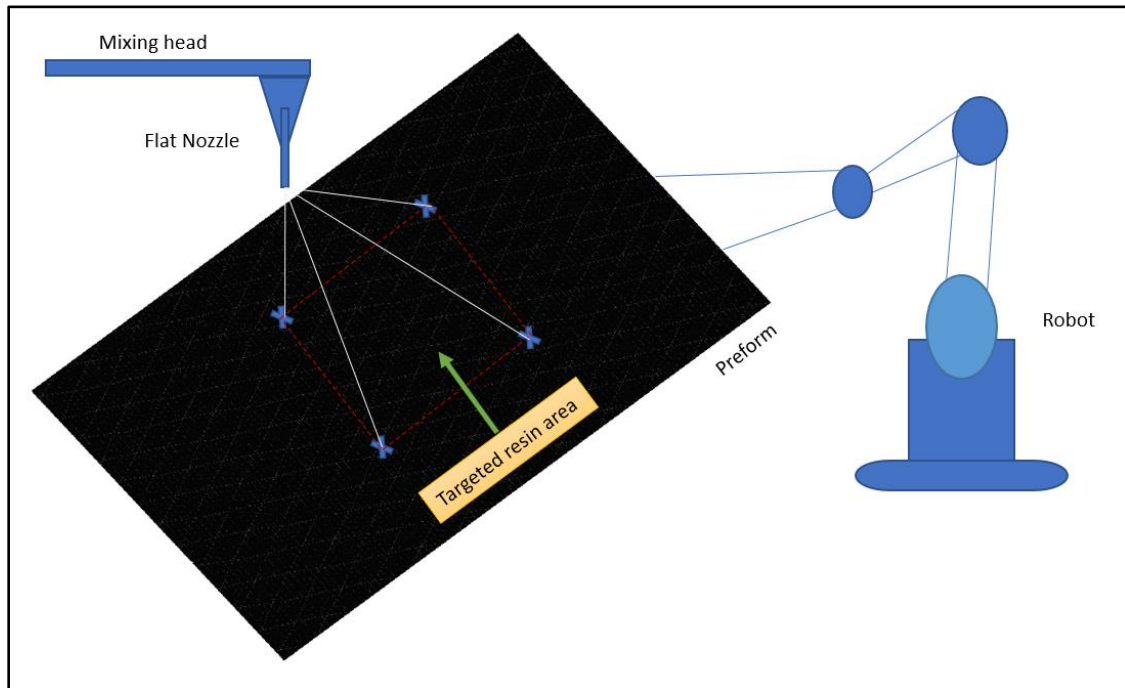


Figure 5-5: Schematic of the targeted resin area - the dimension of the flat nozzle is provided in Figure 3-4: Image of resin distribution nozzle (flat nozzle)

To compute the targeted resin area, the manufacturing system (robot) is running without any resin application to determine the coordinates of the distribution pattern. The resin spread perimeter of the (expected) wetted area on the preform is found based on the robot movement. Then the coordinates of the expected wetted area are measured relative to the center point of the preform. Lastly, based on the coordinates, the targeted resin area is calculated in cm^2 .

5.3.4 Observation of area coverage measurement data

The actual initial wetted area varied in size for each of the produced parts. However, there is a single targeted wetted area for all parts. The initial wetted (resin) for the parts has been plotted as a Whisker and Box plot in Figure 5-6, and the targeted resin area is shown via a horizontal red line. Ideally, all plaques should have equal initial wetted area and targeted resin area, but the results proved they are different. As shown in Figure 5-6, the initial resin area is higher than the targeted resin area in all parts, and this is due to fluid spread in different directions. The area measurements of both the initial and targeted wetted areas are provided in Appendices 11 and 12 respectively. It should be noted that a video recording for area measurement purposes was not available for plaque number 29, thus all presented data plotted in Whisker and Box plot are for 27 plaques instead of 28 parts.

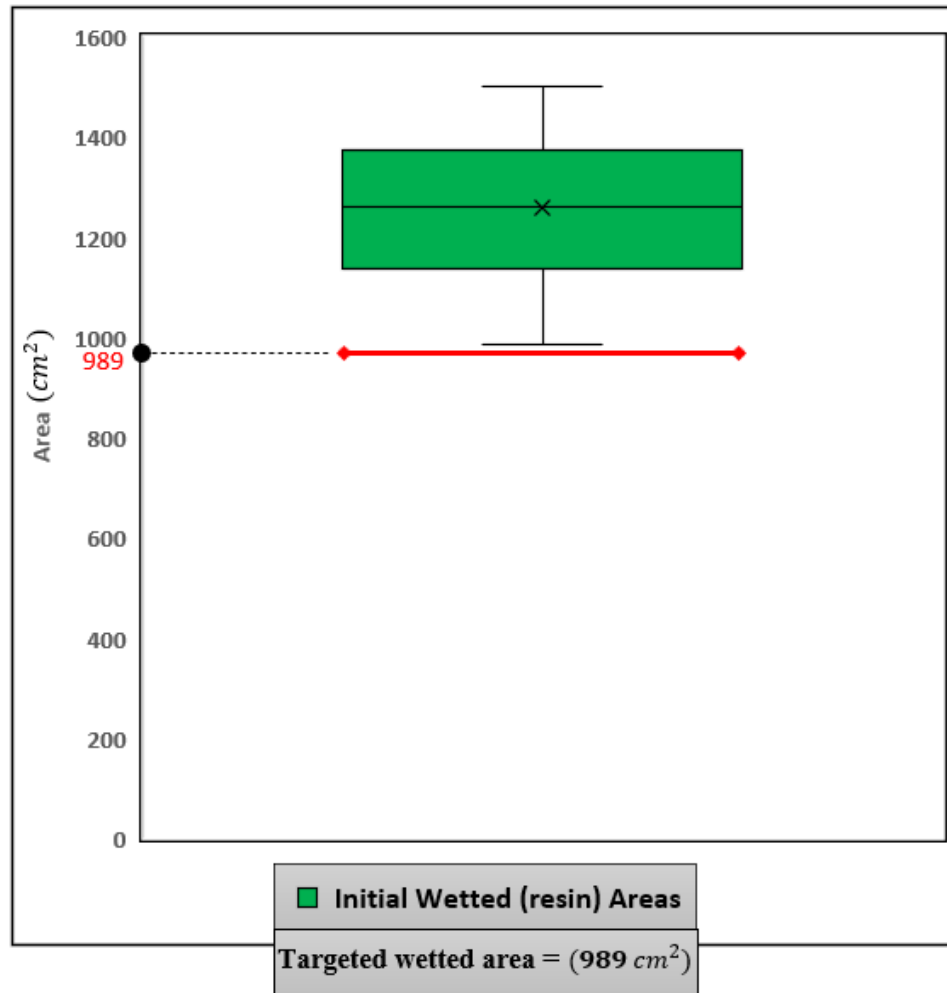


Figure 5-6: Whiskers and Box plot for total initial and targeted resin area

5.4 Area coverage per quadrant

5.4.1 Quadrant's definition

The preform is divided into four symmetrical quadrants (with respect to the centre of the frame) to investigate the initial resin application area in each quadrant.

5.4.2 Initial wetted (resin) area per quadrant measurement

The measurement of initial resin area quadrants is similar to the steps involved in the measurements of the total initial resin area, such as frame selection, background subtraction procedure and thresholding method to acquire binary images, as explained in Section 5.3.2. After obtaining binarized images, the center point of the frame is found, and the image is divided into four quadrants. The wetted area within each quadrant, the upper-left, lower-left, upper-right, and lower-right is calculated in pixels (white pixels) as shown in Figure 5-7. Finally, the area in number of pixels is converted to cm^2 .

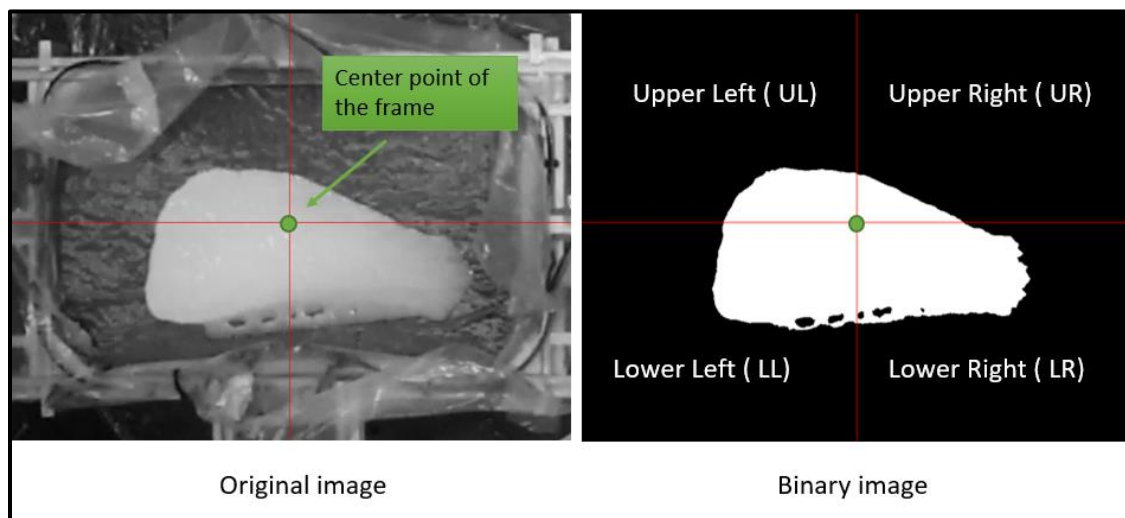


Figure 5-7: Thresholding method for measuring initial wetted area per quadrant

5.4.3 Targeted wetted (resin) area per quadrant measurement

As discussed earlier, the area of the preform where resin is planned to be applied (based on program defined for the robot) is known as the targeted wetted (resin) area. To measure four symmetrical quadrants of targeted resin area, in relation to the frame center point, the targeted resin area is divided into four quadrants, as shown in Figure 5-8.

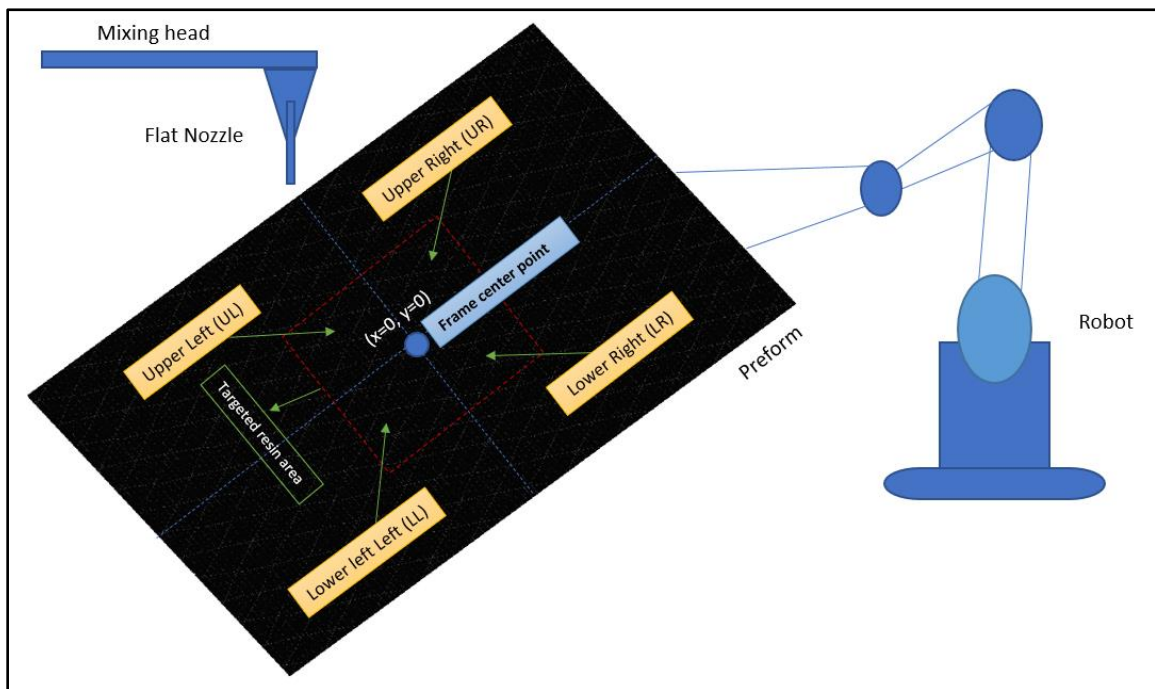


Figure 5-8: Targeted resin area per quadrant

5.4.4 Observation of quadrants measurement for area coverage data

The initial wetted areas per each quadrant varied in size for each of the 27 produced parts, but the targeted wetted area measurements per quadrant were the same size. The area measurements of initial wetted (resin) per quadrant is provided as a Whisker and Box plot in Figure 5-9, and the targeted resin area measurements per quadrant is shown as a horizontal red line. As it is evident from Figure 5-9, the targeted resin area in lower left and lower right is larger than upper left and right quadrants and initial wetted area per quadrant varies (per plaque), with larger area in lower right and lower left.

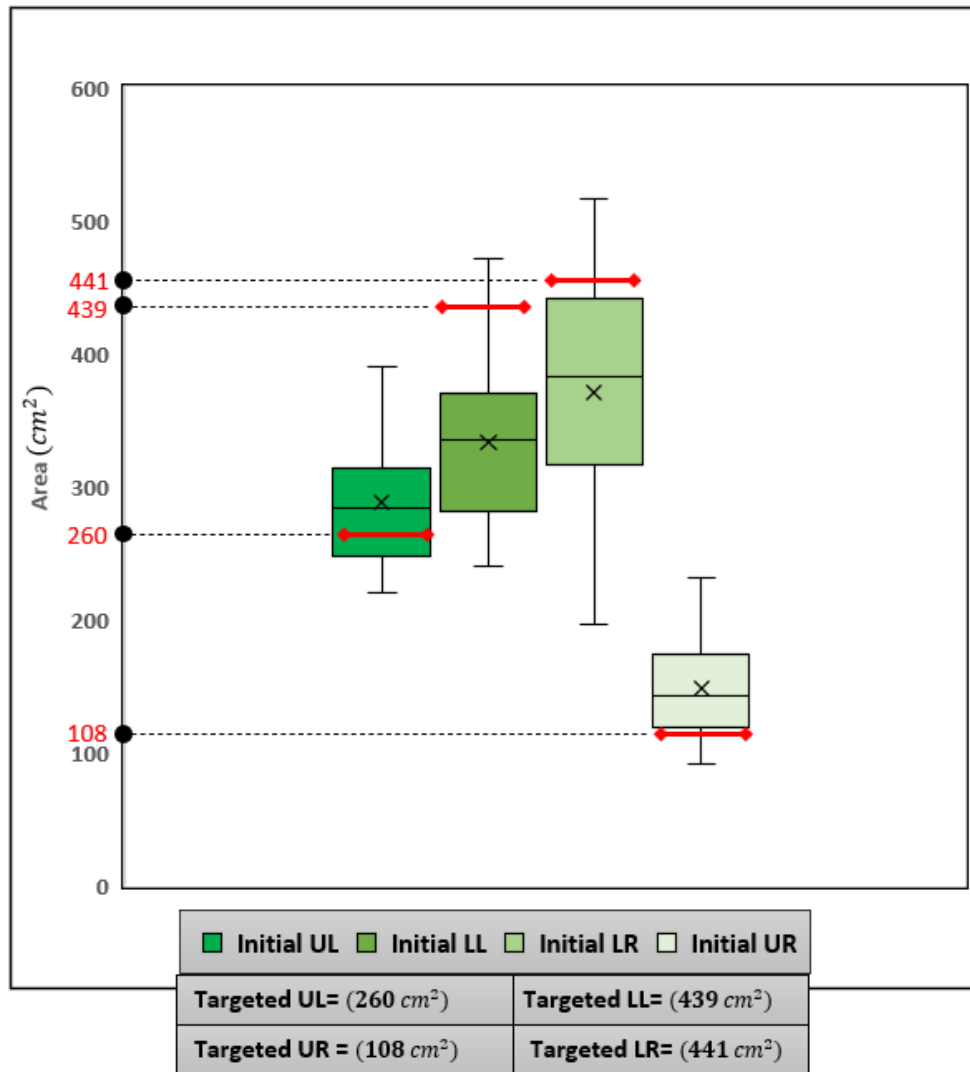


Figure 5-9: Whiskers and Box plot for initial and targeted wetted area - UL: Upper Left, UR: Upper Right, LR: Lower Right, LL: Lower Left

To compare initial resin application area on right and left sides, area per quadrant for each side were summed, and the data were presented using Whisker and Box plot as shown in Figure 5-10. In both targeted and initial wetted (resin) area, the left side has a larger area than the right side. The initial and targeted wetted area measurements per each quadrant and on the right and left sides are provided in Appendices 11 and 12 respectively.

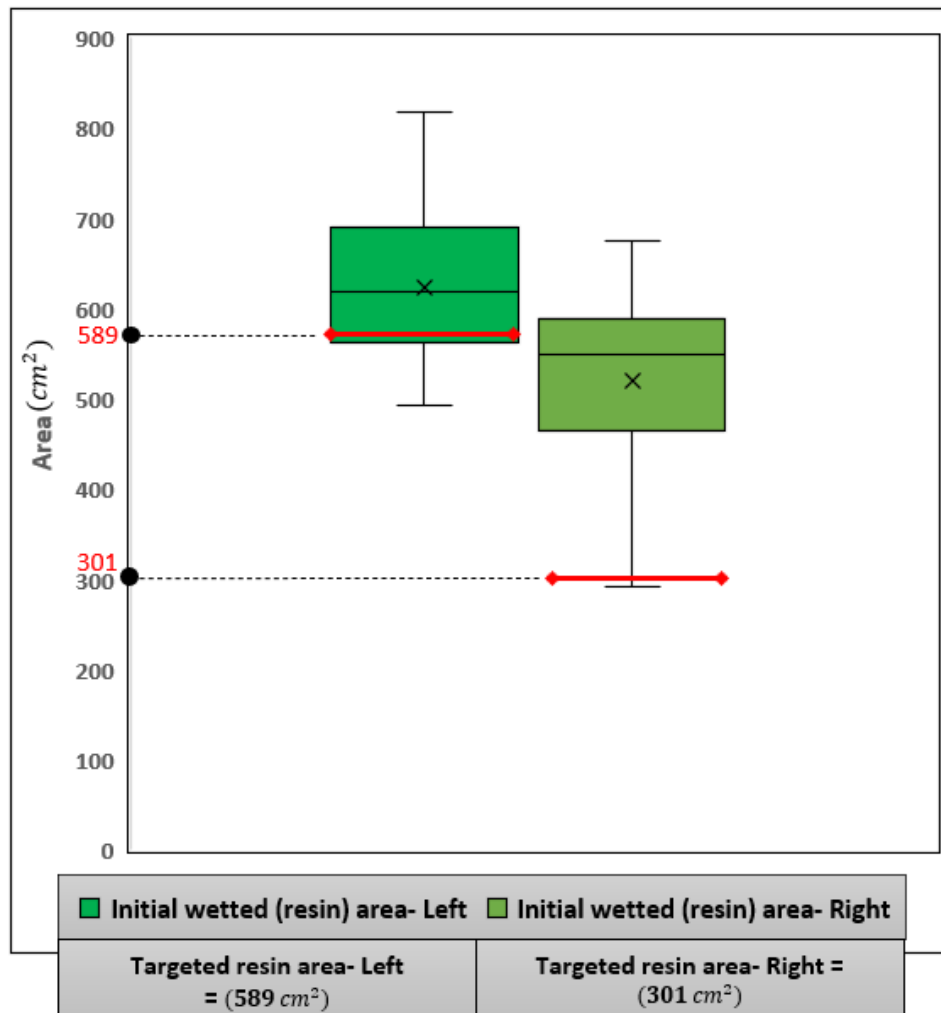


Figure 5-10: Whiskers and Box plot for initial and targeted wetted area in right and left side

It is important to note that due to the space limitation of the WCM manufacturing system (there are fences around the setup to prevent safety hazards), the ABB robot arm could not move freely in all directions. Hence, the movement pattern was configured to accommodate this limitation. In addition, the dispensing nozzle rotated at the end of the first path and then started the second path, which distributed more resin on the left side than the right side of the plaque.

5.5 Wetted vs. non-wetted regions

5.5.1 Definition

Based on the initial wetted and non-wetted (dry) regions, five different sampling areas (coupons) of interest are selected for the mechanical test, as described previously in Section 3.2.2. Figure 5-11 indicates that coupons from sampling areas A and C are selected from initial wetted (resin) areas, and coupons from sampling areas B, D, and E, are chosen from initial non-wetted (dry) areas. This feature of resin application is used to compare Flexural Modulus in the areas where the resin is first applied (sampling areas A and C) to those with no initial resin application (sampling areas B, D, and E).

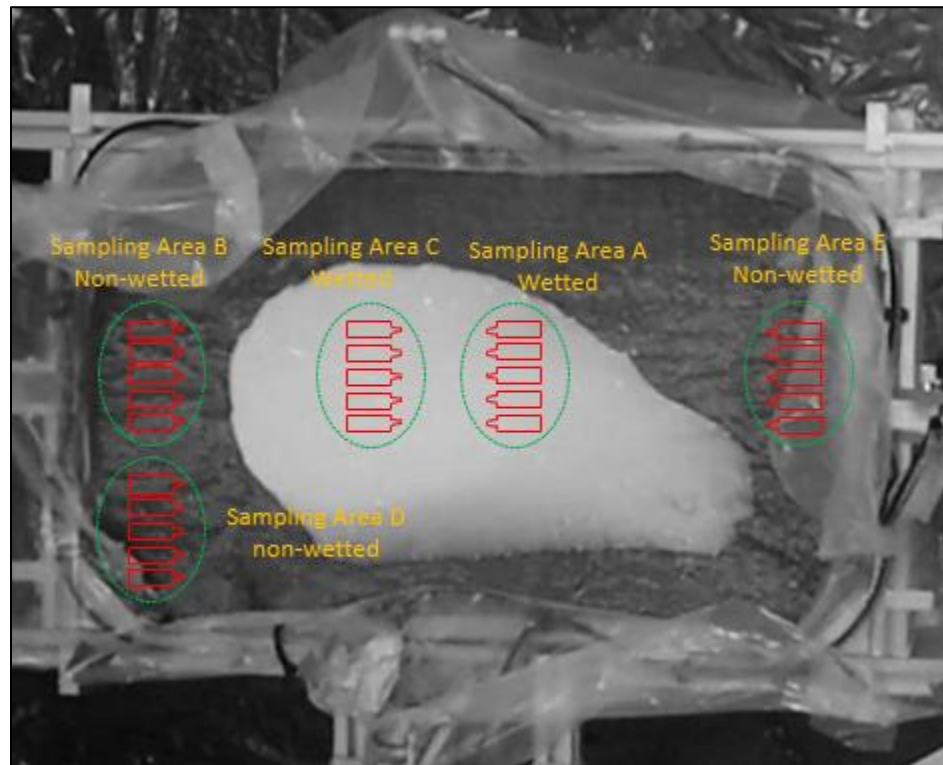


Figure 5-11: Wetted and Non-wetted (dry) sampling areas on an extracted frame

5.5.2 Observation of flexural data for wetted vs. non-wetted regions

Following the procedure, the Flexural Modulus of wetted vs. non-wetted regions are measured, and the data presented using Whisker and Box plot in Figure 5-12. The mechanical property is not symmetric, and sampling areas B, C, and D have almost the same Flexural Modulus on average. On the other hand, sampling areas E and A, have the lowest average Flexural Modulus among the five regions, which is also shown by statistical analysis in Chapter 4 4.4.6).

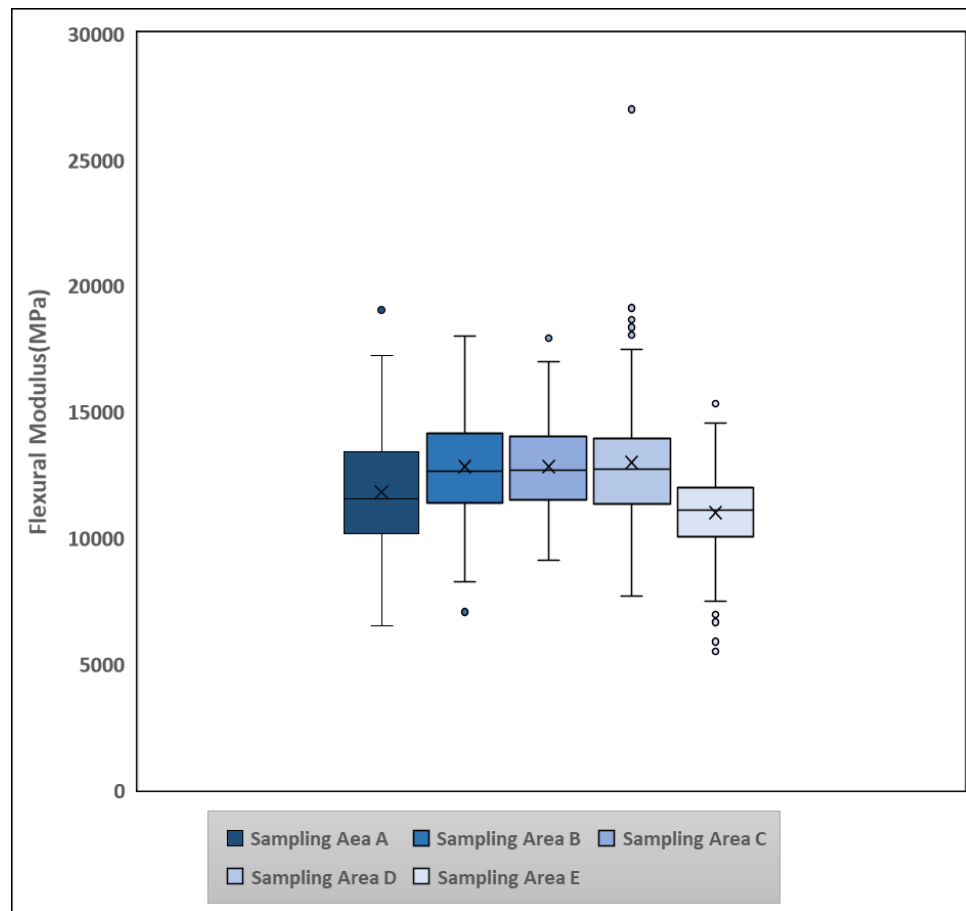


Figure 5-12: Flexural Modulus of wetted (sampling area A and C) vs. non-wetted (sampling area B, D, and E) regions

5.6 Results and discussion

As investigated earlier (in Chapter 4), the property of a part is not symmetrical and varied in different sampling areas. Thus, this part of the research aimed at evaluating the effect of initial resin distribution on the mechanical property of the final parts.

As explained earlier, the area coverage and area per quadrant of initial and targeted resin application are obtained for each of the 27 plaques. Based on the observations in previous sections, it can be concluded that the initial resin distribution pattern (resin flow) and the

mechanical property are not symmetric in the produced part. The higher resin distribution over the plaque surface and better mechanical property are observed for the left side of part. This section of the research aims to answer whether the initial resin distribution pattern can be used as a significant factor that impacts the mechanical property of a plaque.

5.6.1 Investigate the data correlation for wetted regions

The initial resin area measurements per quadrant and the Flexural Modulus of sampling areas A and C are plotted using a Scatter plot, as shown in Figures 5-13 and 5-14. It is evident that there is no visual correlation between the initial wetted area per quadrant and Flexural Modulus, consistent with the low values of R^2 . However, in Figure 5-13, the scatter plot for the Lower Left area and Flexural Modulus shows a slight positive correlation, with $R^2 = 0.36$.

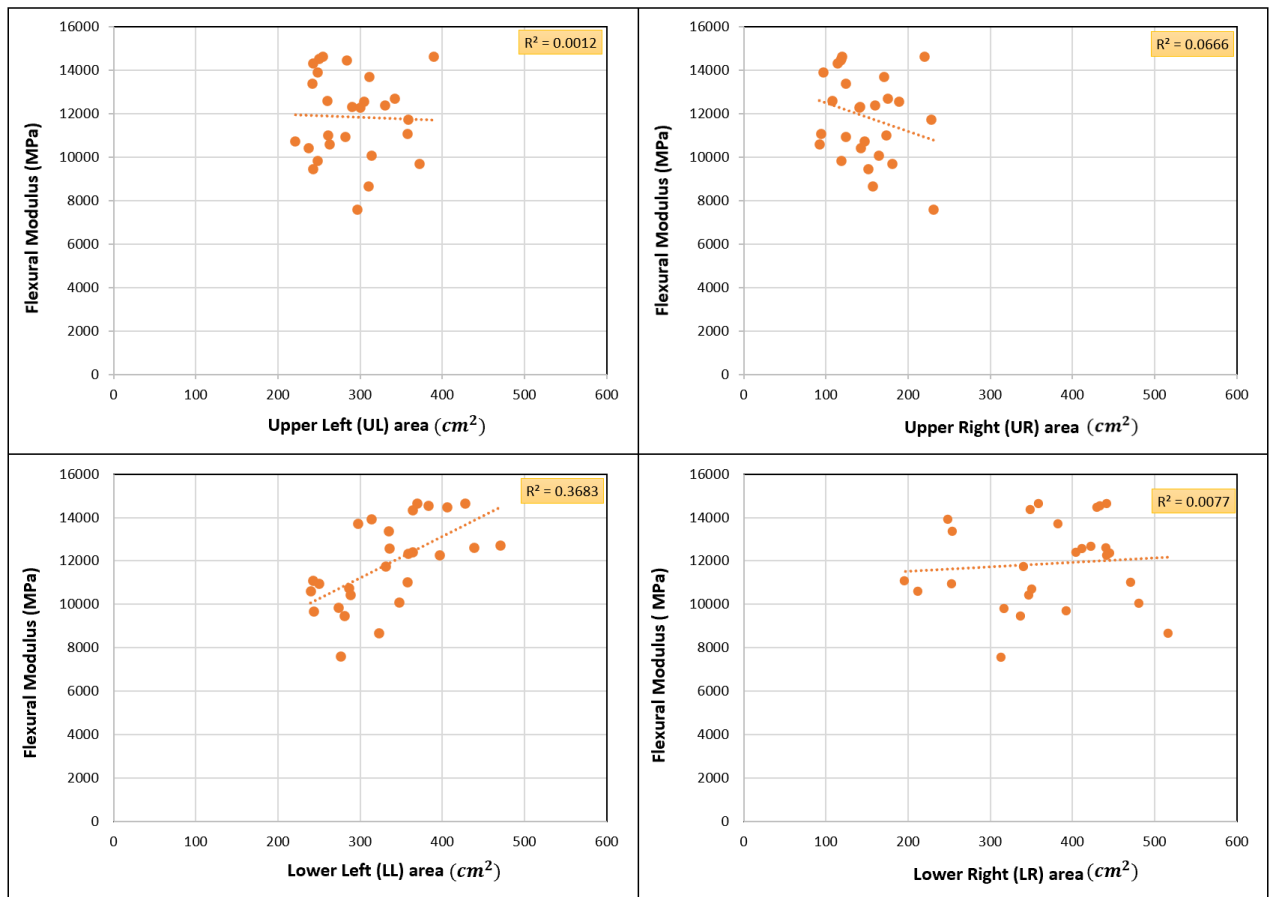


Figure 5-13: Correlation between initial wetted area per quadrant and Flexural Modulus of Sample Area A

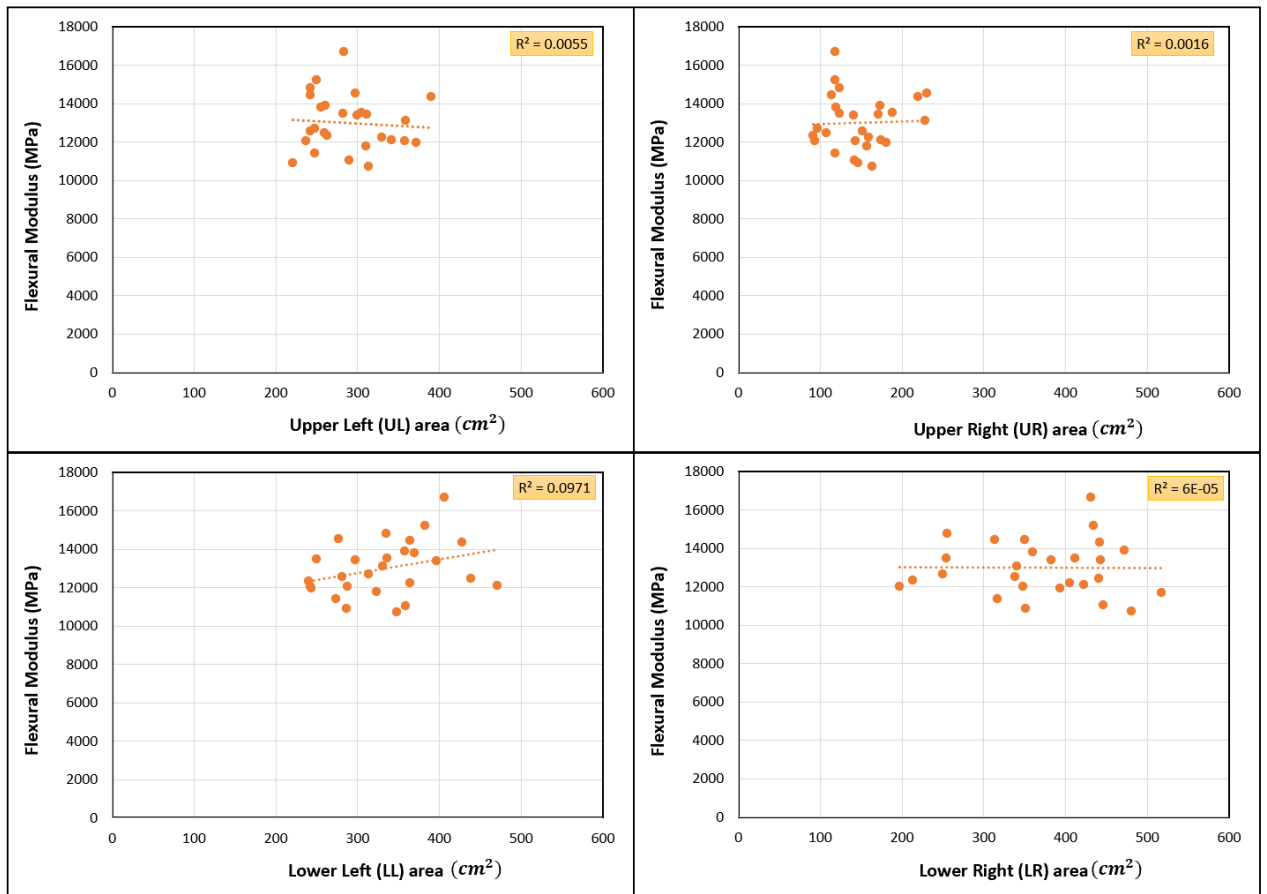


Figure 5-14: Correlation between initial wetted area per quadrant and Flexural Modulus of Sample Area C

5.6.2 Investigate the data correlation for non-wetted regions

Similar to the previous section, the analysis is carried out for non-wetted regions (sampling areas B, D, E), and the results are depicted below in Figures 5-15, 5-16, and 5-17. As seen in those figures, there is no visual correlation between the initial wetted area per quadrant and the flexural modulus variables, which is consistent with the low values of R^2 .

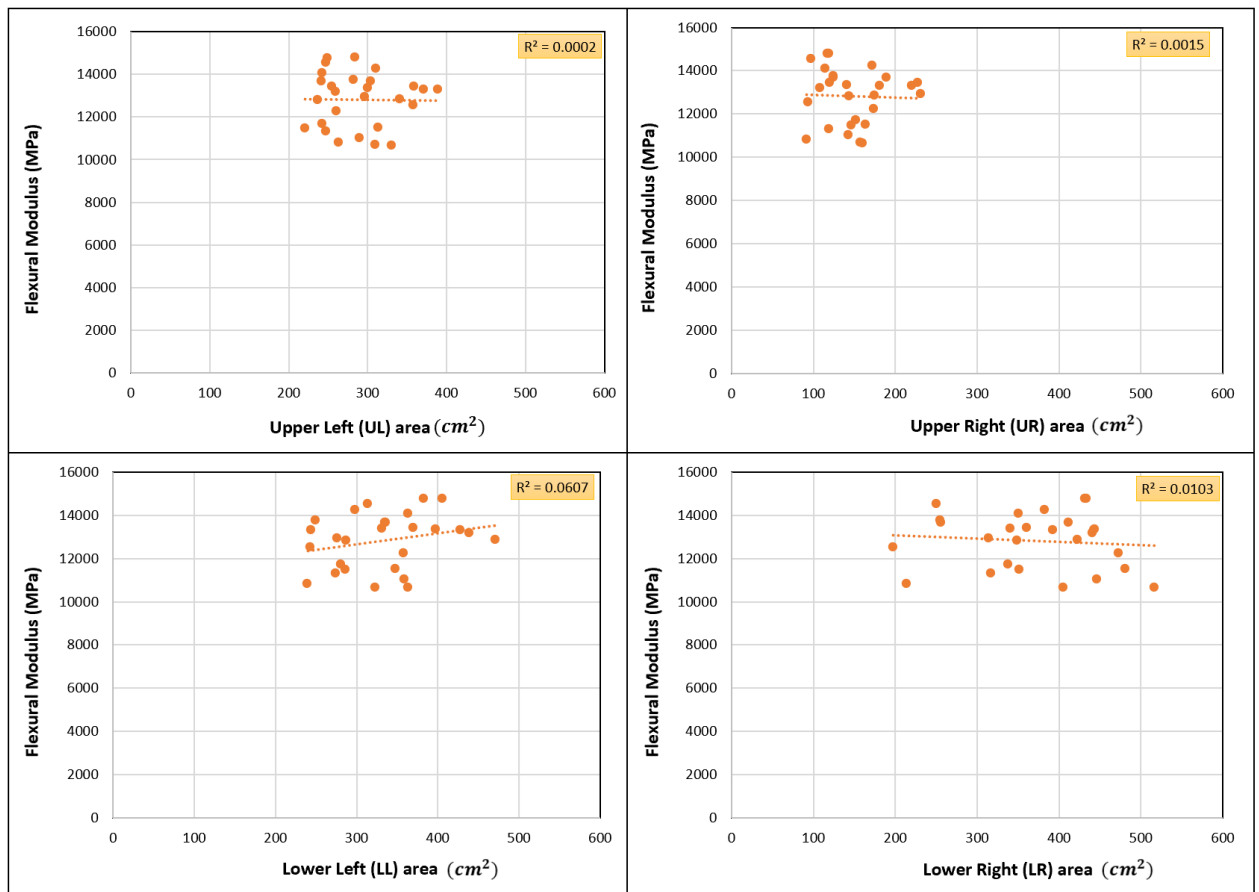


Figure 5-15: Correlation between initial wetted area per quadrant and Flexural Modulus of Sample Area B

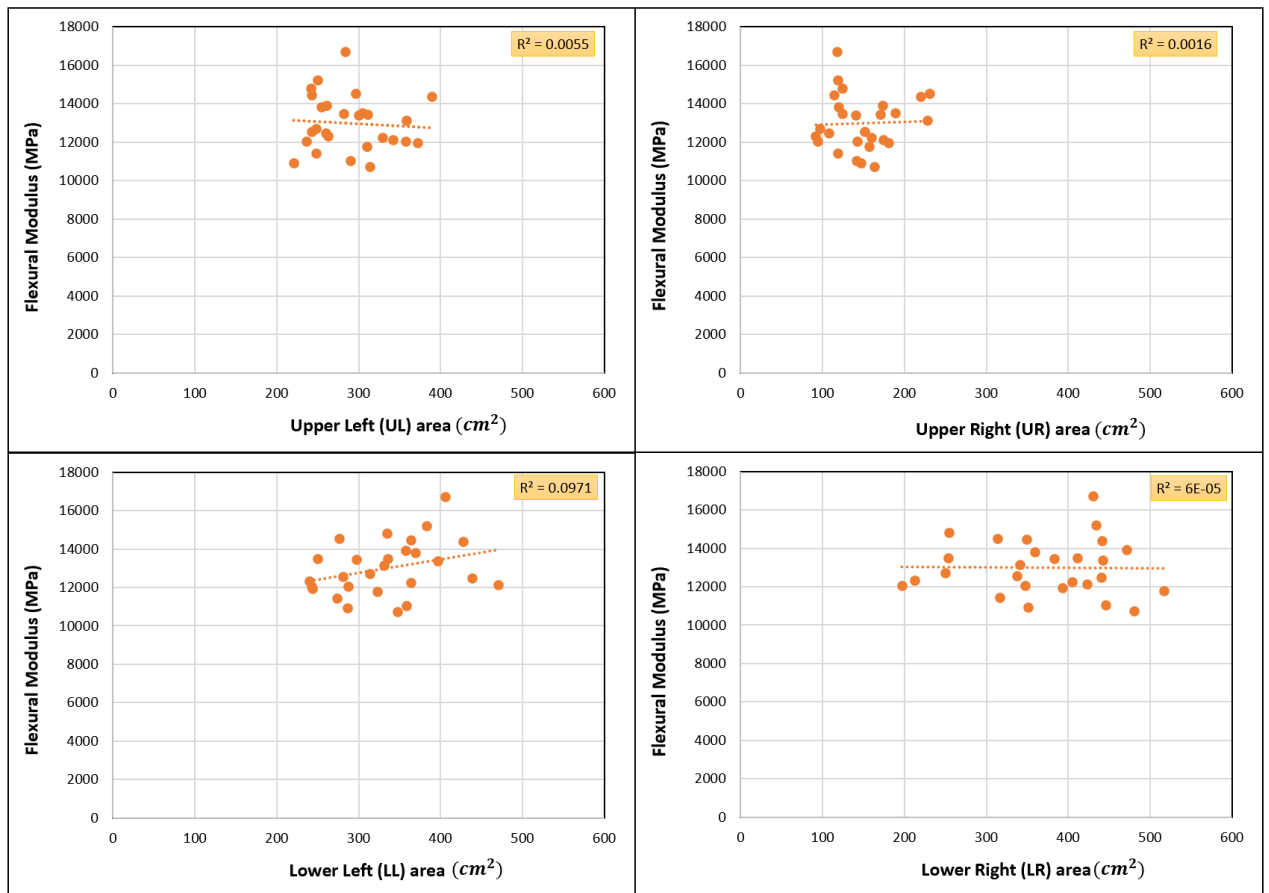


Figure 5-16: Correlation between initial wetted area per quadrant and Flexural Modulus of Sample Area D

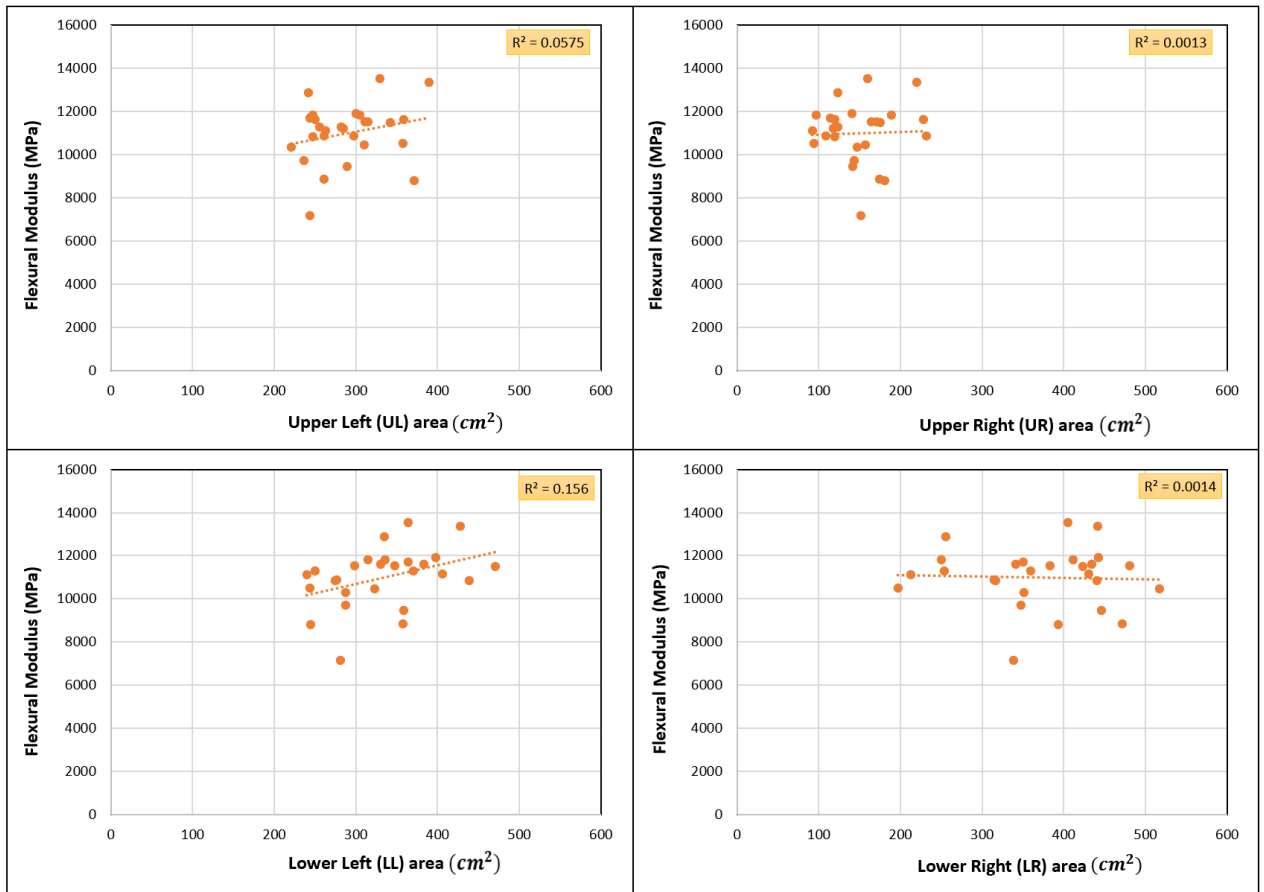


Figure 5-17: Correlation between initial wetted area per quadrant and Flexural Modulus of Sample Area E

5.7 Conclusion

This chapter investigated the effect of initial resin distribution on the final parts' mechanical properties. Based on the statistical analysis results, the initial resin distribution did not significantly influence the mechanical property of the final parts. This means the higher amount of resin on one side of the plaque does not significantly impact the mechanical performance of that side of the plaque.

Chapter 6

6 Conclusion and recommendations

6.1 Conclusion

The WCM equipment at the Fraunhofer Innovation Platform (FIP) for composite research was utilized to fabricate carbon-fiber composites in an epoxy matrix. Several essential process variables significantly affected the quality of the CFRP product; thus, in the present research, the effect of process parameters with different levels, including resin temperature (50, 60, and 70 °C), mold temperature (110 and 130 °C), resin set time (0, 20, and 40 s), Gap Closure Speed (1, 2, and 3 mm/s), and Mold Curing Time (120, 130 s) on part quality are investigated. The Young's Modulus of the resulting composites was evaluated using the three-point bend configuration in accordance with ASTM D-7269 to serve as an indicator of the mechanical property. The influence of process variables on the quality of the parts was investigated by applying Design of Experiments (DoE) and Analysis of Variance (ANOVA). Moreover, in the second part of the research, the impact of initial resin distribution on the mechanical property of the parts was evaluated.

The key conclusions from this study can be summarized as follows:

- Statistical results show that mold temperature, resin temperature, and resin set time significantly affect the mechanical property of the part. However, gap closure speed and mold curing time did not significantly influence the mechanical property of the plaques.
- At the lowest level of mold temperature (110 °C), resin temperature (50 °C), and resin set time (0 s), the mechanical property of the parts was higher; however, at the higher level of the factors the quality of the parts was lower.
- Optical micrographs show that voids (air entrapment) are observed, which was the primary reason for the poor quality of the final parts.

- From statistical results, mechanical property is not uniform across the part meaning that the mechanical property of the parts varies from one sampling location to another. In other words, the sampling area as a factor has a significant contribution to the model.
- Statistical results exhibited no correlation between the initial resin distribution and the mechanical property of the final parts.

6.2 Recommendations for future work

The result obtained from this research can be extended to the suggestions.

- In this project, only the main effects of the process parameters were analyzed. It would also be interesting to investigate factor interactions, which would require a new DoE and more experimental work.
- In this project, plaques were examined and classified (48 produced plaques) based on appearance (visual observations), and just more than half of the plaques were considered in good condition (28 plaques), and the rest, 20 of them, had some sort of manufacturing defects (e.g., dry spots and shifted preform). However, such a relatively low “success rate” is not typical in industry and commercial practices. It is recommended that future research investigates the reasons why such unacceptable parts are produced and try to eliminate them. Also, analyzing unacceptable plaques (with defects) may be worthwhile.
- As was pointed out in this study, only Young’s Modulus (Slope of Stress-Strain curve) was selected as a representative of the mechanical property of parts and used in statistical analysis as the response variable. It is recommended that the Strength and Strain at Break data be considered in addition to Young’s Modulus data when establishing a relationship between process variables and the mechanical property of parts. However, one should keep in mind that in the preparation of specimens for testing, the length of specimens should be chosen based on the higher thickness

(such that breakage would happen in all tests) as opposed to the average thickness approach chosen in this project.

- Three-point beam flexural testing is used in this research. However, it is recommended that other types of mechanical testing, such as tensile and interlaminar shear stress, be employed to investigate other properties of WCM parts.
- In a non-Newtonian fluid, the relation between the shear stress and the shear rate differs, and the fluid can exhibit time-dependent viscosity. The non-Newtonian nature of the resin's rheological behavior may impact voids' size and distribution. We recommend that this is investigated in the future work.
- The existence of voids in the parts was briefly inspected through the OM technique. It is observed that the poor mechanical propriety of parts is related to the void formation during the WCM process. However, the void content needs to be accurately measured to establish the relationship between mechanical property and voids through a quantitative analysis.

References

- Advani, S. G. (1994). Flow and rheology in polymer composites manufacturing/edited by Suresh G. Advani. *Composite materials series; 10., 10.*
- Altmann, A. et al. (2016). A continuum damage model to predict the influence of ply waviness on stiffness and strength in ultra-thick unidirectional Fiber-reinforced Plastics. *Journal of Composite Materials*, 50(20), 2739-2755.
- Baskaran, M. et al. (2014, June). Manufacturing cost comparison of RTM, HP-RTM and CRTM for an automotive roof. *In Proceedings of the 16th European Conference on Composite Materials, ECCM.*
- Bergmann, J. et al. (2016). Interpreting process data of wet pressing process. Part 1: Theoretical approach. *Journal of composite materials*, 50(17), 50(17), 2399-2407.
- Bergmann, J. et al. (2016). Interpreting process data of wet pressing process. Part 2: Verification with real values. *Journal of composite materials*, 50(17), 50(17), 2409-2419.
- Bernath, A. et. al. (2016). Accurate cure modeling for isothermal processing of fast curing epoxy resins. *Polymers*, 8(11), 8(11), 390.
- Bhat, P. et al. (2009). Process analysis of compression resin transfer molding. *Composites Part A: Applied science and manufacturing*, 40(4), 40(4), 431-441.
- Bockelmann, P. (2017). *Process control in compression molding of composites* (. München: Doctoral dissertation, Technische Universität.
- Box et al. (1964). An analysis of transformations. *Journal of the Royal Statistical Society: Series B (Methodological)*, 26(2), 211-243.
- Carbon Neutrality Goals by Country*. (2021, June 17). Retrieved from Motivepower: <https://www.motive-power.com/npuc-resource/carbon-neutral-goals-by-country/>

- Carlone, P. et al. (2015). Unsaturated and saturated flow front tracking in liquid composite molding processes using dielectric sensors. *Applied Composite Materials*, 22, 543-557.
- Chang, C. Y. et al. (2006). Effect of process variables on the quality of compression resin transfer molding. *Journal of Reinforced Plastics and Composites*, 25(10), 25(10), 1027-1037.
- Chang, T. J. (2021). *Characterization of Material for Composite Automotive Components (Doctoral dissertation)*. London: The University of Western Ontario (Canada).
- Chaudhari, R. et al. (2012). CHARACTERIZATION OF HIGH PRESSURE RTM PROCESSES FOR MANUFACTURING OF HIGH PERFORMANCE COMPOSITES.
- Chen, S.C. et al. (2000). Simulation of injection-compression-molding process. II. Influence of process characteristics on part shrinkage. *Journal of Applied Polymer Science*, 75(13), 1640-1654.
- Corporation, Z. (n.d.). *Technical Datasheet ZOLTEK™ PX35 Uni-Directional Fabrics*. Retrieved from www.zoltek.com
- Damani, S. G. et al. (1990). The resin-fiber interface in polyurethane and polyurethane-unsaturated polyester hybrid. *Polymer composites*, 11(3), 11(3), 174-183.
- de Almeida, S. F. M., et al. (1994). Effect of void content on the strength of composite laminates. *Composite structures*, 28(2), 28(2), 139-148.
- Demirci et al. (1995). Control of flow progression during molding processes. *JOURNAL OF MATERIALS PROCESSING & MANUFACTURING SCIENCE*, 3(4), 409-425.

- Ermanni, P. et al. (2011). Molding: liquid composite molding (LCM). *Wiley encyclopedia of composites*, 1-10.
- Fanni, S. (2020). *Void content computation using optical microscopy for carbon fiber composites*.
- Farhang, L. (2014). *Void evolution during processing of out-of-autoclave prepreg laminates*. Doctoral dissertation, University of British Columbia.
- FRIMO. (n.d.). *FRIMO. GLOBAL TECHNOLOGY SOLUTIONS*. (FRIMO. GLOBAL TECHNOLOGY SOLUTIONS) Retrieved from WET COMPRESSION MOLDING: <https://www.frimo.com/en/wet-compression-molding>
- Gardiner, G. (2016, July 31). (CompositesWorld) Retrieved 21, 2016, from Wet Compression Molding: <https://www.compositesworld.com>
- Gereke, T. et al. (2013). Experimental and computational composite textile reinforcement forming: A review. *Composites Part A: Applied Science and Manufacturing*, 46, 46, 1-10.
- Gereke, T. et al. (2013). Experimental and computational composite textile reinforcement forming: A review. *Composites Part A: Applied Science and Manufacturing*, 46, 46, 1-10.
- Ghasemi, A. et al. (2012). Normality tests for statistical analysis: a guide for non-statisticians. *International journal of endocrinology and metabolism*, 10(2), 10(2), 486.
- Ghazimoradi, M. et al. (2021). Deformation characteristics and formability of a tricot-stitched carbon fiber unidirectional non-crimp fabric. *Composites Part A: Applied Science and Manufacturing*, 145, 145, 106366.

- Ghazimoradi, M. et al. (2022). Characterizing the macroscopic response and local deformation mechanisms of a unidirectional non-crimp fabric. *Composites Part A: Applied Science and Manufacturing*, 156, 156, 106857.
- Ghiorse, S. R. (1993). Effect of void content on the mechanical properties of carbon/epoxy laminates. *SAMPE quarterly*, 24(2), 24(2), 54-59.
- Gorss, J. (2003, September 17). *High Performance Carbon Fibers*. Washington, DC, USA: National Historic Chemical Landmarks Program. : American Chemical Society, Office of Communications. Retrieved from www.chemistry.org/landmarks
- Graf, M. et al. (2010). High-pressure resin transfer molding-process advancements. *In SPE Automotive Composites Conference & Exhibition (Vol. 15)*, 15.
- Hamidi et al. (2017). Process induced defects in liquid molding processes of composites. *International Polymer Processing*, 32(5), 32(5), 527-544.
- Han, K. et al. (1998). Analysis of an injection/compression liquid composite molding process. *Polymer composites*, 19(4), 19(4), 487-496.
- Hatz, F. (2011). *Charakterisierung des "High Pressure-Compression RTM "Prozesses zur Herstellung von endlosfaserverstärkten Verbundwerkstoffen .* (Doctoral dissertation, Master Thesis, Fraunhofer ICT).
- Henning, F. et al. (2019). Fast processing and continuous simulation of automotive structural composite components. *Composites Science and Technology*, 171, 171, 261-279.
- Henning, F. et al. (2019). Fast processing and continuous simulation of automotive structural composite components. *Composites Science and Technology*, 171, 171, 261-279.

- Hexion. (2015). *Hexion, Technical Data Sheet EPIKOTE Resin 06170 EPIKURE Curing Agent 06170*. Retrieved from <https://www.hexion.com>
- Hibbeler, R. C. (2017). *Mechanics of Materials*, eBook. Pearson Higher Ed. (n.d.).
- imould. (2019). *Wet compression molding*. (imould.com) Retrieved 12 12, 2019, from imould: <http://www.imould.com/news/Wet+compression+molding-3296.html>
- International, A. (2007). Standard test method for flexural properties of polymer matrix composite materials. *ASTM International*.
- Johnson, R. J. et al. (2006). Simulation of active flow control based on localized preform heating in a VARTM process. *Composites Part A: Applied Science and Manufacturing*, 37(10), 1815-1830.
- Karcher, M.D. et al. (2015). EVALUATION OF A NEW “ INLINEPREPREG ” PROCESS APPROACH TO ESTABLISHED PROCESSES FOR THE MANUFACTURING OF STRUCTURAL COMPONENTS OUT OF CARBON FIBRE REINFORCED PLASTICS.
- Kaynak, C. et al. (2008). Effects of RTM mold temperature and vacuum on the mechanical properties of epoxy/glass fiber composite plates. *Journal of composite materials*, 42(15), 42(15), 1505-1521.
- Kedari, V. R. et al. (2011). Effects of vacuum pressure, inlet pressure, and mold temperature on the void content, volume fraction of polyester/e-glass fiber composites manufactured with VARTM process. *Journal of composite materials*.
- Khan, Z. M. et al. (2016). The influence of multiple nested layer waviness on the compression strength of double nested wave formations in a carbon fiber composite laminate. *Mechanics of Composite Materials*, 51, 751-760.

- Lawrence, J. M. et al. (2002). An approach to couple mold design and on-line control to manufacture complex composite parts by resin transfer molding. *Composites Part A: Applied Science and Manufacturing*, 33(7), 981-990.
- Lawrence, J. M. et al. (2009). Modeling the impact of capillary pressure and air entrapment on fiber tow saturation during resin infusion in LCM. *Composites Part A: Applied Science and Manufacturing*, 40(8), 1053-1064.
- LeBel, F. et al. (2014). Prediction of optimal flow front velocity to minimize void formation in dual scale fibrous reinforcements. *International journal of material forming*, 7, 93-116.
- Leclerc, J. S. et al. (2008). Porosity reduction using optimized flow velocity in Resin Transfer Molding. *Composites Part A: Applied Science and Manufacturing*, 39(12), 1859-1868.
- Lee, D. H. et al. (2006). Analysis and minimization of void formation during resin transfer molding process. *Composites Science and Technology*, 66(16), 3281-3289.
- Lee, S. et al. (2021). CSAI analysis of non-crimp fabric cross-ply laminate manufactured through wet compression molding process. *Composite Structures*, 255, 113056.
- Lettau, M. (n.d.). *Plastics injection Molding*. Retrieved from <https://www.ptonline.com/knowledgecenter/plastic-injection-molding/types-of-technologies/high-pressure-resin-transfer-molding>
- Li, Y. et al. (2016). The effect of fiber misalignment on the homogenized properties of unidirectional fiber reinforced composites. *Mechanics of Materials*, 92, 261-274.

- Liu, L. et al. (2005). Effects of cure pressure induced voids on the mechanical strength of carbon/epoxy laminates. *Journal of Materials Science & Technology*, 21(1), 21(01), 87.
- Lutsey, N. (2010). Review of technical literature and trends related to automobile mass-reduction technology.
- Mehdikhani, M. et al. (2019). Voids in fiber-reinforced polymer composites: A review on their formation, characteristics, and effects on mechanical performance. *Journal of Composite Materials*, 53(12), 53(12), 1579-1669.
- Milton, J. S. et al. (1995). *Introduction to Probability and Statistics (3rd edn). Probability and Statistics.*
- Minitab. (2019). *Minitab® Statistical Software*. Retrieved from www.minitab.com
- Molded Fiber Glass Companies*. (n.d.). Retrieved from <https://moldedfiberglass.com/>
- Molnar, J. A. et al. (1989). Liquid flow in molds with prelocated fiber mats. *Polymer Composites*, 10(6), 10(6), 414-423.
- Montgomery et al. (2010). *Applied statistics and probability for engineers*. John Wiley & sons.
- Montgomery, D. C. (2001). *Design and analysis of experiments*. New York: John Wiley & Sons.
- Naik, N. K. et al. (2014). Permeability characterization of polymer matrix composites by RTM/VARTM. *Progress in aerospace sciences*, 65, 22-40.
- Nielsen, D. et al. (2001). Intelligent model-based control of preform permeation in liquid composite molding processes, with online optimization. *Composites Part A: Applied Science and Manufacturing*, 32(12), 1789-1803.

- Olivier et al. (1995). Effects of cure cycle pressure and voids on some mechanical properties of carbon/epoxy laminates. *Composites*, 26(7), 26(7), 509-515.
- Öztuna, D. et al. (2006). Investigation of four different normality tests in terms of type 1 error rate and power under different distributions. *Turkish Journal of Medical Sciences*, 36(3), 36(3), 171-176.
- Patel, N. et al. . (1993). Influence of processing and material variables on resin-fiber interface in liquid composite molding. *Polymer Composites*, 14(2), 14(2), 161-172.
- Poppe, C. T. (2021). *Process simulation of wet compression moulding for continuous fibre-reinforced polymers*.
- Potter, K. D. (1999). The early history of the resin transfer moulding process for aerospace applications. *Composites Part A: applied science and manufacturing*, 30(5), 30(5), 619-621.
- Raja, M. H. (2005). *Experimental optimization of process parameters to obtain class A surface finish in resin transfer molding process*.
- Rosenberg, P. et al. (2014, May). Investigating cavity pressure behavior in high-pressure RTM process variants. In *AIP Conference Proceedings (Vol. 1593, No. 1, pp. 463-466)*. American Institute of Physics.
- Rudd, C. D. et al. (1997). *Liquid moulding technologies: Resin transfer moulding, structural reaction injection moulding and related processing techniques*. Elsevier.
- Seuffert, J. et al. (2020). Experimental and numerical investigations of pressure-controlled resin transfer molding (PC-RTM). *Advanced Manufacturing: Polymer & Composites Science*, 6(3), 6(3), 154-163.

- Shih et al. (1997). Design of experiments analysis of the on-line consolidation process. *In Proceedings of the Eleventh International Conference on Composite Materials*, 4.
- Simacek, P. et al. (2005). Simulating three-dimensional flow in compression resin transfer molding process. *Revue Européenne des Eléments*, 14(6-7), 14(6-7), 777-802.
- Simacek, P. et al. (2008). Modeling flow in compression resin transfer molding for manufacturing of complex lightweight high-performance automotive parts. *Journal of composite materials*, 42(23), 2523-2545.
- Simacek, P. et al. (2008). Modeling flow in compression resin transfer molding for manufacturing of complex lightweight high-performance automotive parts. *Journal of composite materials*, 42(23), 42(23), 2523-2545.
- Sozer, E. M. et al. (2000). On-line strategic control of liquid composite mould filling process. *Composites Part A: Applied Science and Manufacturing*, 31(12), 1383-1394.
- Suhot, M. A. et al. (2014). The effects of voids on the flexural properties and failure mechanisms of carbon/epoxy composites. *Jurnal Teknologi*, 71(2), 71(2).
- Suratkar, A. P. (2022). *Damage in Non-Crimp Fabric carbon fiber reinforced epoxy composites under various mechanical loading conditions*. London, Canada: The university of Western Ontario.
- Svensson, N. et al. (1998). Manufacturing of thermoplastic composites from commingled yarns-A review. *Journal of Thermoplastic Composite Materials*, 11(1), 11(1), 22-56.
- Swentek, I. et al. (2015). Impact of HP-RTM process parameters on mechanical properties using epoxy and polyurethane., (pp. 26-29). Dallas, Texas, USA,.

Thermoplastics Vs. Thermoset. (2017). Retrieved from Modor Plastics:

<http://www.modorplastics.com/thermoset-vs-thermoplastics>

Trejo et al. (2020). Assessing strain fields in unbalanced unidirectional non-crimp fabrics.

Composites Part A: Applied Science and Manufacturing, 130, 105758.

Villière, M. et al. (2015). Dynamic saturation curve measurement in liquid composite

molding by heat transfer analysis. *Composites Part A: Applied Science and*

Manufacturing, 69, 255-265.

Vita, A. et al. (2019). Comparative life cycle assessment of low-pressure RTM,

compression RTM and high-pressure RTM manufacturing processes to produce

CFRP car hoods. *Procedia CIRP*, 80, 80, 352-357.

Xueshu et al. (2016). A review of void formation and its effects on the mechanical

performance of carbon fiber reinforced plastic. *Engineering Transactions*, 64(1),

64(1), 33-51.

Yang, M. (2019). *Molecular Weight and Thermal Properties of Fiber Reinforced*

Polyamide-Based Composites Throughout the Direct Long-Fiber Reinforced

Thermoplastic Process (Doctoral dissertation). The University of Western

Ontario (Canada).

List of Appendices

Appendix 1: ZOLTEK™ PX35 unidirectional fabric data sheet

Technical Datasheet

ZOLTEK™ PX35 Uni-Directional Fabrics



Stitch-Bonded Uni-Directional Carbon Fabrics

COMPOSITE PROPERTIES	SI	US	METHOD
Tensile Strength	1,400 MPa	203 ksi	DIN EN ISO 527
Tensile Modulus	119 GPa	17.2 msi	DIN EN ISO 527
Compressive Strength	980 MPa	142 ksi	DIN EN ISO 14126
Compressive Modulus	118 GPa	17.5 msi	DIN EN ISO 14126
Flexural Strength	1,290 MPa	187 ksi	DIN EN ISO 14125
Flexural Modulus	112 GPa	16.2 msi	DIN EN ISO 14125

Typical Fiber Volume Fraction (FVF) is 55%.
Standard Epoxy Resin System

The properties listed in this datasheet do not constitute any warranty or guarantee of values. This information should only be used for the purposes of material selection. Please contact us for more details.

TYPICAL PACKAGING

Wound on cardboard cone, sealed in polyethylene bag, and placed in cardboard box. Rolls stacked horizontally on pallets when shipping.

+ Requirements other than standard widths and roll lengths should be specified by purchase order.

CERTIFICATION

ZOLTEK PX35 Fabrics are manufactured in accordance with ZOLTEK's written and published data. A Certificate of Conformance is provided with each shipment.

SAFETY

Obtain, read, and understand the Material Safety Data Sheet (SDS) before use of this or any other ZOLTEK product.

APPROVAL

DNV-GL has granted approval to ZOLTEK PX35 Uni-Directional Fabrics for use in wind energy applications.



ZOLTEK™ PX35



ZOLTEK Corporation | 3101 McKelvey Road | Bridgeton, MO 63044
P: 314-291-5110 | F: 314-291-8536 | www.zoltek.com

Technical Datasheet

ZOLTEK™ PX35 Uni-Directional Fabrics



Stitch-Bonded Uni-Directional Carbon Fabrics

DESCRIPTION

ZOLTEK PX35 Stitch-Bonded Uni-Directional Carbon Fabrics are produced from our ZOLTEK PX35 50K Continuous Tow Carbon Fiber. Unique fiber spreading techniques are utilized to obtain a wide range of UD fabric weights for a varied set of composite part applications. Quick composite part build-up is cost effectively achieved with our diverse weight range of low-cost carbon fabric products.



MATERIAL OVERVIEW	UD150	UD200	UD300	UD400	UD500	UD600	UD900V
0° Carbon ZOLTEK PX35 50K	158	200	309	403	500	600	865
90° Glass 34 dtex	10	10	10	10	10	10	—
Polyester Veil	—	—	—	—	—	—	30
Polyester Stitch 76 dtex	6	6	6	6	6	6	5
Total Fabric Weight	182 g/m ² 5.37 oz/yd ²	224 g/m ² 6.61 oz/yd ²	333 g/m ² 9.82 oz/yd ²	419 g/m ² 12.36 oz/yd ²	516 g/m ² 15.22 oz/yd ²	624 g/m ² 18.40 oz/yd ²	900 g/m ² 26.54 oz/yd ²

Average Values Shown

*Epoxy resin binder available upon customer request.

FABRIC CONSTRUCTION	UD150	UD200	UD300	UD400	UD500	UD600	UD900V
Stitch Length	A variety of stitch lengths are available to meet application requirements.						
Stitch Pattern	A variety of stitch patterns are available to meet application requirements.						
Cured Thickness/Ply	.21 mm	.25 mm	.37 mm	.46 mm	.57 mm	.69 mm	1.00 mm
Roll Width	30 cm - 61 cm - 122 cm						122 cm
Roll Length	100 m				50 m		30 m

Average Values Shown

The properties listed in this datasheet do not constitute any warranty or guarantee of values. This information should only be used for the purposes of material selection. Please contact us for more details.

ZOLTEK™ PX35



ZOLTEK Corporation | 3101 McKelvey Road | Bridgeton, MO 63044
P: 314-291-5110 | F: 314-291-8536 | www.zoltek.com

Appendix 2: EPIKOTE™ Resin TRAC 06170 resin data sheet



Technical Data Sheet

Most recent revision date:

3/19/2015

EPIKOTE™ Resin TRAC 06170

(Formerly named TRAC-0031-R)

EPIKURE™ Curing Agent TRAC 06170

(Formerly named EK GCW-RD-639-KW)

HELOXY™ Additive TRAC 06805

(Formerly named HELOXY™ Additive 112)

Product Description

EPIKOTE™ Resin TRAC 06170 is a medium viscous epoxy resin.

EPIKURE™ Curing Agent TRAC 06170 is a low viscous very fast amine hardener.

HELOXY™ Additive TRAC 06805 is a silicone- and wax-free internal mold release agent.

Application Areas/Suggested Uses

Low viscous resin system designed for RTM and LCM applications with excellent wetting and adhesion characteristics on glass-, carbon- or aramid-fibers. Benefits of this system are a very low viscosity during infusion and a fast development of the Glass Transition temperature T_g to above the molding temperature, which allows an easy de-molding, combined with very short cycle times.

Typical suggested uses include but are not limited to mass production of structural automotive parts such as parts of the frame or chassis, floor pans, firewalls, monocoque structure.

Benefits

- Low viscosity during injection.
- Easy to process due to thermo latent behavior:
 - Infusion time easily adjustable by selecting a process temperature (100°C to 145°C)
 - Fast glass transition temperature (T_g) development
 - Short curing cycle (e.g. 4 min at 100°C, or ~40 sec at 140°C)
- Excellent fiber wetting properties.
- Excellent thermal and mechanical performance.
- Excellent demolding characteristics.

page 1 of 6

The information provided herein was believed by Hexion Inc. and its affiliated companies ("Hexion") to be accurate at the time of preparation or prepared from sources believed to be reliable, but it is the responsibility of the user to investigate and understand other pertinent sources of information, to comply with all laws and regulations applicable to the sale, handling and use of the product and to determine the suitability of the product for its intended use. All products supplied by Hexion are subject to Hexion's terms and conditions of sale. HEXION MAKES NO WARRANTY, EXPRESS OR IMPLIED, CONCERNING THE PRODUCT OR THE MERCHANTABILITY OR FITNESS THEREOF FOR ANY PURPOSE OR CONCERNING THE ACCURACY OF ANY INFORMATION PROVIDED BY HEXION, except that the product shall conform to Hexion's specifications at the time of delivery. Nothing contained herein constitutes any offer for the sale of any product.
© 2015 Hexion Inc. All rights reserved.

® and TM marks trademarks owned or licensed by Hexion Inc.

Vestner Straße 40
47133 Duisburg-Meerbusch

Postfach 120952
47125 Duisburg

Germany

www.hexion.com

020015


Technical Data Sheet

Most recent revision date:

3/19/2015

Sales Specification
EPIKOTE™ Resin TRAC 06170

Property	Unit	Value	Test Method / Standard
Viscosity at 25°C	mPa·s	9000 ± 1000	DIN 53015 = ISO 12058-1
Color	Gardner	2 max.	ISO 4630-1
Color	Hazen	100 max.	ASTM D1209
Refractive index	-	1,572 ± 0,003	DIN 51423-2 = ISO 489

EPIKURE™ Curing Agent TRAC 06170

Property	Unit	Value	Test Method / Standard
Viscosity at 25°C	mPa·s	15 ± 10	DIN 53015 = ISO 12058-1
Refractive Index at 25°C	-	1,495 ± 0,003	DIN 51423-2 = ISO 489

HELOXY™ Additive TRAC 06805

Property	Unit	Value	Test Method
Viscosity at 30°C	mPa·s	750 ± 450	DIN 53015

Typical Properties
EPIKOTE™ Resin TRAC 06170

Property	Unit	Value	Test Method / Standard
Delivery form		Clear liquid	
Density at 20°C	kg/l	1.15 – 1.19	ISO 2811

EPIKURE™ Curing Agent TRAC 06170

Property	Unit	Value	Test Method / Standard
Delivery form		Clear to slightly yellow / brown liquid	
Density at 20°C	kg/l	0,97 ± 0,03	ISO 2811-3

HELOXY™ Additive TRAC 06805

Property	Unit	Value	Test Method
Delivery form		liquid	
Density at 20°C	kg/l	1.01 ± 1.05	DIN 51755
Appearance		yellow/brown	

page 2 of 6

The information provided herein was believed by Hexion Inc. and its affiliated companies ("Hexion") to be accurate at the time of preparation or prepared from sources believed to be reliable, but it is the responsibility of the user to investigate and understand other pertinent sources of information, to comply with all laws and procedures applicable to the safe handling and use of the product and to determine the suitability of the product for its intended use. All products supplied by Hexion are subject to Hexion's terms and conditions of sale. HEXION MAKES NO WARRANTY, EXPRESS OR IMPLIED, CONCERNING THE PRODUCT OR THE MERCHANTABILITY OR FITNESS THEREOF FOR ANY PURPOSE OR CONCERNING THE ACCURACY OF ANY INFORMATION PROVIDED BY HEXION, except that the product shall conform to Hexion's specifications at the time of delivery. Nothing contained herein constitutes any offer for the sale of any product. © 2015 Hexion Inc. All rights reserved. ® and TM denote trademarks owned or licensed by Hexion Inc.

Vardner Straße 40
47125 Duisburg-Meiderich
Postfach 120952
47125 Duisburg
Germany
www.hexion.com

022015


Technical Data Sheet

Most recent revision date: 3/19/2015

Processing Details
Mixing ratio

EPIKOTE™ Resin TRAC 06170	100	parts by weight
EPIKURE™ Curing Agent TRAC 06170	16	parts by weight
HELOXY™ Additive TRAC 06805	1-2	parts by weight

Mixing tolerance

The maximum allowable mixing tolerance (resin & hardener) is ± 0.5 pbw, but it is particularly important to preserve the recommended mixing ratio as accurately as possible. Incorrect dosing of the hardener is not an appropriate approach to accelerate or retard the reaction; rather it will lead to an incomplete cure. The reaction speed can be properly adjusted by changing the processing temperature, as indicated below. Resin and hardener must be mixed very thoroughly. Mix until no clouding is visible, pay special attention to the walls and the bottom of the mixing container.

Material preheating

To optimize the process a preheating of the components is recommended.

EPIKOTE™ Resin TRAC 06170	60-80	°C
EPIKURE™ Curing Agent TRAC 06170	RT-30	°C
HELOXY™ Additive TRAC 06805	25-30	°C

page 3 of 6

The information provided herein was believed by Hexion Inc. and its affiliated companies ("Hexion") to be accurate at the time of preparation or prepared from sources believed to be reliable, but it is the responsibility of the user to investigate and understand other pertinent sources of information, to comply with all laws and procedures applicable to the safe handling and use of the product and to determine the suitability of the product for its intended use. All products supplied by Hexion are subject to Hexion's terms and conditions of sale. HEXION MAKES NO WARRANTY, EXPRESS OR IMPLIED, CONCERNING THE PRODUCT OR THE MERCHANTABILITY OR FITNESS THEREOF FOR ANY PURPOSE OR CONCERNING THE ACCURACY OF ANY INFORMATION PROVIDED BY HEXION, except that the product shall conform to Hexion's specifications at the time of delivery. Nothing contained herein constitutes any offer for the sale of any product.
 © 2015 Hexion Inc. All rights reserved.
 ® and TM denote trademarks owned or licensed by Hexion Inc.

 Victor Straße 49
 47135 Duisburg-Meideroth

 Postfach 120552
 47120 Duisburg

Germany

www.Hexion.com

102015


Technical Data Sheet

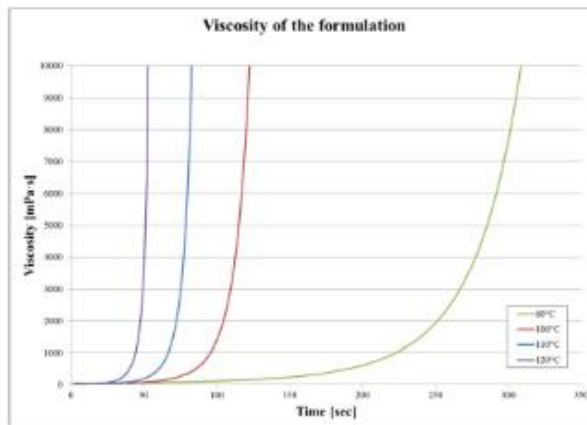
Most recent revision date: 3/19/2015

Processing Temperature and Pot Life

The EPIKOTE™ Resin TRAC 06170 / EPIKURE™ Curing Agent TRAC 06170 system has an infusion time which is easily adjustable by adjusting the process temperature over a relatively wide target range. The system exhibits good processing in the temperature range between 80 and 145 °C, and full curing can typically be achieved in 2 minutes cure at 120°C. Higher processing temperatures are possible but will shorten the pot life. A rise in temperature of 10 °C reduces the pot life by approx. 50%. Different temperatures during processing have no significant effect on the mechanical properties of the hardened product.

Do not mix large quantities at elevated processing temperatures as this can lead to an uncontrolled exothermic reaction where the mixture may heat up very quickly to more than 200 °C in the mixing container.

Processing Data		Unit	Value
Viscosity of the formulation	at 80°C	mPas	41 ± 10
	at 100°C	mPas	19 ± 10
	at 110°C	mPas	15 ± 5
	at 120°C	mPas	11 ± 5
Viscosity development of the formulation after 30s/60s/90s	at 80°C	mPas	49/67/97
	at 100°C	mPas	37/120/678
	at 110°C	mPas	95/486/61150
	at 120°C	mPas	114/65500/>100000
B-time of the formulation (Hot plate)	at 100°C	s	120 ± 30
	at 110°C	s	72 ± 20
	at 120°C	s	45 ± 10
Pot life of the formulation	at 25°C	mm:ss	42:00 ± 05:00 (260°C peak max)



page 4 of 6

The information provided herein was believed by Hexion Inc. and its affiliated companies ("Hexion") to be accurate at the time of preparation or prepared from sources believed to be reliable, but it is the responsibility of the user to investigate and understand other pertinent sources of information, to comply with all laws and procedures applicable to the safe handling and use of the product and to determine the suitability of the product for its intended use. All products supplied by Hexion are subject to Hexion's terms and conditions of sale. HEXION MAKES NO WARRANTY, EXPRESS OR IMPLIED, CONCERNING THE PRODUCT OR THE MERCHANTABILITY OR FITNESS THEREOF FOR ANY PURPOSE OR CONCERNING THE ACCURACY OF ANY INFORMATION PROVIDED BY HEXION, except that the product shall conform to Hexion's specifications at the time of delivery. Nothing contained herein constitutes any offer for the sale of any product.
 © 2015 Hexion Inc. All rights reserved.
 ® and ™ marks trademarks owned or licensed by Hexion Inc.

 Völkner Straße 46
 47125 Duisburg-Meiderich

 Rüdolph 1 02052
 47125 Duisburg

Germany

www.hexion.com


Technical Data Sheet

Most recent revision date:

3/19/2015

Typical Properties of the cured, non-reinforced system

Cure cycle: 2min @ 120°C

Property	Unit	Value	Test Method
TG, DSC first run			
Onset	°C	122 ± 3	DSC (10K/min)
Midpoint	°C	124 ± 3	DIN 53445
DMA			
Onset	°C	133 ± 3	DMA (2K/min)
Peak max	°C	140 ± 5	DIN EN 61006
Tensile test @ room temperature			
Tensile strength	MPa	74 ± 10	DIN EN ISO 527-1
Tensile modulus	MPa	2570 ± 50	
Elongation at break	%	7,3 ± 1	
Bending test @ room temperature			
Flexural strength	MPa	100 ± 13	DIN EN ISO 178
Flexural modulus	N/mm ²	2500 ± 200	
Fracture toughness at RT (K1C)	MPa.m ^{1/2}	0,87 ± 0,03	ISO 17281
Density	g/cm ³	1,177 ± 0,003	DIN 53479 A

Safety, Storage & Handling

Please refer to the MSDS for the most current Safety and Handling information.

EPIKOTE™ Resin TRAC 06170 should be stored at room temperature in its carefully sealed original containers. Under these conditions the shelf life is a minimum of three years from date of certification.

EPIKURE™ Curing Agent TRAC 06170 should be stored at room temperature in its carefully sealed original containers, so that moisture is excluded. Under these conditions the shelf life is a minimum of two years from date of certification. Care should be taken to avoid storage environments resulting in moisture contamination. Exposure to moisture will cause an increase in viscosity and reactivity, the degree of increase depending on the amount of moisture, which has been absorbed.

HELOXY™ Additive TRAC 06805 should be stored at room temperature in its carefully sealed original containers, so that moisture is excluded. Under these conditions the shelf life is a minimum of 6 months. HELOXY™ Additive TRAC 06805 should not be stored at temperatures above 30°C. Before use it is necessary to homogenize the material by shaking or stirring.

Occasionally, it is possible that the resin or the hardener crystallize at temperatures below 15°C. The crystallization is visible as a clouding or solidification of the content of the container. Before processing, the crystallization must be removed by warming up. Slow warming up to 50 - 60°C in a water bath or oven and stirring or shaking will clarify the contents in the container without any loss of quality. Use only completely clear products. Before warming up, open containers slightly to permit equalization of pressure. Caution during warm up! Do not warm up over open flame! While stirring up use safety equipment (gloves, eyeglasses, respirator equipment).

page 5 of 6

The information provided herein was believed by Hexion Inc. and its affiliated companies ("Hexion") to be accurate at the time of preparation or prepared from sources believed to be reliable, but it is the responsibility of the user to investigate and understand other pertinent sources of information, to comply with all laws and procedures applicable to the safe handling and use of the product and to determine the suitability of the product for its intended use. All products supplied by Hexion are subject to Hexion's terms and conditions of sale. HEXION MAKES NO WARRANTY, EXPRESS OR IMPLIED, CONCERNING THE PRODUCT OR THE MERCHANTABILITY OR FITNESS THEREOF FOR ANY PURPOSE OR CONCERNING THE ACCURACY OF ANY INFORMATION PROVIDED BY HEXION, except that the product shall conform to Hexion's specifications at the time of delivery. Nothing contained herein constitutes any offer for the sale of any product.
© 2015 Hexion Inc. All rights reserved.

Vertrieb Straße 40
47125 Duisburg-Meideroth
Postfach 120002
47125 Duisburg
Germany

Appendix 3: Experimental test matrix

Plaque Number	Operating condition					
	Resin temp (°C)	Mold temp (°C)	Resin set time (sec)	Gap closure speed last 2 mm (sec/sec)	Press force (kN)	Mold curing time (sec)
1	50	110	0	1	3000	120
2	50	110	0	1	3000	120
3	50	110	0	1	3000	120
4	50	110	0	1	3000	120
5	50	110	0	1	3000	300
6	70	110	0	1	3000	300
7	70	110	0	1	3000	300
8	70	110	0	1	3000	300
9	70	130	0	1	3000	120
10	70	130	0	1	3000	120
16	60	110	0	1	3000	300
17	60	110	20	1	3000	300
18	60	110	20	1	3000	300
19	60	110	40	1	3000	300
20	60	110	40	1	3000	300
21	60	110	40	1	3000	300
22	60	110	0	2	3000	300
23	60	110	0	2	3000	300
24	60	110	0	2	3000	300
25	60	110	0	2	3000	300
26	60	110	0	3	3000	300
27	60	110	0	3	3000	300
28	60	110	0	3	3000	300
29	60	110	0	1	3000	300
30	60	110	20	1	3000	300
31	60	110	40	1	3000	300
32	50	130	0	1	3000	120
34	50	130	0	1	3000	120

Operating condition						
Plaque number	Resin temp (°C)	Mold temp (°C)	Resin set time (sec)	Gap closure speed last 2 mm (sec/sec)	Press force (kN)	Mold curing time (sec)
35	50	130	0	1	3000	120
36	50	130	40	1	3000	120
37	50	130	40	1	3000	120
38	70	130	0	1	3000	120
40	70	130	0	1	3000	120
41	70	130	40	1	3000	120
42	70	130	40	1	3000	120
43	70	130	40	1	3000	120
44	60	130	40	1	3000	120
45	60	130	40	1	3000	120
46	60	130	40	1	3000	120
47	60	130	0	1	3000	120
48	60	130	0	1	3000	120
49	60	130	0	1	3000	120
52	60	110	0	1	3000	300
53	60	110	0	1	3000	300
54	60	110	0	1	3000	300
55	60	110	0	1	3000	300
56	60	110	0	1	3000	300
57	60	110	20	1	3000	300

Appendix 4: A developed spreadsheet for the plaques screening

Plaque number	Dry spot	Shifted preforms
1	Yes	
2		
3		
4		
5		
6		
7		
8		
9		
10		
16		
17	Yes	
18		
19		Yes
20		Yes
21		Yes
22		Yes
23	Yes	
24		
25		
26		
27		
28		
29		
30		
31		
32		
34		
35		Yes

Plaque number	Dry spot	Shifted preforms
36	Yes	
37		Yes
38		
40		
41		
42	Yes	Yes
43		
44		
45		
46		
47		Yes
48		Yes
49		
52		Yes
53	Yes	Yes
54		
55		Yes
56		
57		Yes

Appendix 5: Flexural properties of produced plaques-sampling area A

Sample	Specimen No.	Width (mm)	Thickness (mm)	Span (mm)	Strength (MPa)	Strain @ break (mm/mm)	Flexural Modulus (MPa)
2-A-RC	1	11.93	1.22	39.36	2.95E+02	3.04E-02	1.18E+04
	2	11.94	1.24		2.99E+02	3.06E-02	1.23E+04
	3	11.9	1.2		3.62E+02	2.95E-02	1.50E+04
	4	11.93	1.22		2.87E+02	3.07E-02	1.15E+04
	5	11.95	1.26		3.01E+02	2.91E-02	1.22E+04
Average					3.09E+02	3.01E-02	1.26E+04
Standard Deviation					3.00E+01	7.23E-04	1.39E+03

Sample	Specimen No.	Width (mm)	Thickness (mm)	Span (mm)	Strength (MPa)	Strain @ break (mm/mm)	Flexural Modulus (MPa)
3-A-RC	1	11.92	1.2	39.04	3.50E+02	2.87E-02	1.42E+04
	2	11.92	1.23		3.53E+02	2.99E-02	1.48E+04
	3	11.92	1.21		3.60E+02	2.76E-02	1.49E+04
	4	11.89	1.2		3.65E+02	2.74E-02	1.50E+04
	5	11.9	1.24		3.29E+02	2.82E-02	1.35E+04
Average					3.52E+02	2.84E-02	1.45E+04
Standard Deviation					1.37E+01	1.03E-03	6.45E+02

Sample	Specimen No.	Width (mm)	Thickness (mm)	Span (mm)	Strength (MPa)	Strain @ break (mm/mm)	Flexural Modulus (MPa)
4-A-RC	1	11.93	1.2	39.04	3.70E+02	2.94E-02	1.48E+04
	2	11.92	1.24		3.09E+02	3.05E-02	1.22E+04
	3	11.91	1.22		3.82E+02	2.73E-02	1.61E+04
	4	11.9	1.18		3.95E+02	2.95E-02	1.65E+04
	5	11.92	1.25		3.20E+02	2.78E-02	1.30E+04
Average					3.55E+02	2.89E-02	1.45E+04
Standard Deviation					3.85E+01	1.33E-03	1.87E+03

Sample	Specimen No.	Width (mm)	Thickness (mm)	Span (mm)	Strength (MPa)	Strain @ break (mm/mm)	Flexural Modulus (MPa)
5-A-RC	1	11.93	1.2	38.72	3.33E+02	3.03E-02	1.36E+04
	2	11.94	1.21		1.80E+03	3.68E-02	1.32E+04
	3	11.92	1.18		3.92E+02	2.93E-02	1.66E+04
	4	11.92	1.21		3.94E+02	3.41E-02	1.52E+04
	5	11.92	1.24		3.17E+02	2.96E-02	1.32E+04
					6.47E+02	3.20E-02	1.43E+04
Standard Deviation					6.46E+02	3.29E-03	1.51E+03

Sample	Specimen No.	Width (mm)	Thickness (mm)	Span (mm)	Strength (MPa)	Strain @ break (mm/mm)	Flexural Modulus (MPa)
6-A-RC	1	11.93	1.2	37.12	3.30E+02	3.09E-02	1.31E+04
	2	11.94	1.18		3.66E+02	3.40E-02	1.17E+04
	3	11.9	1.15		4.16E+02	3.02E-02	1.71E+04
	4	11.9	1.15		4.29E+02	3.26E-02	1.72E+04
	5	11.9	1.16		3.58E+02	2.85E-02	1.41E+04
Average					3.80E+02	3.12E-02	1.46E+04
Standard Deviation					4.14E+01	2.13E-03	2.45E+03

Sample	Specimen No.	Width (mm)	Thickness (mm)	Span (mm)	Strength (MPa)	Strain @ break (mm/mm)	Flexural Modulus (MPa)
7-A-RC	1	11.92	1.17	38.08	3.14E+02	2.94E-02	1.24E+04
	2	11.94	1.19		2.92E+02	2.75E-02	1.19E+04
	3	11.88	1.18		4.35E+02	2.47E-02	1.90E+04
	4	11.89	1.17		4.15E+02	3.07E-02	1.67E+04
	5	11.92	1.23		3.30E+02	2.78E-02	1.33E+04
Average					3.57E+02	2.80E-02	1.46E+04
Standard Deviation					6.37E+01	2.28E-03	3.08E+03

Sample	Specimen No.	Width (mm)	Thickness (mm)	Span (mm)	Strength (MPa)	Strain @ break (mm/mm)	Flexural Modulus (MPa)
8-A-RC	1	11.91	1.24	40.96	4.91E+02	3.37E-02	1.17E+04
	2	11.95	1.28		4.10E+02	3.48E-02	1.13E+04
	3	11.93	1.29		3.89E+02	2.77E-02	1.60E+04
	4	11.92	1.24		4.65E+02	3.37E-02	1.25E+04
	5	11.92	1.29		3.06E+02	3.07E-02	1.20E+04
Average					4.12E+02	3.21E-02	1.27E+04
Standard Deviation					7.24E+01	2.92E-03	1.92E+03

Sample	Specimen No.	Width (mm)	Thickness (mm)	Span (mm)	Strength (MPa)	Strain @ break (mm/mm)	Flexural Modulus (MPa)
9-A-RC	1	11.96	1.4	45.76	3.43E+02	2.92E-02	1.44E+04
	2	11.99	1.45		2.46E+02	2.94E-02	1.04E+04
	3	11.94	1.44		2.79E+02	3.13E-02	1.14E+04
	4	11.93	1.4		3.58E+02	3.02E-02	1.52E+04
	5	11.96	1.44		2.36E+02	2.54E-02	1.03E+04
Average					2.92E+02	2.91E-02	1.23E+04
Standard Deviation					5.56E+01	2.20E-03	2.31E+03

Sample	Specimen No.	Width (mm)	Thickness (mm)	Span (mm)	Strength (MPa)	Strain @ break (mm/mm)	Flexural Modulus (MPa)
10-A-RC	1	11.95	1.32	42.56	2.64E+02	3.27E-02	1.05E+04
	2	11.95	1.33		2.97E+02	2.86E-02	1.23E+04
	3	11.91	1.33		3.32E+02	2.70E-02	1.42E+04
	4	11.93	1.31		3.50E+02	3.30E-02	1.42E+04
	5	11.93	1.36		2.88E+02	2.98E-02	1.17E+04
Average					3.06E+02	3.02E-02	1.26E+04
Standard Deviation					3.48E+01	2.59E-03	1.62E+03

Sample	Specimen No.	Width (mm)	Thickness (mm)	Span (mm)	Strength (MPa)	Strain @ break (mm/mm)	Flexural Modulus (MPa)
16-A-RC	1	11.94	1.25	38.72	2.91E+02	3.13E-02	1.15E+04
	2	11.93	1.23		3.52E+02	3.21E-02	1.43E+04
	3	11.92	1.2		3.71E+02	3.13E-02	1.52E+04
	4	11.93	1.19		3.31E+02	3.06E-02	1.30E+04
	5	11.95	1.21		3.75E+02	3.38E-02	1.28E+04
Average					3.44E+02	3.18E-02	1.34E+04
Standard Deviation					3.42E+01	1.23E-03	1.43E+03

Sample	Specimen No.	Width (mm)	Thickness (mm)	Span (mm)	Strength (MPa)	Strain @ break (mm/mm)	Flexural Modulus (MPa)
25-A-RC	1	11.93	1.24	40.64	7.00E+02	3.42E-02	1.12E+04
	2	11.94	1.28		3.56E+02	3.53E-02	1.22E+04
	3	11.91	1.26		4.07E+02	3.45E-02	1.30E+04
	4	11.91	1.25		3.59E+02	3.36E-02	1.21E+04
	5	11.92	1.3		3.26E+02	3.16E-02	1.35E+04
Average					4.30E+02	3.39E-02	1.24E+04
Standard Deviation					1.54E+02	1.40E-03	8.63E+02

Sample	Specimen No.	Width (mm)	Thickness (mm)	Span (mm)	Strength (MPa)	Strain @ break (mm/mm)	Flexural Modulus (MPa)
26-A-RC	1	11.93	1.23	40.32	3.16E+02	2.89E-02	1.32E+04
	2	11.94	1.28		3.46E+02	3.41E-02	1.44E+04
	3	11.92	1.26		4.54E+02	3.53E-02	1.23E+04
	4	11.91	1.24		4.24E+02	3.46E-02	1.40E+04
	5	11.93	1.29		3.51E+02	3.15E-02	1.47E+04
Average					3.78E+02	3.29E-02	1.37E+04
Standard Deviation					5.81E+01	2.68E-03	9.93E+02

Sample	Specimen No.	Width (mm)	Thickness (mm)	Span (mm)	Strength (MPa)	Strain @ break (mm/mm)	Flexural Modulus (MPa)
27-A-RC	1	11.91	1.27	41.6	2.81E+02	3.16E-02	1.12E+04
	2	11.94	1.32		2.79E+02	2.50E-02	1.20E+04
	3	11.92	1.3		2.74E+02	2.52E-02	1.18E+04
	4	11.91	1.27		2.62E+02	2.78E-02	1.09E+04
	5	11.93	1.32		2.88E+02	2.70E-02	1.26E+04
Average					2.77E+02	2.73E-02	1.17E+04
Standard Deviation					9.68E+00	2.66E-03	6.62E+02

Sample	Specimen No.	Width (mm)	Thickness (mm)	Span (mm)	Strength (MPa)	Strain @ break (mm/mm)	Flexural Modulus (MPa)
28-A-RC	1	11.94	1.27	41.6	3.00E+02	3.35E-02	9.42E+03
	2	11.97	1.31		3.36E+02	3.45E-02	1.49E+04
	3	11.93	1.3		3.01E+02	3.41E-02	1.36E+04
	4	11.92	1.28		3.02E+02	3.36E-02	1.32E+04
	5	11.92	1.33		2.31E+02	3.50E-02	1.02E+04
Average					2.94E+02	3.41E-02	1.23E+04
Standard Deviation					3.83E+01	6.62E-04	2.34E+03

Sample	Specimen No.	Width (mm)	Thickness (mm)	Span (mm)	Strength (MPa)	Strain @ break (mm/mm)	Flexural Modulus (MPa)
29-A-RC	1	12.34	1.31	42.88	2.84E+02	3.25E-02	9.13E+03
	2	12.36	1.36		2.65E+02	3.32E-02	9.80E+03
	3	12.35	1.33		3.04E+02	3.25E-02	1.11E+04
	4	12.28	1.32		2.77E+02	3.27E-02	1.04E+04
	5	12.21	1.37		2.57E+02	3.33E-02	9.72E+03
Average					2.77E+02	3.28E-02	1.00E+04
Standard Deviation					1.84E+01	3.65E-04	7.60E+02

Sample	Specimen No.	Width (mm)	Thickness (mm)	Span (mm)	Strength (MPa)	Strain @ break (mm/mm)	Flexural Modulus (MPa)
31-A-RC	1	12.36	1.4	45.44	2.09E+02	2.94E-02	7.48E+03
	2	12.41	1.42		1.72E+02	2.40E-02	7.07E+03
	3	12.39	1.42		2.54E+02	3.04E-02	9.75E+03
	4	12.37	1.38		1.75E+02	3.05E-02	6.51E+03
	5	12.36	1.43		1.79E+02	2.98E-02	7.10E+03
Average					1.98E+02	2.88E-02	7.58E+03
Standard Deviation					3.49E+01	2.73E-03	1.26E+03

Sample	Specimen No.	Width (mm)	Thickness (mm)	Span (mm)	Strength (MPa)	Strain @ break (mm/mm)	Flexural Modulus (MPa)
32-A-RC	1	12.35	1.25	40.64	3.80E+02	3.26E-02	1.05E+04
	2	12.39	1.27		5.03E+02	3.50E-02	1.09E+04
	3	12.33	1.27		3.87E+02	3.38E-02	1.05E+04
	4	12.33	1.24		8.27E+02	3.42E-02	1.05E+04
	5	12.33	1.29		2.75E+02	2.98E-02	1.05E+04
Average					4.74E+02	3.31E-02	1.06E+04
Standard Deviation					2.13E+02	2.04E-03	1.91E+02

Sample	Specimen No.	Width (mm)	Thickness (mm)	Span (mm)	Strength (MPa)	Strain @ break (mm/mm)	Flexural Modulus (MPa)
34-A-RC	1	12.33	1.26	41.28	3.68E+02	3.30E-02	1.08E+04
	2	12.4	1.27		3.34E+02	3.31E-02	1.22E+04
	3	12.43	1.28		3.81E+02	3.39E-02	1.02E+04
	4	12.34	1.25		4.14E+02	3.35E-02	1.19E+04
	5	12.34	1.32		3.40E+02	3.53E-02	9.60E+03
Average					3.67E+02	3.38E-02	1.09E+04
Standard Deviation					3.24E+01	9.56E-04	1.11E+03

Sample	Specimen No.	Width (mm)	Thickness (mm)	Span (mm)	Strength (MPa)	Strain @ break (mm/mm)	Flexural Modulus (MPa)
38-A-RC	1	12.35	1.34	43.84	2.99E+02	3.01E-02	1.14E+04
	2	12.39	1.39		2.54E+02	3.01E-02	9.35E+03
	3	12.31	1.35		2.93E+02	3.00E-02	1.15E+04
	4	12.32	1.35		2.78E+02	2.39E-02	1.19E+04
	5	12.34	1.38		2.82E+02	2.60E-02	1.10E+04
Average					2.82E+02	2.80E-02	1.10E+04
Standard Deviation					1.73E+01	2.90E-03	9.84E+02

Sample	Specimen No.	Width (mm)	Thickness (mm)	Span (mm)	Strength (MPa)	Strain @ break (mm/mm)	Flexural Modulus (MPa)
40-A-RC	1	12.37	1.35	43.84	2.52E+02	3.20E-02	9.10E+03
	2	12.36	1.38		2.69E+02	3.27E-02	1.00E+04
	3	12.32	1.36		2.88E+02	3.06E-02	1.10E+04
	4	12.3	1.35		2.77E+02	3.04E-02	1.05E+04
	5	12.2	1.38		2.53E+02	2.99E-02	9.77E+03
Average					2.68E+02	3.11E-02	1.01E+04
Standard Deviation					1.54E+01	1.18E-03	7.10E+02

Sample	Specimen No.	Width (mm)	Thickness (mm)	Span (mm)	Strength (MPa)	Strain @ break (mm/mm)	Flexural Modulus (MPa)
41-A-RC	1	12.4	1.42	45.12	2.07E+02	2.27E-02	9.04E+03
	2	12.37	1.44		2.57E+02	3.11E-02	1.03E+04
	3	12.34	1.38		2.20E+02	2.92E-02	8.87E+03
	4	12.35	1.39		2.21E+02	2.62E-02	8.96E+03
	5	12.34	1.39		2.54E+02	2.99E-02	1.01E+04
Average					2.32E+02	2.78E-02	9.46E+03
Standard Deviation					2.25E+01	3.37E-03	6.92E+02

Sample	Specimen No.	Width (mm)	Thickness (mm)	Span (mm)	Strength (MPa)	Strain @ break (mm/mm)	Flexural Modulus (MPa)
43-A-RC	1	12.32	1.41	46.72	2.89E+02	2.94E-02	1.22E+04
	2	12.34	1.47		2.62E+02	2.87E-02	1.08E+04
	3	12.31	1.47		2.37E+02	2.71E-02	9.84E+03
	4	12.33	1.43		2.41E+02	2.78E-02	1.02E+04
	5	12.33	1.48		2.65E+02	2.79E-02	1.07E+04
Average					2.59E+02	2.82E-02	1.07E+04
Standard Deviation					2.09E+01	9.04E-04	8.88E+02

Sample	Specimen No.	Width (mm)	Thickness (mm)	Span (mm)	Strength (MPa)	Strain @ break (mm/mm)	Flexural Modulus (MPa)
44-A-RC	1	12.37	1.42	46.72	3.07E+02	2.83E-02	1.30E+04
	2	12.39	1.5		2.37E+02	3.12E-02	9.60E+03
	3	12.34	1.44		2.12E+02	2.76E-02	9.28E+03
	4	12.34	1.44		2.44E+02	2.92E-02	1.02E+04
	5	12.36	1.49		2.39E+02	2.63E-02	1.00E+04
Average					2.48E+02	2.85E-02	1.04E+04
Standard Deviation					3.52E+01	1.83E-03	1.48E+03

Sample	Specimen No.	Width (mm)	Thickness (mm)	Span (mm)	Strength (MPa)	Strain @ break (mm/mm)	Flexural Modulus (MPa)
45-A-RC	1	12.36	1.4	45.76	2.87E+02	3.00E-02	1.14E+04
	2	12.34	1.44		2.71E+02	2.90E-02	1.06E+04
	3	12.29	1.41		2.34E+02	3.06E-02	9.45E+03
	4	12.3	1.4		2.01E+02	2.38E-02	8.10E+03
	5	12.29	1.45		2.43E+02	3.02E-02	9.62E+03
Average					2.47E+02	2.87E-02	9.83E+03
Standard Deviation					3.34E+01	2.80E-03	1.24E+03

Sample	Specimen No.	Width (mm)	Thickness (mm)	Span (mm)	Strength (MPa)	Strain @ break (mm/mm)	Flexural Modulus (MPa)
49-A-RC	1	12.38	1.36	45.12	2.22E+02	3.04E-02	9.41E+03
	2	12.37	1.42		2.04E+02	2.93E-02	8.27E+03
	3	12.32	1.39		2.34E+02	2.86E-02	1.01E+04
	4	12.33	1.41		1.99E+02	3.13E-02	7.87E+03
	5	12.36	1.42		1.89E+02	2.72E-02	7.64E+03
Average					2.09E+02	2.94E-02	8.66E+03
Standard Deviation					1.82E+01	1.61E-03	1.05E+03

Sample	Specimen No.	Width (mm)	Thickness (mm)	Span (mm)	Strength (MPa)	Strain @ break (mm/mm)	Flexural Modulus (MPa)
54-A-RC	1	12.3	1.43	46.4	3.26E+02	2.63E-02	1.35E+04
	2	12.38	1.49		2.69E+02	3.15E-02	1.07E+04
	3	12.38	1.45		2.46E+02	2.94E-02	1.03E+04
	4	12.35	1.43		2.51E+02	2.75E-02	1.09E+04
	5	12.36	1.45		2.44E+02	3.07E-02	9.93E+03
Average					2.67E+02	2.91E-02	1.11E+04
Standard Deviation					3.43E+01	2.18E-03	1.42E+03

Sample	Specimen No.	Width (mm)	Thickness (mm)	Span (mm)	Strength (MPa)	Strain @ break (mm/mm)	Flexural Modulus (MPa)
56-A-RC	1	12.32	1.19	38.72	1.63E+03	3.61E-02	1.38E+04
	2	12.31	1.2		3.54E+02	2.99E-02	1.37E+04
	3	12.31	1.2		7.95E+02	3.57E-02	1.30E+04
	4	12.26	1.19		3.59E+02	2.75E-02	1.40E+04
	5	12.33	1.23		4.04E+02	3.43E-02	1.49E+04
Average					7.09E+02	3.27E-02	1.39E+04
Standard Deviation					5.48E+02	3.82E-03	6.82E+02

Appendix 6: Flexural properties of produced plaques-sampling area B

Sample	Specimen No.	Width (mm)	Thickness (mm)	Span (mm)	Strength (MPa)	Strain @ break (mm/mm)	Flexural Modulus (MPa)
2-B-L	1	11.97	1.16	37.12	3.28E+02	3.28E-02	1.19E+04
	2	11.95	1.16		4.01E+02	3.02E-02	1.69E+04
	3	11.98	1.16		3.02E+02	2.68E-02	1.08E+04
	4	11.95	1.15		2.55E+02	2.44E-02	1.29E+04
	5	11.97	1.15		3.57E+02	3.26E-02	1.35E+04
Average					3.29E+02	2.93E-02	1.32E+04
Standard Deviation					5.51E+01	3.70E-03	2.33E+03

Sample	Specimen No.	Width (mm)	Thickness (mm)	Span (mm)	Strength (MPa)	Strain @ break (mm/mm)	Flexural Modulus (MPa)
3-B-L	1	11.96	1.14	36.48	2.90E+02	2.41E-02	1.35E+04
	2	11.95	1.15		3.48E+02	2.88E-02	1.57E+04
	3	11.93	1.15		3.67E+02	2.75E-02	1.62E+04
	4	11.93	1.14		3.54E+02	3.20E-02	1.44E+04
	5	11.94	1.14		3.43E+02	2.97E-02	1.43E+04
Average					3.40E+02	2.84E-02	1.48E+04
Standard Deviation					2.96E+01	2.89E-03	1.07E+03

Sample	Specimen No.	Width (mm)	Thickness (mm)	Span (mm)	Strength (MPa)	Strain @ break (mm/mm)	Flexural Modulus (MPa)
4-B-L	1	11.95	1.14	36.16	3.30E+02	2.91E-02	1.39E+04
	2	11.96	1.13		2.86E+02	2.89E-02	1.23E+04
	3	11.95	1.14		3.36E+02	2.14E-02	1.60E+04
	4	11.91	1.13		3.58E+02	2.87E-02	1.56E+04
	5	11.93	1.13		3.57E+02	2.70E-02	1.61E+04
Average					3.33E+02	2.70E-02	1.48E+04
Standard Deviation					2.94E+01	3.24E-03	1.61E+03

Sample	Specimen No.	Width (mm)	Thickness (mm)	Span (mm)	Strength (MPa)	Strain @ break (mm/mm)	Flexural Modulus (MPa)
5-B-L	1	11.97	1.13	36.16	3.40E+02	2.74E-02	1.46E+04
	2	11.94	1.14		3.52E+02	3.03E-02	1.45E+04
	3	11.92	1.14		3.42E+02	2.92E-02	1.37E+04
	4	11.95	1.13		3.13E+02	3.01E-02	1.25E+04
	5	11.99	1.12		3.52E+02	2.79E-02	1.51E+04
Average					3.40E+02	2.90E-02	1.41E+04
Standard Deviation					1.60E+01	1.29E-03	1.04E+03

Sample	Specimen No.	Width (mm)	Thickness (mm)	Span (mm)	Strength (MPa)	Strain @ break (mm/mm)	Flexural Modulus (MPa)
6-B-L	1	11.94	1.09	35.2	3.29E+02	3.01E-02	1.33E+04
	2	11.93	1.09		2.78E+02	2.68E-02	1.15E+04
	3	11.93	1.1		4.04E+02	3.40E-02	1.41E+04
	4	11.92	1.09		4.11E+02	3.23E-02	1.59E+04
	5	11.95	1.1		3.04E+02	2.78E-02	1.24E+04
Average					3.45E+02	3.02E-02	1.34E+04
Standard Deviation					5.96E+01	3.00E-03	1.68E+03

Sample	Specimen No.	Width (mm)	Thickness (mm)	Span (mm)	Strength (MPa)	Strain @ break (mm/mm)	Flexural Modulus (MPa)
7-B-L	1	11.96	1.1	35.2	3.77E+02	3.25E-02	1.09E+04
	2	11.95	1.11		3.75E+02	3.33E-02	1.17E+04
	3	11.96	1.1		4.26E+02	2.66E-02	1.80E+04
	4	11.95	1.1		5.40E+02	3.46E-02	1.39E+04
	5	11.93	1.09		3.50E+02	3.21E-02	1.21E+04
Average					4.13E+02	3.18E-02	1.33E+04
Standard Deviation					7.58E+01	3.05E-03	2.84E+03

Sample	Specimen No.	Width (mm)	Thickness (mm)	Span (mm)	Strength (MPa)	Strain @ break (mm/mm)	Flexural Modulus (MPa)
8-B-L	1	11.94	1.16	37.44	3.01E+02	2.80E-02	1.33E+04
	2	11.96	1.17		2.65E+02	3.02E-02	1.12E+04
	3	11.94	1.18		3.67E+02	2.73E-02	1.64E+04
	4	11.94	1.18		2.97E+02	3.11E-02	1.26E+04
	5	11.95	1.17		2.51E+02	2.96E-02	1.07E+04
Average					2.96E+02	2.93E-02	1.29E+04
Standard Deviation					4.47E+01	1.57E-03	2.24E+03

Sample	Specimen No.	Width (mm)	Thickness (mm)	Span (mm)	Strength (MPa)	Strain @ break (mm/mm)	Flexural Modulus (MPa)
9-B-L	1	11.97	1.28	40.96	3.28E+02	2.69E-02	1.47E+04
	2	11.96	1.29		1.65E+02	2.09E-02	7.24E+03
	3	11.95	1.28		2.95E+02	3.21E-02	1.11E+04
	4	11.95	1.28		3.00E+02	3.31E-02	1.19E+04
	5	11.94	1.27		3.31E+02	3.45E-02	1.02E+04
Average					2.84E+02	2.95E-02	1.10E+04
Standard Deviation					6.83E+01	5.62E-03	2.69E+03

Sample	Specimen No.	Width (mm)	Thickness (mm)	Span (mm)	Strength (MPa)	Strain @ break (mm/mm)	Flexural Modulus (MPa)
10-B-L	1	11.98	1.24	39.68	2.65E+02	3.05E-02	1.15E+04
	2	11.98	1.24		3.11E+02	3.17E-02	1.34E+04
	3	11.95	1.24		3.51E+02	2.99E-02	1.52E+04
	4	11.93	1.24		3.69E+02	3.39E-02	1.51E+04
	5	11.96	1.23		3.99E+02	3.56E-02	1.32E+04
Average					3.39E+02	3.24E-02	1.37E+04
Standard Deviation					5.23E+01	2.37E-03	1.53E+03

Sample	Specimen No.	Width (mm)	Thickness (mm)	Span (mm)	Strength (MPa)	Strain @ break (mm/mm)	Flexural Modulus (MPa)
16-B-L	1	11.94	1.14	36.8	3.76E+02	3.11E-02	1.38E+04
	2	11.95	1.14		4.00E+02	3.09E-02	1.61E+04
	3	11.92	1.15		3.21E+02	3.31E-02	1.24E+04
	4	11.91	1.13		3.67E+02	3.25E-02	1.28E+04
	5	11.94	1.14		3.30E+02	2.82E-02	1.34E+04
Average					3.59E+02	3.12E-02	1.37E+04
Standard Deviation					3.30E+01	1.89E-03	1.43E+03

Sample	Specimen No.	Width (mm)	Thickness (mm)	Span (mm)	Strength (MPa)	Strain @ break (mm/mm)	Flexural Modulus (MPa)
25-B-L	1	11.95	1.18	38.08	2.59E+02	3.15E-02	8.24E+03
	2	11.95	1.19		2.65E+02	3.20E-02	1.02E+04
	3	11.93	1.19		2.85E+02	3.11E-02	1.13E+04
	4	11.91	1.19		3.21E+02	3.02E-02	1.30E+04
	5	11.92	1.19		2.72E+02	3.20E-02	1.06E+04
Average					2.80E+02	3.14E-02	1.07E+04
Standard Deviation					2.49E+01	7.48E-04	1.74E+03

Sample	Specimen No.	Width (mm)	Thickness (mm)	Span (mm)	Strength (MPa)	Strain @ break (mm/mm)	Flexural Modulus (MPa)
26-B-L	1	11.95	1.19	37.44	3.60E+02	2.63E-02	1.59E+04
	2	11.95	1.18		3.13E+02	2.61E-02	1.32E+04
	3	11.93	1.18		3.05E+02	3.08E-02	1.26E+04
	4	11.93	1.16		3.63E+02	3.20E-02	1.44E+04
	5	11.94	1.17		3.68E+02	2.79E-02	1.53E+04
Average					3.42E+02	2.86E-02	1.42E+04
Standard Deviation					3.02E+01	2.66E-03	1.38E+03

Sample	Specimen No.	Width (mm)	Thickness (mm)	Span (mm)	Strength (MPa)	Strain @ break (mm/mm)	Flexural Modulus (MPa)
27-B-L	1	11.93	1.18	38.08	2.98E+02	3.03E-02	1.22E+04
	2	11.96	1.19		3.07E+02	2.68E-02	1.31E+04
	3	11.93	1.19		3.33E+02	3.01E-02	1.41E+04
	4	11.92	1.2		3.04E+02	3.23E-02	1.23E+04
	5	11.94	1.19		3.58E+02	2.99E-02	1.54E+04
Average					3.20E+02	2.99E-02	1.34E+04
Standard Deviation					2.49E+01	1.98E-03	1.34E+03

Sample	Specimen No.	Width (mm)	Thickness (mm)	Span (mm)	Strength (MPa)	Strain @ break (mm/mm)	Flexural Modulus (MPa)
28-B-L	1	11.96	1.18	38.08	2.83E+02	2.03E-02	1.12E+04
	2	11.94	1.2		3.71E+02	2.81E-02	1.58E+04
	3	11.92	1.2		2.93E+02	2.24E-02	1.51E+04
	4	11.93	1.2		2.86E+02	2.65E-02	1.22E+04
	5	11.96	1.18		2.72E+02	2.33E-02	1.26E+04
Average					3.01E+02	2.41E-02	1.34E+04
Standard Deviation					3.99E+01	3.18E-03	1.99E+03

Sample	Specimen No.	Width (mm)	Thickness (mm)	Span (mm)	Strength (MPa)	Strain @ break (mm/mm)	Flexural Modulus (MPa)
29-B-L	1	11.96	1.2	38.4	2.76E+02	2.82E-02	1.13E+04
	2	11.94	1.19		3.32E+02	2.95E-02	1.37E+04
	3	11.94	1.2		3.38E+02	3.13E-02	1.33E+04
	4	11.9	1.21		2.94E+02	3.14E-02	1.12E+04
	5	11.94	1.19		2.93E+02	2.70E-02	1.21E+04
Average					3.06E+02	2.95E-02	1.23E+04
Standard Deviation					2.70E+01	1.94E-03	1.13E+03

Sample	Specimen No.	Width (mm)	Thickness (mm)	Span (mm)	Strength (MPa)	Strain @ break (mm/mm)	Flexural Modulus (MPa)
31-B-L	1	11.94	1.19	37.76	3.57E+02	3.00E-02	1.49E+04
	2	11.95	1.19		2.88E+02	2.68E-02	1.22E+04
	3	11.94	1.19		3.28E+02	2.76E-02	1.45E+04
	4	11.94	1.18		2.95E+02	2.58E-02	1.26E+04
	5	11.94	1.18		2.56E+02	2.72E-02	1.05E+04
Average					3.05E+02	2.75E-02	1.30E+04
Standard Deviation					3.90E+01	1.56E-03	1.81E+03

Sample	Specimen No.	Width (mm)	Thickness (mm)	Span (mm)	Strength (MPa)	Strain @ break (mm/mm)	Flexural Modulus (MPa)
32-B-L	1	11.95	1.17	37.76	2.28E+02	3.19E-02	7.05E+03
	2	11.95	1.19		2.80E+02	3.25E-02	1.22E+04
	3	11.96	1.19		2.69E+02	3.14E-02	1.17E+04
	4	11.92	1.18		2.56E+02	2.86E-02	1.11E+04
	5	11.95	1.16		2.54E+02	2.53E-02	1.20E+04
Average					2.57E+02	2.99E-02	1.08E+04
Standard Deviation					1.94E+01	3.00E-03	2.15E+03

Sample	Specimen No.	Width (mm)	Thickness (mm)	Span (mm)	Strength (MPa)	Strain @ break (mm/mm)	Flexural Modulus (MPa)
34-B-L	1	11.94	1.17	37.44	3.06E+02	2.91E-02	1.18E+04
	2	11.95	1.19		3.30E+02	3.07E-02	1.38E+04
	3	11.94	1.17		3.48E+02	3.26E-02	1.35E+04
	4	11.92	1.18		3.84E+02	3.28E-02	1.56E+04
	5	11.93	1.17		3.58E+02	3.21E-02	1.41E+04
Average					3.45E+02	3.15E-02	1.38E+04
Standard Deviation					2.94E+01	1.53E-03	1.35E+03

Sample	Specimen No.	Width (mm)	Thickness (mm)	Span (mm)	Strength (MPa)	Strain @ break (mm/mm)	Flexural Modulus (MPa)
38-B-L	1	11.94	1.24	39.36	3.86E+02	3.65E-02	1.35E+04
	2	11.95	1.24		3.22E+02	3.53E-02	1.07E+04
	3	11.94	1.23		3.33E+02	3.23E-02	1.43E+04
	4	11.95	1.23		3.03E+02	3.31E-02	1.24E+04
	5	11.96	1.22		2.51E+02	3.02E-02	1.04E+04
Average					3.19E+02	3.35E-02	1.23E+04
Standard Deviation					4.88E+01	2.50E-03	1.70E+03

Sample	Specimen No.	Width (mm)	Thickness (mm)	Span (mm)	Strength (MPa)	Strain @ break (mm/mm)	Flexural Modulus (MPa)
40-B-L	1	11.94	1.23	39.68	2.45E+02	3.18E-02	1.09E+04
	2	11.96	1.25		6.44E+02	3.62E-02	1.01E+04
	3	11.94	1.24		2.59E+02	3.07E-02	1.18E+04
	4	11.93	1.24		2.62E+02	2.48E-02	1.27E+04
	5	11.96	1.23		2.60E+02	2.87E-02	1.21E+04
Average					3.34E+02	3.04E-02	1.15E+04
Standard Deviation					1.73E+02	4.18E-03	1.04E+03

Sample	Specimen No.	Width (mm)	Thickness (mm)	Span (mm)	Strength (MPa)	Strain @ break (mm/mm)	Flexural Modulus (MPa)
41-B-L	1	11.97	1.26	40	3.14E+02	3.00E-02	1.30E+04
	2	11.97	1.25		2.93E+02	2.81E-02	1.23E+04
	3	11.94	1.25		3.30E+02	2.86E-02	1.27E+04
	4	11.95	1.25		3.17E+02	3.38E-02	1.08E+04
	5	11.96	1.25		2.75E+02	3.32E-02	9.88E+03
Average					3.06E+02	3.07E-02	1.17E+04
Standard Deviation					2.16E+01	2.61E-03	1.33E+03

Sample	Specimen No.	Width (mm)	Thickness (mm)	Span (mm)	Strength (MPa)	Strain @ break (mm/mm)	Flexural Modulus (MPa)
43-B-L	1	11.98	1.28	40.96	2.63E+02	2.94E-02	1.10E+04
	2	11.97	1.27		2.86E+02	3.45E-02	1.17E+04
	3	11.96	1.29		2.48E+02	2.40E-02	1.05E+04
	4	11.97	1.29		3.15E+02	3.47E-02	1.26E+04
	5	11.97	1.28		2.83E+02	3.06E-02	1.16E+04
Average					2.79E+02	3.06E-02	1.15E+04
Standard Deviation					2.54E+01	4.38E-03	7.91E+02

Sample	Specimen No.	Width (mm)	Thickness (mm)	Span (mm)	Strength (MPa)	Strain @ break (mm/mm)	Flexural Modulus (MPa)
44-B-L	1	11.95	1.28	40.64	3.40E+02	2.63E-02	1.45E+04
	2	11.96	1.28		2.92E+02	2.85E-02	1.26E+04
	3	11.95	1.27		2.64E+02	3.00E-02	1.09E+04
	4	11.95	1.27		3.21E+02	2.88E-02	1.38E+04
	5	11.96	1.27		2.85E+02	2.72E-02	1.23E+04
Average					3.00E+02	2.82E-02	1.28E+04
Standard Deviation					2.99E+01	1.44E-03	1.39E+03

Sample	Specimen No.	Width (mm)	Thickness (mm)	Span (mm)	Strength (MPa)	Strain @ break (mm/mm)	Flexural Modulus (MPa)
45-B-L	1	11.97	1.28	40.96	3.01E+02	3.47E-02	1.25E+04
	2	11.97	1.29		2.41E+02	3.02E-02	1.10E+04
	3	11.95	1.29		2.24E+02	3.48E-02	9.39E+03
	4	11.96	1.28		2.58E+02	3.43E-02	1.19E+04
	5	11.93	1.28		2.65E+02	3.48E-02	1.19E+04
Average					2.58E+02	3.38E-02	1.13E+04
Standard Deviation					2.89E+01	1.99E-03	1.21E+03

Sample	Specimen No.	Width (mm)	Thickness (mm)	Span (mm)	Strength (MPa)	Strain @ break (mm/mm)	Flexural Modulus (MPa)
46-B-L	1	11.97	1.27	40.64	3.01E+02	2.85E-02	1.26E+04
	2	11.95	1.27		3.35E+02	2.84E-02	1.44E+04
	3	11.93	1.27		3.10E+02	2.83E-02	1.34E+04
	4	11.94	1.28		3.02E+02	2.68E-02	1.30E+04
	5	11.96	1.27		3.04E+02	3.09E-02	1.31E+04
Average					3.11E+02	2.86E-02	1.33E+04
Standard Deviation					1.41E+01	1.48E-03	6.62E+02

Sample	Specimen No.	Width (mm)	Thickness (mm)	Span (mm)	Strength (MPa)	Strain @ break (mm/mm)	Flexural Modulus (MPa)
49-B-L	1	11.97	1.26	40.64	2.42E+02	2.95E-02	9.90E+03
	2	11.97	1.28		2.65E+02	3.01E-02	1.04E+04
	3	11.93	1.28		2.71E+02	2.73E-02	1.12E+04
	4	11.94	1.27		3.22E+02	3.51E-02	1.13E+04
	5	11.97	1.27		2.81E+02	3.23E-02	1.07E+04
Average					2.76E+02	3.08E-02	1.07E+04
Standard Deviation					2.97E+01	2.96E-03	5.77E+02

Sample	Specimen No.	Width (mm)	Thickness (mm)	Span (mm)	Strength (MPa)	Strain @ break (mm/mm)	Flexural Modulus (MPa)
54-B-L	1	11.96	1.35	42.88	3.51E+02	3.26E-02	1.41E+04
	2	11.95	1.34		2.49E+02	3.01E-02	1.01E+04
	3	11.96	1.33		3.04E+02	2.64E-02	1.36E+04
	4	11.95	1.35		3.39E+02	3.02E-02	1.38E+04
	5	11.97	1.34		2.81E+02	3.03E-02	1.12E+04
Average					3.05E+02	2.99E-02	1.25E+04
Standard Deviation					4.19E+01	2.23E-03	1.81E+03

Sample	Specimen No.	Width (mm)	Thickness (mm)	Span (mm)	Strength (MPa)	Strain @ break (mm/mm)	Flexural Modulus (MPa)
56-B-L	1	11.95	1.11	35.84	4.24E+02	3.35E-02	1.61E+04
	2	11.95	1.13		3.47E+02	3.17E-02	1.38E+04
	3	11.93	1.11		3.32E+02	2.69E-02	1.36E+04
	4	11.92	1.12		3.87E+02	3.35E-02	1.45E+04
	5	11.9	1.12		3.80E+02	3.29E-02	1.48E+04
Average					3.74E+02	3.17E-02	1.46E+04
Standard Deviation					3.59E+01	2.79E-03	9.99E+02

Appendix 7: Flexural properties of produced plaques-sampling area C

Sample	Specimen No.	Width (mm)	Thickness (mm)	Span (mm)	Strength (MPa)	Strain @ break (mm/mm)	Flexural Modulus (MPa)
2-C-LC	1	11.96	1.19	38.72	3.38E+02	2.69E-02	1.43E+04
	2	11.96	1.21		3.64E+02	3.01E-02	1.48E+04
	3	11.94	1.2		3.42E+02	3.11E-02	1.32E+04
	4	11.93	1.2		3.12E+02	2.78E-02	1.24E+04
	5	11.96	1.23		3.94E+02	2.83E-02	1.59E+04
Average					3.50E+02	2.88E-02	1.41E+04
Standard Deviation					3.07E+01	1.73E-03	1.38E+03

Sample	Specimen No.	Width (mm)	Thickness (mm)	Span (mm)	Strength (MPa)	Strain @ break (mm/mm)	Flexural Modulus (MPa)
3-C-LC	1	11.95	1.2	38.72	3.55E+02	2.82E-02	1.45E+04
	2	11.96	1.2		3.85E+02	3.04E-02	1.61E+04
	3	11.94	1.2		4.14E+02	3.30E-02	1.69E+04
	4	11.94	1.18		3.53E+02	2.99E-02	1.43E+04
	5	11.96	1.22		3.29E+02	3.29E-02	1.33E+04
Average					3.67E+02	3.09E-02	1.50E+04
Standard Deviation					3.30E+01	2.05E-03	1.44E+03

Sample	Specimen No.	Width (mm)	Thickness (mm)	Span (mm)	Strength (MPa)	Strain @ break (mm/mm)	Flexural Modulus (MPa)
4-C-LC	1	11.97	1.19	38.4	3.57E+02	3.29E-02	1.30E+04
	2	11.95	1.2		3.72E+02	3.36E-02	1.20E+04
	3	11.94	1.19		1.83E+03	3.68E-02	1.56E+04
	4	11.95	1.17		9.82E+02	3.57E-02	1.65E+04
	5	11.94	1.22		3.35E+02	3.14E-02	1.38E+04
Average					7.75E+02	3.41E-02	1.42E+04
Standard Deviation					6.49E+02	2.18E-03	1.85E+03

Sample	Specimen No.	Width (mm)	Thickness (mm)	Span (mm)	Strength (MPa)	Strain @ break (mm/mm)	Flexural Modulus (MPa)
5-C-LC	1	11.95	1.18	38.08	3.74E+02	2.90E-02	1.67E+04
	2	11.93	1.19		3.47E+02	3.00E-02	1.42E+04
	3	11.94	1.17		3.67E+02	3.05E-02	1.55E+04
	4	11.93	1.18		3.26E+02	2.94E-02	1.30E+04
	5	11.96	1.22		3.11E+02	3.06E-02	1.29E+04
Average					3.45E+02	2.99E-02	1.45E+04
Standard Deviation					2.70E+01	6.98E-04	1.64E+03

Sample	Specimen No.	Width (mm)	Thickness (mm)	Span (mm)	Strength (MPa)	Strain @ break (mm/mm)	Flexural Modulus (MPa)
6-C-LC	1	11.95	1.18	37.44	7.97E+02	3.69E-02	1.19E+04
	2	11.94	1.19		7.27E+02	3.67E-02	1.02E+04
		11.94	1.16		9.49E+02	3.77E-02	1.35E+04
	4	11.94	1.14		8.43E+02	3.64E-02	1.46E+04
	5	11.96	1.18		3.08E+02	3.20E-02	1.19E+04
Average					7.25E+02	3.59E-02	1.24E+04
Standard Deviation					2.46E+02	2.25E-03	1.69E+03

Sample	Specimen No.	Width (mm)	Thickness (mm)	Span (mm)	Strength (MPa)	Strain @ break (mm/mm)	Flexural Modulus (MPa)
7-C-LC		11.96	1.16	37.44	7.11E+02	3.77E-02	1.08E+04
	2	11.96	1.16		5.47E+02	3.50E-02	1.12E+04
	3	11.95	1.16		4.48E+02	3.16E-02	1.79E+04
	4	11.94	1.15		6.89E+02	3.61E-02	1.44E+04
	5	11.96	1.18		3.15E+02	3.31E-02	1.18E+04
Average					4.54E+03	3.47E-02	1.32E+04
Standard Deviation					9.04E+03	2.42E-03	2.96E+03

Sample	Specimen No.	Width (mm)	Thickness (mm)	Span (mm)	Strength (MPa)	Strain @ break (mm/mm)	Flexural Modulus (MPa)
8-C-LC	1	11.95	1.23	40	3.58E+02	3.48E-02	1.23E+04
	2	11.97	1.24		3.55E+02	3.53E-02	1.10E+04
	3	11.96	1.26		3.48E+02	3.59E-02	1.37E+04
	4	11.96	1.23		3.14E+02	3.44E-02	1.04E+04
	5	11.96	1.26		2.85E+02	3.07E-02	1.15E+04
Average					3.32E+02	3.42E-02	1.18E+04
Standard Deviation					3.16E+01	2.04E-03	1.27E+03

Sample	Specimen No.	Width (mm)	Thickness (mm)	Span (mm)	Strength (MPa)	Strain @ break (mm/mm)	Flexural Modulus (MPa)
9-C-LC	1	12	1.4	44.8	3.33E+02	2.94E-02	1.38E+04
	2	12	1.39		2.55E+02	2.98E-02	1.02E+04
	3	11.96	1.42		2.63E+02	3.22E-02	9.91E+03
	4	11.95	1.39		3.76E+02	3.08E-02	1.47E+04
	5	11.96	1.39		2.71E+02	2.96E-02	1.05E+04
Average					3.00E+02	3.04E-02	1.18E+04
Standard Deviation					5.26E+01	1.17E-03	2.25E+03

Sample	Specimen No.	Width (mm)	Thickness (mm)	Span (mm)	Strength (MPa)	Strain @ break (mm/mm)	Flexural Modulus (MPa)
10-C-LC	1	11.95	1.3	42.24	2.93E+02	3.32E-02	1.10E+04
	2	11.95	1.32		3.07E+02	3.37E-02	1.21E+04
	3	11.94	1.31		2.82E+02	2.56E-02	1.18E+04
	4	11.97	1.3		3.36E+02	3.31E-02	1.36E+04
	5	11.97	1.34		2.87E+02	3.15E-02	1.17E+04
Average					3.01E+02	3.14E-02	1.20E+04
Standard Deviation					2.19E+01	3.37E-03	9.72E+02

Sample	Specimen No.	Width (mm)	Thickness (mm)	Span (mm)	Strength (MPa)	Strain @ break (mm/mm)	Flexural Modulus (MPa)
16-C-LC	1	11.95	1.23	38.72	3.46E+02	3.25E-02	1.45E+04
	2	11.96	1.24		3.69E+02	3.58E-02	1.42E+04
	3	11.92	1.17		4.15E+02	3.28E-02	1.63E+04
	4	11.94	1.22		3.09E+02	3.30E-02	1.24E+04
	5	11.95	1.23		3.76E+02	3.53E-02	1.28E+04
Average					3.63E+02	3.39E-02	1.40E+04
Standard Deviation					3.94E+01	1.56E-03	1.56E+03

Sample	Specimen No.	Width (mm)	Thickness (mm)	Span (mm)	Strength (MPa)	Strain @ break (mm/mm)	Flexural Modulus (MPa)
25-C-LC	1	11.96	1.23	40	3.59E+02	3.50E-02	1.24E+04
	2	11.95	1.24		3.35E+02	3.11E-02	1.37E+04
	3	11.95	1.25		3.61E+02	3.39E-02	1.47E+04
	4	11.94	1.22		3.31E+02	3.39E-02	1.28E+04
	5	11.95	1.26		3.90E+02	2.92E-02	1.63E+04
Average					3.55E+02	3.26E-02	1.40E+04
Standard Deviation					2.38E+01	2.40E-03	1.57E+03

Sample	Specimen No.	Width (mm)	Thickness (mm)	Span (mm)	Strength (MPa)	Strain @ break (mm/mm)	Flexural Modulus (MPa)
26-C-LC	1	11.96	1.23	39.68	3.28E+02	3.12E-02	1.35E+04
	2	11.96	1.23		3.26E+02	2.92E-02	1.41E+04
	3	11.95	1.23		4.23E+02	3.56E-02	1.19E+04
	4	11.95	1.22		3.17E+02	2.72E-02	1.33E+04
	5	11.97	1.26		3.49E+02	3.63E-02	1.28E+04
Average					3.48E+02	3.19E-02	1.31E+04
Standard Deviation					4.31E+01	3.99E-03	8.33E+02

Sample	Specimen No.	Width (mm)	Thickness (mm)	Span (mm)	Strength (MPa)	Strain @ break (mm/mm)	Flexural Modulus (MPa)
27-C-LC	1	11.95	1.25	40.64	1.73E+03	3.43E-02	1.17E+04
	2	11.96	1.27		3.73E+02	2.96E-02	1.54E+04
	3	11.94	1.25		1.71E+03	3.45E-02	1.27E+04
	4	11.96	1.26		1.26E+03	3.48E-02	1.33E+04
	5	11.97	1.28		3.96E+02	3.27E-02	1.33E+04
Average					1.09E+03	3.32E-02	1.33E+04
Standard Deviation					6.74E+02	2.16E-03	1.37E+03

Sample	Specimen No.	Width (mm)	Thickness (mm)	Span (mm)	Strength (MPa)	Strain @ break (mm/mm)	Flexural Modulus (MPa)
28-C-LC	1	11.97	1.26	41.28	2.82E+02	3.07E-02	1.16E+04
	2	11.95	1.29		3.56E+02	3.29E-02	1.45E+04
	3	11.95	1.27		3.66E+02	3.30E-02	1.51E+04
	4	11.94	1.25		3.49E+02	3.35E-02	1.36E+04
	5	11.97	1.31		2.81E+02	3.45E-02	1.09E+04
Average					3.27E+02	3.29E-02	1.31E+04
Standard Deviation					4.19E+01	1.39E-03	1.84E+03

Sample	Specimen No.	Width (mm)	Thickness (mm)	Span (mm)	Strength (MPa)	Strain @ break (mm/mm)	Flexural Modulus (MPa)
29-C-LC	1	11.94	1.27	40.96	3.23E+02	3.34E-02	1.15E+04
	2	11.95	1.28		4.04E+02	3.45E-02	1.25E+04
	3	11.95	1.27		3.50E+02	3.42E-02	1.38E+04
	4	11.94	1.28		3.28E+02	3.48E-02	1.18E+04
	5	11.97	1.29		3.12E+02	3.05E-02	1.26E+04
Average					3.43E+02	3.35E-02	1.24E+04
Standard Deviation					3.68E+01	1.73E-03	9.03E+02

Sample	Specimen No.	Width (mm)	Thickness (mm)	Span (mm)	Strength (MPa)	Strain @ break (mm/mm)	Flexural Modulus (MPa)
31-C-LC	1	11.96	1.26	40.96	3.50E+02	3.36E-02	1.32E+04
	2	11.97	1.27		2.94E+02	3.01E-02	1.22E+04
	3	11.94	1.25		4.28E+02	3.01E-02	1.79E+04
	4	11.94	1.27		4.16E+02	3.45E-02	1.12E+04
	5	11.97	1.31		3.21E+02	3.09E-02	1.30E+04
Average					3.62E+02	3.19E-02	1.35E+04
Standard Deviation					5.89E+01	2.07E-03	2.57E+03

Sample	Specimen No.	Width (mm)	Thickness (mm)	Span (mm)	Strength (MPa)	Strain @ break (mm/mm)	Flexural Modulus (MPa)
32-C-LC	1	11.96	1.2	39.04	4.03E+02	3.39E-02	1.27E+04
	2	11.95	1.21		1.85E+03	3.62E-02	1.23E+04
	3	11.93	1.21		4.59E+02	3.52E-02	1.28E+04
	4	11.93	1.19		1.80E+03	3.56E-02	1.29E+04
	5	11.94	1.23		3.52E+02	3.44E-02	1.31E+04
Average					9.74E+02	3.50E-02	1.28E+04
Standard Deviation					7.80E+02	9.37E-04	3.19E+02

Sample	Specimen No.	Width (mm)	Thickness (mm)	Span (mm)	Strength (MPa)	Strain @ break (mm/mm)	Flexural Modulus (MPa)
34-C-LC	1	11.96	1.2	38.72	3.70E+02	3.11E-02	1.58E+04
	2	11.95	1.21		3.59E+02	3.25E-02	1.48E+04
	3	11.94	1.2		1.70E+03	3.64E-02	1.34E+04
	4	11.94	1.19		3.81E+02	3.20E-02	1.57E+04
	5	11.96	1.24		2.90E+02	3.16E-02	1.20E+04
Average					6.21E+02	3.27E-02	1.43E+04
Standard Deviation					6.06E+02	2.10E-03	1.63E+03

Sample	Specimen No.	Width (mm)	Thickness (mm)	Span (mm)	Strength (MPa)	Strain @ break (mm/mm)	Flexural Modulus (MPa)
38-C-LC	1	11.96	1.28	41.6	2.80E+02	2.65E-02	1.18E+04
	2	11.98	1.31		2.58E+02	2.69E-02	1.03E+04
	3	11.95	1.29		2.96E+02	3.03E-02	1.19E+04
	4	11.94	1.28		3.18E+02	3.35E-02	1.25E+04
	5	11.96	1.32		2.59E+02	2.92E-02	9.81E+03
Average					2.82E+02	2.93E-02	1.12E+04
Standard Deviation					2.54E+01	2.85E-03	1.14E+03

Sample	Specimen No.	Width (mm)	Thickness (mm)	Span (mm)	Strength (MPa)	Strain @ break (mm/mm)	Flexural Modulus (MPa)
40-C-LC	1	11.98	1.31	42.24	2.65E+02	3.10E-02	1.09E+04
	2	11.97	1.31		2.86E+02	2.73E-02	1.22E+04
	3	11.95	1.32		3.12E+02	2.83E-02	1.33E+04
	4	11.93	1.29		3.81E+02	2.99E-02	1.70E+04
	5	11.97	1.35		2.87E+02	2.72E-02	1.23E+04
Average					3.06E+02	2.87E-02	1.31E+04
Standard Deviation					4.51E+01	1.65E-03	2.30E+03

Sample	Specimen No.	Width (mm)	Thickness (mm)	Span (mm)	Strength (MPa)	Strain @ break (mm/mm)	Flexural Modulus (MPa)
41-C-LC	1	11.97	1.35	42.88	2.59E+02	3.08E-02	1.07E+04
	2	11.98	1.38		3.03E+02	3.09E-02	1.23E+04
	3	11.96	1.32		2.56E+02	2.79E-02	1.06E+04
	4	11.97	1.32		2.93E+02	3.18E-02	1.18E+04
	5	11.97	1.35		2.89E+02	2.80E-02	1.23E+04
Average					2.80E+02	2.99E-02	1.15E+04
Standard Deviation					2.12E+01	1.78E-03	8.48E+02

Sample	Specimen No.	Width (mm)	Thickness (mm)	Span (mm)	Strength (MPa)	Strain @ break (mm/mm)	Flexural Modulus (MPa)
43-C-LC	1	11.97	1.37	44.16	2.99E+02	3.20E-02	1.17E+04
	2	11.97	1.37		2.96E+02	3.12E-02	1.20E+04
	3	11.96	1.36		2.86E+02	3.17E-02	1.16E+04
	4	11.96	1.35		2.78E+02	3.09E-02	1.12E+04
	5	11.98	1.4		3.24E+02	3.24E-02	1.30E+04
Average					2.97E+02	3.16E-02	1.19E+04
Standard Deviation					1.75E+01	6.05E-04	6.96E+02

Sample	Specimen No.	Width (mm)	Thickness (mm)	Span (mm)	Strength (MPa)	Strain @ break (mm/mm)	Flexural Modulus (MPa)
44-C-LC	1	11.98	1.34	43.84	3.57E+02	3.18E-02	1.49E+04
	2	11.98	1.36		2.47E+02	3.22E-02	1.01E+04
	3	11.95	1.34		2.46E+02	3.01E-02	1.01E+04
	4	11.94	1.35		3.13E+02	3.06E-02	1.30E+04
	5	11.96	1.4		2.63E+02	3.24E-02	1.06E+04
Average					2.85E+02	3.14E-02	1.18E+04
Standard Deviation					4.84E+01	1.03E-03	2.14E+03

Sample	Specimen No.	Width (mm)	Thickness (mm)	Span (mm)	Strength (MPa)	Strain @ break (mm/mm)	Flexural Modulus (MPa)
45-C-LC	1	11.99	1.34	43.2	3.32E+02	2.98E-02	1.34E+04
	2	11.95	1.35		3.22E+02	2.62E-02	1.36E+04
	3	11.96	1.33		2.58E+02	3.01E-02	1.02E+04
	4	11.97	1.33		2.40E+02	2.73E-02	9.74E+03
	5	11.98	1.38		2.66E+02	2.96E-02	1.07E+04
					2.84E+02	2.86E-02	1.15E+04
Standard Deviation					4.10E+01	1.74E-03	1.82E+03

Sample	Specimen No.	Width (mm)	Thickness (mm)	Span (mm)	Strength (MPa)	Strain @ break (mm/mm)	Flexural Modulus (MPa)
46-C-LC	1	11.98	1.34	43.2	2.65E+02	3.23E-02	1.07E+04
	2	11.94	1.35		2.99E+02	3.04E-02	1.20E+04
	3	11.95	1.32		3.39E+02	2.94E-02	1.43E+04
	4	11.96	1.34		3.00E+02	3.00E-02	1.22E+04
	5	11.97	1.38		3.13E+02	3.14E-02	1.31E+04
Average					3.03E+02	3.07E-02	1.25E+04
Standard Deviation					2.68E+01	1.17E-03	1.35E+03

Sample	Specimen No.	Width (mm)	Thickness (mm)	Span (mm)	Strength (MPa)	Strain @ break (mm/mm)	Flexural Modulus (MPa)
54-C-LC	1	11.97	1.38	44.8	3.10E+02	3.05E-02	1.26E+04
	2	11.95	1.43		2.36E+02	3.11E-02	9.35E+03
	3	11.96	1.43		2.29E+02	3.22E-02	9.09E+03
	4	11.96	1.37		2.81E+02	2.99E-02	1.13E+04
	5	11.98	1.4		2.55E+02	3.01E-02	1.02E+04
Average					2.62E+02	3.08E-02	1.05E+04
Standard Deviation					3.35E+01	9.49E-04	1.47E+03

Sample	Specimen No.	Width (mm)	Thickness (mm)	Span (mm)	Strength (MPa)	Strain @ break (mm/mm)	Flexural Modulus (MPa)
56-C-LC	1	11.95	1.15	37.12	2.25E+04	3.81E-02	1.38E+04
	2	11.96	1.14		3.98E+02	3.48E-02	1.43E+04
	3	11.94	1.14		2.47E+04	3.77E-02	1.35E+04
	4	11.92	1.16		1.45E+04	3.84E-02	1.47E+04
	5	11.97	1.19		4.24E+02	3.58E-02	1.55E+04
Average					1.25E+04	3.70E-02	1.43E+04
Standard Deviation					1.17E+04	1.55E-03	7.74E+02

Appendix 8: Flexural properties of produced plaques-sampling area D

Sample	Specimen No.	Width (mm)	Thickness (mm)	Span (mm)	Strength (MPa)	Strain @ break (mm/mm)	Flexural Modulus (MPa)
2-D-LE	1	11.95	1.17	38.08	2.67E+02	3.02E-02	1.12E+04
	2	11.97	1.17		3.07E+02	3.00E-02	1.26E+04
	3	11.94	1.18		3.18E+02	3.10E-02	1.29E+04
	4	11.94	1.19		2.98E+02	3.05E-02	1.22E+04
	5	11.96	1.19		3.16E+02	3.03E-02	1.33E+04
Average					3.01E+02	3.04E-02	1.25E+04
Standard Deviation					2.06E+01	3.99E-04	7.82E+02

Sample	Specimen No.	Width (mm)	Thickness (mm)	Span (mm)	Strength (MPa)	Strain @ break (mm/mm)	Flexural Modulus (MPa)
3-D-LE	1	11.97	1.15	37.12	4.61E+02	2.01E-02	2.70E+04
	2	11.95	1.15		3.05E+02	2.85E-02	1.27E+04
	3	11.95	1.15		3.91E+02	3.32E-02	1.24E+04
	4	11.95	1.17		4.45E+02	3.48E-02	1.40E+04
	5	11.98	1.17		4.18E+02	3.15E-02	1.75E+04
Average					4.04E+02	2.96E-02	1.67E+04
Standard Deviation					6.16E+01	5.79E-03	6.09E+03

Sample	Specimen No.	Width (mm)	Thickness (mm)	Span (mm)	Strength (MPa)	Strain @ break (mm/mm)	Flexural Modulus (MPa)
4-D-LE	1	11.95	1.15	37.12	3.30E+02	2.60E-02	1.41E+04
	2	11.94	1.14		3.53E+02	3.25E-02	1.50E+04
	3	11.92	1.16		4.66E+02	3.10E-02	1.91E+04
	4	11.93	1.16		3.50E+02	2.55E-02	1.57E+04
	5	11.97	1.18		2.72E+02	2.63E-02	1.21E+04
Average					3.54E+02	2.83E-02	1.52E+04
Standard Deviation					7.06E+01	3.25E-03	2.56E+03

Sample	Specimen No.	Width (mm)	Thickness (mm)	Span (mm)	Strength (MPa)	Strain @ break (mm/mm)	Flexural Modulus (MPa)
5-D-LE	1	11.97	1.13	36.8	3.62E+02	2.92E-02	1.48E+04
	2	11.94	1.14		3.52E+02	2.87E-02	1.36E+04
	3	11.91	1.14		3.29E+02	2.65E-02	1.38E+04
	4	11.92	1.14		4.35E+02	3.03E-02	1.81E+04
	5	11.95	1.16		4.69E+02	3.43E-02	1.19E+04
Average					3.89E+02	2.98E-02	1.44E+04
Standard Deviation					5.97E+01	2.87E-03	2.31E+03

Sample	Specimen No.	Width (mm)	Thickness (mm)	Span (mm)	Strength (MPa)	Strain @ break (mm/mm)	Flexural Modulus (MPa)
6-D-LE	1	11.96	1.08	35.2	3.59E+02	2.63E-02	1.55E+04
	2	11.97	1.08		2.98E+02	2.27E-02	1.29E+04
	3	11.93	1.1		4.11E+02	2.63E-02	1.83E+04
	4	11.94	1.1		3.27E+02	2.42E-02	1.46E+04
	5	11.95	1.11		3.68E+03	3.60E-02	7.70E+03
Average					7.02E+03	2.71E-02	1.38E+04
Standard Deviation					1.49E+04	5.20E-03	3.94E+03

Sample	Specimen No.	Width (mm)	Thickness (mm)	Span (mm)	Strength (MPa)	Strain @ break (mm/mm)	Flexural Modulus (MPa)
7-D-LE	1	11.95	1.1	35.52	4.28E+02	2.72E-02	1.88E+04
	2	11.9	1.1		3.66E+02	3.05E-02	1.51E+04
	3	11.9	1.12		3.09E+02	2.88E-02	1.22E+04
	4	11.93	1.12		3.25E+02	3.35E-02	1.28E+04
	5	11.94	1.11		3.16E+02	2.62E-02	1.29E+04
Average					3.49E+02	2.92E-02	1.44E+04
Standard Deviation					4.95E+01	2.90E-03	2.73E+03

Sample	Specimen No.	Width (mm)	Thickness (mm)	Span (mm)	Strength (MPa)	Strain @ break (mm/mm)	Flexural Modulus (MPa)
8-D-LE	1	11.93	1.17	37.76	3.29E+02	2.79E-02	1.36E+04
	2	11.95	1.18		2.74E+02	2.81E-02	1.20E+04
	3	11.94	1.18		1.34E+04	3.77E-02	1.13E+04
	4	11.94	1.18		2.64E+02	3.03E-02	1.11E+04
	5	11.95	1.18		2.95E+02	3.35E-02	1.25E+04
Average					2.92E+03	3.15E-02	1.21E+04
Standard Deviation					5.87E+03	4.14E-03	1.02E+03

Sample	Specimen No.	Width (mm)	Thickness (mm)	Span (mm)	Strength (MPa)	Strain @ break (mm/mm)	Flexural Modulus (MPa)
9-D-LE	1	11.97	1.28	41.28	2.24E+02	2.76E-02	9.45E+03
	2	11.97	1.29		3.64E+02	3.23E-02	1.50E+04
	3	11.95	1.28		2.60E+02	2.85E-02	1.12E+04
	4	11.95	1.28		2.33E+02	3.11E-02	9.50E+03
	5	11.96	1.29		2.40E+02	2.72E-02	1.00E+04
Average					2.64E+02	2.94E-02	1.10E+04
Standard Deviation					5.72E+01	2.25E-03	2.33E+03

Sample	Specimen No.	Width (mm)	Thickness (mm)	Span (mm)	Strength (MPa)	Strain @ break (mm/mm)	Flexural Modulus (MPa)
10-D-LE	1	11.96	1.24	40.32	3.26E+02	2.95E-02	1.38E+04
	2	11.96	1.24		4.14E+02	3.47E-02	1.60E+04
	3	11.93	1.26		3.37E+02	3.46E-02	1.34E+04
	4	11.95	1.26		3.61E+02	3.49E-02	1.09E+04
	5	11.97	1.27		3.25E+02	3.10E-02	1.34E+04
Average					3.53E+02	3.29E-02	1.35E+04
Standard Deviation					3.71E+01	2.53E-03	1.82E+03

Sample	Specimen No.	Width (mm)	Thickness (mm)	Span (mm)	Strength (MPa)	Strain @ break (mm/mm)	Flexural Modulus (MPa)
16-D-LE	1	11.95	1.15	37.12	4.42E+02	2.76E-02	1.87E+04
	2	11.94	1.15		3.82E+02	3.11E-02	1.56E+04
	3	11.93	1.14		1.56E+03	3.75E-02	1.23E+04
	4	11.93	1.15		7.17E+02	3.79E-02	1.17E+04
	5	11.96	1.17		3.90E+02	3.32E-02	1.58E+04
Average					8.70E+03	3.35E-02	1.48E+04
Standard Deviation					1.14E+04	4.34E-03	2.88E+03

Sample	Specimen No.	Width (mm)	Thickness (mm)	Span (mm)	Strength (MPa)	Strain @ break (mm/mm)	Flexural Modulus (MPa)
25-D-LE	1	11.95	1.19	38.4	8.97E+02	3.68E-02	1.30E+04
	2	11.95	1.2		3.33E+02	2.45E-02	1.47E+04
	3	11.93	1.19		3.28E+02	3.40E-02	1.15E+04
	4	11.93	1.18		2.94E+02	2.90E-02	1.17E+04
	5	11.97	1.21		2.54E+02	2.69E-02	1.01E+04
Average					4.21E+02	3.03E-02	1.22E+04
Standard Deviation					2.68E+02	5.06E-03	1.76E+03

Sample	Specimen No.	Width (mm)	Thickness (mm)	Span (mm)	Strength (MPa)	Strain @ break (mm/mm)	Flexural Modulus (MPa)
26-D-LE	1	11.95	1.18	38.08	2.94E+02	2.40E-02	1.28E+04
	2	11.96	1.19		2.73E+02	2.59E-02	1.11E+04
	3	11.92	1.19		4.34E+02	2.60E-02	1.80E+04
	4	11.95	1.18		3.09E+02	2.63E-02	1.29E+04
	5	11.95	1.19		2.98E+02	2.75E-02	1.24E+04
Average					3.22E+02	2.59E-02	1.34E+04
Standard Deviation					6.39E+01	1.24E-03	2.67E+03

Sample	Specimen No.	Width (mm)	Thickness (mm)	Span (mm)	Strength (MPa)	Strain @ break (mm/mm)	Flexural Modulus (MPa)
27-D-LE	1	11.95	1.2	38.72	3.84E+02	2.86E-02	1.65E+04
	2	11.95	1.2		3.39E+02	3.31E-02	1.34E+04
	3	11.94	1.2		3.02E+02	2.96E-02	1.26E+04
	4	11.94	1.2		2.47E+02	2.62E-02	1.07E+04
	5	11.97	1.22		2.82E+02	2.56E-02	1.23E+04
Average					3.11E+02	2.86E-02	1.31E+04
Standard Deviation					5.30E+01	3.01E-03	2.15E+03

Sample	Specimen No.	Width (mm)	Thickness (mm)	Span (mm)	Strength (MPa)	Strain @ break (mm/mm)	Flexural Modulus (MPa)
28-D-LE	1	11.96	1.2	38.72	3.47E+02	2.77E-02	1.43E+04
	2	11.95	1.2		3.22E+02	2.75E-02	1.34E+04
	3	11.94	1.21		3.37E+02	3.25E-02	1.30E+04
	4	11.94	1.2		3.07E+02	2.77E-02	1.24E+04
	5	11.93	1.22		3.12E+02	2.49E-02	1.37E+04
Average					3.25E+02	2.81E-02	1.34E+04
Standard Deviation					1.68E+01	2.73E-03	7.08E+02

Sample	Specimen No.	Width (mm)	Thickness (mm)	Span (mm)	Strength (MPa)	Strain @ break (mm/mm)	Flexural Modulus (MPa)
29-D-LE	1	11.98	1.2	39.04	2.66E+02	2.59E-02	1.07E+04
	2	11.95	1.21		2.97E+02	2.90E-02	1.21E+04
	3	11.93	1.21		2.86E+02	2.93E-02	1.13E+04
	4	11.94	1.21		2.83E+02	2.86E-02	1.12E+04
	5	11.9	1.22		4.16E+02	2.51E-02	1.87E+04
Average					3.10E+02	2.76E-02	1.28E+04
Standard Deviation					6.05E+01	1.95E-03	3.32E+03

Sample	Specimen No.	Width (mm)	Thickness (mm)	Span (mm)	Strength (MPa)	Strain @ break (mm/mm)	Flexural Modulus (MPa)
31-D-LE	1	11.95	1.19	39.04	3.96E+02	2.77E-02	1.66E+04
	2	11.92	1.22		3.90E+02	3.21E-02	1.56E+04
	3	11.92	1.2		3.49E+02	2.57E-02	1.44E+04
	4	11.91	1.22		2.95E+02	3.18E-02	1.14E+04
	5	11.95	1.23		3.63E+02	3.21E-02	1.46E+04
Average					3.58E+02	2.99E-02	1.45E+04
Standard Deviation					4.06E+01	3.01E-03	1.93E+03

Sample	Specimen No.	Width (mm)	Thickness (mm)	Span (mm)	Strength (MPa)	Strain @ break (mm/mm)	Flexural Modulus (MPa)
32-D-LE	1	11.96	1.19	38.4	3.14E+02	2.79E-02	1.43E+04
	2	11.97	1.19		1.27E+03	3.67E-02	1.06E+04
	3	11.96	1.2		3.34E+02	3.57E-02	1.06E+04
	4	11.94	1.19		7.23E+02	3.67E-02	1.25E+04
	5	11.95	1.2		3.26E+02	2.73E-02	1.35E+04
Average					5.93E+02	3.29E-02	1.23E+04
Standard Deviation					4.14E+02	4.82E-03	1.68E+03

Sample	Specimen No.	Width (mm)	Thickness (mm)	Span (mm)	Strength (MPa)	Strain @ break (mm/mm)	Flexural Modulus (MPa)
34-D-LE	1	11.95	1.18	38.08	2.56E+02	2.96E-02	1.08E+04
	2	11.95	1.18		3.69E+02	3.43E-02	1.24E+04
	3	11.92	1.19		4.20E+03	3.74E-02	1.28E+04
	4	11.92	1.19		3.78E+02	2.58E-02	1.72E+04
	5	11.96	1.2		3.34E+02	2.71E-02	1.41E+04
Average					3.11E+03	3.08E-02	1.35E+04
Standard Deviation					6.20E+03	4.91E-03	2.40E+03

Sample	Specimen No.	Width (mm)	Thickness (mm)	Span (mm)	Strength (MPa)	Strain @ break (mm/mm)	Flexural Modulus (MPa)
38-D-LE	1	11.96	1.23	40	3.15E+02	2.89E-02	1.38E+04
	2	11.97	1.25		2.39E+02	2.87E-02	1.05E+04
	3	11.95	1.24		3.92E+02	3.16E-02	1.64E+04
	4	11.95	1.24		3.29E+02	3.34E-02	1.36E+04
	5	11.97	1.25		3.62E+02	3.23E-02	1.51E+04
Average					3.28E+02	3.10E-02	1.39E+04
Standard Deviation					5.76E+01	2.09E-03	2.19E+03

Sample	Specimen No.	Width (mm)	Thickness (mm)	Span (mm)	Strength (MPa)	Strain @ break (mm/mm)	Flexural Modulus (MPa)
40-D-LE	1	11.96	1.25	40.32	2.40E+02	2.74E-02	1.09E+04
	2	11.97	1.26		2.37E+02	2.85E-02	1.04E+04
	3	11.94	1.26		2.13E+02	2.12E-02	9.99E+03
	4	11.94	1.28		2.37E+02	2.55E-02	9.95E+03
	5	11.96	1.26		2.98E+02	2.80E-02	1.23E+04
Average					2.45E+02	2.61E-02	1.07E+04
Standard Deviation					3.16E+01	2.97E-03	9.73E+02

Sample	Specimen No.	Width (mm)	Thickness (mm)	Span (mm)	Strength (MPa)	Strain @ break (mm/mm)	Flexural Modulus (MPa)
41-D-LE	1	11.96	1.24	40.32	3.41E+02	2.70E-02	1.45E+04
	2	11.97	1.24		3.18E+02	3.28E-02	1.26E+04
	3	11.96	1.25		3.21E+02	3.11E-02	1.30E+04
	4	11.96	1.27		2.91E+02	2.96E-02	1.18E+04
	5	11.95	1.27		2.57E+02	2.61E-02	1.08E+04
Average					3.06E+02	2.93E-02	1.25E+04
Standard Deviation					3.25E+01	2.77E-03	1.36E+03

Sample	Specimen No.	Width (mm)	Thickness (mm)	Span (mm)	Strength (MPa)	Strain @ break (mm/mm)	Flexural Modulus (MPa)
43-D-LE	1	11.98	1.3	41.92	2.43E+02	2.72E-02	1.03E+04
	2	11.92	1.31		2.40E+02	3.40E-02	9.50E+03
	3	11.94	1.29		2.58E+02	3.22E-02	1.07E+04
	4	11.96	1.3		3.31E+02	3.37E-02	1.37E+04
	5	11.97	1.31		2.32E+02	2.38E-02	1.04E+04
Average					2.61E+02	3.02E-02	1.09E+04
Standard Deviation					4.04E+01	4.49E-03	1.60E+03

Sample	Specimen No.	Width (mm)	Thickness (mm)	Span (mm)	Strength (MPa)	Strain @ break (mm/mm)	Flexural Modulus (MPa)
44-D-LE	1	11.96	1.27	41.28	2.99E+02	2.63E-02	1.36E+04
	2	11.96	1.29		2.88E+02	3.27E-02	1.20E+04
	3	11.95	1.29		3.07E+02	3.14E-02	1.33E+04
	4	11.95	1.28		3.08E+02	3.40E-02	1.30E+04
	5	11.95	1.3		2.06E+02	3.10E-02	8.24E+03
Average					2.81E+02	3.11E-02	1.20E+04
Standard Deviation					4.30E+01	2.94E-03	2.20E+03

Sample	Specimen No.	Width (mm)	Thickness (mm)	Span (mm)	Strength (MPa)	Strain @ break (mm/mm)	Flexural Modulus (MPa)
45-D-LE	1	11.98	1.29	41.92	2.48E+02	2.83E-02	9.91E+03
	2	11.97	1.31		2.49E+02	2.60E-02	9.36E+03
	3	11.96	1.3		3.15E+02	3.37E-02	1.21E+04
	4	11.95	1.31		3.30E+02	3.38E-02	1.37E+04
	5	11.96	1.32		2.86E+02	2.98E-02	1.20E+04
Average					2.85E+02	3.03E-02	1.14E+04
Standard Deviation					3.76E+01	3.39E-03	1.78E+03

Sample	Specimen No.	Width (mm)	Thickness (mm)	Span (mm)	Strength (MPa)	Strain @ break (mm/mm)	Flexural Modulus (MPa)
46-D-LE	1	11.96	1.28	41.28	3.26E+02	2.70E-02	1.38E+04
	2	11.94	1.29		3.27E+02	3.45E-02	1.04E+04
	3	11.94	1.29		3.23E+02	3.43E-02	1.30E+04
	4	11.93	1.29		2.64E+02	3.34E-02	1.07E+04
	5	11.95	1.3		2.80E+02	2.71E-02	1.19E+04
Average					3.04E+02	3.13E-02	1.19E+04
Standard Deviation					2.96E+01	3.87E-03	1.48E+03

Sample	Specimen No.	Width (mm)	Thickness (mm)	Span (mm)	Strength (MPa)	Strain @ break (mm/mm)	Flexural Modulus (MPa)
49-D-LE	1	11.95	1.28	41.28	2.54E+02	2.75E-02	1.15E+04
	2	11.97	1.28		2.62E+02	2.52E-02	1.22E+04
	3	11.97	1.28		2.48E+02	2.47E-02	1.15E+04
	4	11.97	1.3		2.57E+02	2.83E-02	1.14E+04
	5	11.93	1.31		2.90E+02	3.44E-02	1.22E+04
Average					2.62E+02	2.80E-02	1.18E+04
Standard Deviation					1.63E+01	3.88E-03	3.77E+02

Sample	Specimen No.	Width (mm)	Thickness (mm)	Span (mm)	Strength (MPa)	Strain @ break (mm/mm)	Flexural Modulus (MPa)
54-D-LE	1	11.97	1.33	43.2	2.47E+02	1.79E-02	1.28E+04
	2	11.97	1.34		2.70E+02	2.43E-02	1.19E+04
	3	11.94	1.35		2.95E+02	2.30E-02	1.37E+04
	4	11.94	1.35		2.80E+02	2.06E-02	1.33E+04
	5	11.96	1.35		2.20E+02	2.84E-02	8.29E+03
Average					2.62E+02	2.28E-02	1.20E+04
Standard Deviation					2.92E+01	3.98E-03	2.20E+03

Sample	Specimen No.	Width (mm)	Thickness (mm)	Span (mm)	Strength (MPa)	Strain @ break (mm/mm)	Flexural Modulus (MPa)
56-D-LE	1	11.94	1.13	36.48	4.47E+02	3.40E-02	1.33E+04
	2	11.95	1.14		3.20E+02	2.61E-02	1.35E+04
	3	11.94	1.14		2.91E+02	2.61E-02	1.11E+04
	4	11.93	1.13		4.52E+02	3.29E-02	1.13E+04
	5	11.93	1.15		3.38E+02	3.10E-02	1.43E+04
Average					3.70E+02	3.00E-02	1.27E+04
Standard Deviation					7.47E+01	3.75E-03	1.45E+03

Appendix 9: Flexural properties of produced plaques-sampling area E

Sample	Specimen No.	Width (mm)	Thickness (mm)	Span (mm)	Strength (MPa)	Strain @ break (mm/mm)	Flexural Modulus (MPa)
2-E-R	1	12.36	1.24	40.32	2.64E+02	2.69E-02	1.00E+04
	2	12.35	1.24		2.91E+02	2.97E-02	1.07E+04
	3	12.35	1.26		2.96E+02	3.01E-02	1.10E+04
	4	12.31	1.26		3.05E+02	3.02E-02	1.13E+04
	5	12.39	1.27		3.06E+02	2.97E-02	1.11E+04
Average					2.92E+02	2.93E-02	1.08E+04
Standard Deviation					1.74E+01	1.35E-03	5.07E+02

Sample	Specimen No.	Width (mm)	Thickness (mm)	Span (mm)	Strength (MPa)	Strain @ break (mm/mm)	Flexural Modulus (MPa)
3-E-R	1	12.4	1.2	40	3.38E+02	3.17E-02	1.26E+04
	2	12.41	1.2		2.92E+02	2.82E-02	1.18E+04
	3	12.32	1.24		2.84E+02	3.23E-02	1.01E+04
	4	12.34	1.25		3.17E+02	3.02E-02	1.20E+04
	5	12.36	1.27		6.08E+02	3.54E-02	9.21E+03
Average					3.68E+02	3.16E-02	1.12E+04
Standard Deviation					1.36E+02	2.65E-03	1.43E+03

Sample	Specimen No.	Width (mm)	Thickness (mm)	Span (mm)	Strength (MPa)	Strain @ break (mm/mm)	Flexural Modulus (MPa)
4-E-R	1	12.38	1.19	38.72	7.63E+02	3.46E-02	1.16E+04
	2	12.41	1.18		1.41E+04	3.59E-02	1.12E+04
	3	12.41	1.23		3.36E+02	3.19E-02	1.25E+04
	4	12.3	1.23		3.97E+02	3.54E-02	1.29E+04
	5	12.38	1.21		2.59E+02	3.06E-02	9.58E+03
Average					3.16E+03	3.37E-02	1.16E+04
Standard Deviation					6.09E+03	2.33E-03	1.30E+03

Sample	Specimen No.	Width (mm)	Thickness (mm)	Span (mm)	Strength (MPa)	Strain @ break (mm/mm)	Flexural Modulus (MPa)
5-E-R	1	12.37	1.17	38.08	8.83E+03	3.46E-02	1.07E+04
	2	12.38	1.17		1.22E+03	3.50E-02	1.28E+04
	3	12.33	1.2		3.12E+02	3.24E-02	1.16E+04
	4	12.29	1.19		4.78E+03	3.61E-02	1.13E+04
	5	12.34	1.18		2.98E+02	3.18E-02	1.19E+04
Average					3.09E+03	3.40E-02	1.17E+04
Standard Deviation					3.70E+03	1.84E-03	7.97E+02

Sample	Specimen No.	Width (mm)	Thickness (mm)	Span (mm)	Strength (MPa)	Strain @ break (mm/mm)	Flexural Modulus (MPa)
6-E-R	1	12.36	1.1	35.52	3.98E+02	3.17E-02	1.33E+04
	2	12.39	1.1		2.66E+02	2.91E-02	9.89E+03
	3	12.34	1.1		3.11E+02	2.78E-02	1.21E+04
	4	12.32	1.13		6.66E+03	3.62E-02	1.10E+04
	5	12.35	1.13		1.59E+04	3.64E-02	9.96E+03
Average					4.71E+03	3.22E-02	1.12E+04
Standard Deviation					6.84E+03	3.97E-03	1.44E+03

Sample	Specimen No.	Width (mm)	Thickness (mm)	Span (mm)	Strength (MPa)	Strain @ break (mm/mm)	Flexural Modulus (MPa)
7-E-R	1	12.38	1.13	36.8	4.74E+02	3.33E-02	1.22E+04
	2	12.42	1.16		3.76E+02	3.06E-02	1.39E+04
	3	12.36	1.15		5.55E+02	3.55E-02	1.46E+04
	4	12.3	1.13		9.17E+02	3.48E-02	1.26E+04
	5	12.37	1.15		3.94E+02	3.33E-02	1.34E+04
Average					5.43E+02	3.35E-02	1.33E+04
Standard Deviation					2.21E+02	1.89E-03	9.60E+02

Sample	Specimen No.	Width (mm)	Thickness (mm)	Span (mm)	Strength (MPa)	Strain @ break (mm/mm)	Flexural Modulus (MPa)
8-E-R	1	12.34	1.19	38.72	1.68E+03	3.49E-02	1.07E+04
	2	12.4	1.23		3.61E+02	3.46E-02	1.06E+04
	3	12.34	1.2		3.89E+02	2.91E-02	1.53E+04
	4	12.32	1.2		1.37E+04	3.57E-02	9.80E+03
	5	12.32	1.21		2.85E+02	3.26E-02	1.07E+04
Average					3.28E+03	3.34E-02	1.14E+04
Standard Deviation					5.84E+03	2.67E-03	2.21E+03

Sample	Specimen No.	Width (mm)	Thickness (mm)	Span (mm)	Strength (MPa)	Strain @ break (mm/mm)	Flexural Modulus (MPa)
9-E-R	1	12.35	1.46	45.44	2.37E+02	2.82E-02	9.40E+03
	2	12.39	1.43		1.58E+02	2.11E-02	7.70E+03
	3	12.34	1.42		2.53E+02	2.81E-02	1.05E+04
	4	12.33	1.42		2.44E+02	2.89E-02	9.63E+03
	5	12.3	1.41		2.31E+02	2.98E-02	9.82E+03
Average					2.24E+02	2.72E-02	9.41E+03
Standard Deviation					3.82E+01	3.47E-03	1.04E+03

Sample	Specimen No.	Width (mm)	Thickness (mm)	Span (mm)	Strength (MPa)	Strain @ break (mm/mm)	Flexural Modulus (MPa)
10-E-R	1	12.37	1.27	40.64	4.90E+02	3.51E-02	1.05E+04
	2	12.39	1.27		3.62E+02	3.46E-02	1.13E+04
	3	12.36	1.27		4.11E+02	3.51E-02	1.24E+04
	4	12.3	1.26		4.21E+02	3.48E-02	1.30E+04
	5	12.33	1.26		3.72E+02	3.48E-02	1.16E+04
Average					4.11E+02	3.49E-02	1.18E+04
Standard Deviation					5.06E+01	2.03E-04	9.79E+02

Sample	Specimen No.	Width (mm)	Thickness (mm)	Span (mm)	Strength (MPa)	Strain @ break (mm/mm)	Flexural Modulus (MPa)
16-E-R	1	12.35	1.18	38.08	3.55E+02	3.23E-02	1.27E+04
	2	12.37	1.19		3.56E+02	3.27E-02	1.17E+04
	3	12.31	1.19		3.25E+02	2.99E-02	1.32E+04
	4	12.28	1.19		3.60E+02	2.90E-02	1.41E+04
	5	12.34	1.19		3.49E+02	3.27E-02	1.26E+04
Average					3.49E+02	3.13E-02	1.28E+04
Standard Deviation					1.42E+01	1.75E-03	8.72E+02

Sample	Specimen No.	Width (mm)	Thickness (mm)	Span (mm)	Strength (MPa)	Strain @ break (mm/mm)	Flexural Modulus (MPa)
25-E-R	1	12.37	1.2	39.04	3.25E+02	2.55E-02	1.30E+04
	2	12.34	1.21		3.78E+02	2.65E-02	1.53E+04
	3	12.32	1.22		3.07E+02	3.01E-02	1.17E+04
	4	12.3	1.23		3.73E+02	3.26E-02	1.40E+04
	5	12.36	1.22		3.59E+02	3.12E-02	1.36E+04
Average					3.48E+02	2.92E-02	1.35E+04
Standard Deviation					3.09E+01	3.06E-03	1.32E+03

Sample	Specimen No.	Width (mm)	Thickness (mm)	Span (mm)	Strength (MPa)	Strain @ break (mm/mm)	Flexural Modulus (MPa)
26-E-R	1	12.34	1.23	39.36	3.24E+02	3.30E-02	9.85E+03
	2	12.33	1.22		3.16E+02	2.85E-02	1.26E+04
	3	12.27	1.22		1.33E+03	3.59E-02	1.14E+04
	4	12.31	1.23		3.76E+02	3.48E-02	1.26E+04
	5	12.31	1.24		7.34E+02	3.65E-02	1.11E+04
Average					6.15E+02	3.37E-02	1.15E+04
Standard Deviation					4.34E+02	3.20E-03	1.16E+03

Sample	Specimen No.	Width (mm)	Thickness (mm)	Span (mm)	Strength (MPa)	Strain @ break (mm/mm)	Flexural Modulus (MPa)
27-E-R	1	12.35	1.24	40	2.69E+02	3.04E-02	1.07E+04
	2	12.35	1.24		3.35E+02	2.87E-02	1.38E+04
	3	12.32	1.25		3.17E+02	3.43E-02	1.04E+04
	4	12.3	1.24		2.79E+02	2.81E-02	1.12E+04
	5	12.32	1.23		3.41E+02	3.36E-02	1.20E+04
Average					3.08E+02	3.10E-02	1.16E+04
Standard Deviation					3.28E+01	2.79E-03	1.36E+03

Sample	Specimen No.	Width (mm)	Thickness (mm)	Span (mm)	Strength (MPa)	Strain @ break (mm/mm)	Flexural Modulus (MPa)
28-E-R	1	12.35	1.22	39.68	5.97E+02	3.41E-02	1.02E+04
	2	12.3	1.24		4.03E+02	3.41E-02	1.34E+04
	3	12.32	1.24		3.09E+02	2.82E-02	1.19E+04
	4	12.28	1.24		3.55E+02	2.86E-02	1.36E+04
	5	12.34	1.24		2.84E+02	3.18E-02	1.02E+04
Average					3.90E+02	3.14E-02	1.19E+04
Standard Deviation					1.25E+02	2.87E-03	1.67E+03

Sample	Specimen No.	Width (mm)	Thickness (mm)	Span (mm)	Strength (MPa)	Strain @ break (mm/mm)	Flexural Modulus (MPa)
29-E-R	1	12.37	1.26	40	6.42E+03	3.59E-02	8.55E+03
	2	12.38	1.26		4.91E+02	3.59E-02	1.22E+04
	3	12.4	1.26		4.54E+02	3.59E-02	1.23E+04
	4	12.32	1.24		7.32E+02	3.53E-02	1.07E+04
	5	12.33	1.25		5.29E+02	3.56E-02	1.08E+04
Average					1.72E+03	3.57E-02	1.09E+04
Standard Deviation					2.63E+03	2.64E-04	1.52E+03

Sample	Specimen No.	Width (mm)	Thickness (mm)	Span (mm)	Strength (MPa)	Strain @ break (mm/mm)	Flexural Modulus (MPa)
31-E-R	1	12.35	1.23	39.68	3.10E+02	2.81E-02	1.19E+04
	2	12.4	1.24		3.09E+02	3.30E-02	1.08E+04
	3	12.33	1.24		3.30E+02	3.37E-02	1.15E+04
	4	12.31	1.24		1.10E+04	3.59E-02	8.95E+03
	5	12.29	1.25		5.96E+02	3.62E-02	1.11E+04
Average					2.50E+03	3.34E-02	1.08E+04
Standard Deviation					4.73E+03	3.26E-03	1.14E+03

Sample	Specimen No.	Width (mm)	Thickness (mm)	Span (mm)	Strength (MPa)	Strain @ break (mm/mm)	Flexural Modulus (MPa)
32-E-R	1	12.35	1.22	39.04	2.90E+02	2.56E-02	1.17E+04
	2	12.35	1.22		3.79E+02	3.38E-02	1.10E+04
	3	12.34	1.22		2.78E+02	2.93E-02	1.06E+04
	4	12.32	1.21		3.27E+02	3.34E-02	1.23E+04
	5	12.32	1.23		6.14E+02	3.68E-02	9.96E+03
Average					2.38E+03	3.18E-02	1.11E+04
Standard Deviation					4.60E+03	4.36E-03	8.97E+02

Sample	Specimen No.	Width (mm)	Thickness (mm)	Span (mm)	Strength (MPa)	Strain @ break (mm/mm)	Flexural Modulus (MPa)
34-E-R	1	12.36	1.26	39.68	3.51E+02	3.65E-02	1.13E+04
	2	12.37	1.26		3.84E+02	3.53E-02	1.20E+04
	3	12.36	1.24		2.89E+02	3.04E-02	1.10E+04
	4	12.32	1.23		3.51E+02	3.40E-02	1.14E+04
	5	12.34	1.22		1.35E+03	3.53E-02	1.04E+04
Average					5.45E+02	3.43E-02	1.12E+04
Standard Deviation					4.51E+02	2.38E-03	6.05E+02

Sample	Specimen No.	Width (mm)	Thickness (mm)	Span (mm)	Strength (MPa)	Strain @ break (mm/mm)	Flexural Modulus (MPa)
38-E-R	1	12.41	1.3	41.28	1.43E+02	2.15E-02	6.78E+03
	2	12.34	1.27		2.55E+02	3.11E-02	7.06E+03
	3	12.35	1.3		3.05E+02	3.23E-02	1.14E+04
	4	12.33	1.3		3.69E+02	3.48E-02	9.57E+03
	5	12.3	1.29		3.45E+02	3.44E-02	9.35E+03
Average					2.83E+02	3.08E-02	8.82E+03
Standard Deviation					8.96E+01	5.43E-03	1.91E+03

Sample	Specimen No.	Width (mm)	Thickness (mm)	Span (mm)	Strength (MPa)	Strain @ break (mm/mm)	Flexural Modulus (MPa)
40-E-R	1	12.4	1.27	40.96	2.87E+02	3.17E-02	1.11E+04
	2	12.34	1.27		3.37E+02	3.37E-02	1.16E+04
	3	12.31	1.27		3.10E+02	3.09E-02	1.18E+04
	4	12.34	1.29		3.39E+02	3.44E-02	1.17E+04
	5	12.31	1.28		2.92E+02	2.98E-02	1.12E+04
Average					3.13E+02	3.21E-02	1.15E+04
Standard Deviation					2.43E+01	1.91E-03	3.01E+02

Sample	Specimen No.	Width (mm)	Thickness (mm)	Span (mm)	Strength (MPa)	Strain @ break (mm/mm)	Flexural Modulus (MPa)
41-E-R	1	12.29	1.31	42.24	1.89E+02	3.11E-02	5.49E+03
	2	12.32	1.31		1.66E+02	3.35E-02	6.64E+03
	3	12.33	1.33		1.93E+02	3.40E-02	5.87E+03
	4	12.3	1.31		2.16E+02	3.18E-02	7.48E+03
	5	12.34	1.32		2.43E+02	3.36E-02	1.02E+04
Average					2.01E+02	3.28E-02	7.13E+03
Standard Deviation					2.95E+01	1.27E-03	1.87E+03

Sample	Specimen No.	Width (mm)	Thickness (mm)	Span (mm)	Strength (MPa)	Strain @ break (mm/mm)	Flexural Modulus (MPa)
43-E-R	1	12.39	1.36	42.88	2.90E+02	3.06E-02	1.13E+04
	2	12.36	1.33		2.47E+02	2.91E-02	1.01E+04
	3	12.37	1.33		2.59E+02	3.26E-02	1.02E+04
	4	12.27	1.34		2.66E+02	3.28E-02	1.05E+04
	5	12.33	1.34		2.43E+02	3.13E-02	9.37E+03
Average					2.61E+02	3.13E-02	1.03E+04
Standard Deviation					1.87E+01	1.53E-03	6.99E+02

Sample	Specimen No.	Width (mm)	Thickness (mm)	Span (mm)	Strength (MPa)	Strain @ break (mm/mm)	Flexural Modulus (MPa)
44-E-R	1	12.36	1.35	43.52	3.03E+02	3.24E-02	1.19E+04
	2	12.4	1.36		1.94E+02	2.86E-02	7.78E+03
	3	12.36	1.46		1.87E+02	3.51E-02	6.94E+03
	4	12.26	1.31		2.73E+02	2.75E-02	1.12E+04
	5	12.35	1.34		2.74E+02	3.15E-02	1.06E+04
Average					2.46E+02	3.10E-02	9.68E+03
Standard Deviation					5.23E+01	3.04E-03	2.19E+03

Sample	Specimen No.	Width (mm)	Thickness (mm)	Span (mm)	Strength (MPa)	Strain @ break (mm/mm)	Flexural Modulus (MPa)
45-E-R	1	12.37	1.33	43.2	3.04E+02	3.24E-02	1.17E+04
	2	12.46	1.35		2.93E+02	3.15E-02	1.15E+04
	3	12.38	1.37		2.58E+02	2.93E-02	1.03E+04
	4	12.34	1.33		2.53E+02	3.23E-02	1.00E+04
	5	12.34	1.35		2.51E+02	2.85E-02	1.05E+04
Average					2.72E+02	3.08E-02	1.08E+04
Standard Deviation					2.48E+01	1.78E-03	7.46E+02

Sample	Specimen No.	Width (mm)	Thickness (mm)	Span (mm)	Strength (MPa)	Strain @ break (mm/mm)	Flexural Modulus (MPa)
46-E-R	1	12.36	1.36	43.52	2.41E+02	3.07E-02	9.55E+03
	2	12.35	1.35		2.30E+02	2.93E-02	8.49E+03
	3	12.35	1.34		2.32E+02	3.01E-02	8.98E+03
	4	12.34	1.36		2.04E+02	3.00E-02	7.71E+03
	5	12.35	1.37		2.33E+02	3.27E-02	9.00E+03
Average					2.28E+02	3.06E-02	8.75E+03
Standard Deviation					1.42E+01	1.31E-03	6.91E+02

Sample	Specimen No.	Width (mm)	Thickness (mm)	Span (mm)	Strength (MPa)	Strain @ break (mm/mm)	Flexural Modulus (MPa)
49-E-R	1	12.38	1.31	41.92	2.83E+02	2.88E-02	1.12E+04
	2	12.36	1.32		2.27E+02	2.79E-02	9.09E+03
	3	12.38	1.31		2.58E+02	3.05E-02	1.00E+04
	4	12.34	1.32		3.01E+02	3.41E-02	1.03E+04
	5	12.33	1.31		3.05E+02	3.13E-02	1.16E+04
Average					2.75E+02	3.05E-02	1.04E+04
Standard Deviation					3.26E+01	2.42E-03	9.90E+02

Sample	Specimen No.	Width (mm)	Thickness (mm)	Span (mm)	Strength (MPa)	Strain @ break (mm/mm)	Flexural Modulus (MPa)
54-E-R	1	12.38	1.35	43.52	2.67E+02	3.24E-02	1.07E+04
	2	12.41	1.36		3.54E+02	3.26E-02	1.35E+04
	3	12.35	1.38		2.44E+02	3.32E-02	9.45E+03
	4	12.34	1.33		2.35E+02	3.17E-02	9.33E+03
	5	12.35	1.37		2.37E+02	2.83E-02	9.56E+03
Average					2.68E+02	3.16E-02	1.05E+04
Standard Deviation					5.01E+01	1.94E-03	1.74E+03

Sample	Specimen No.	Width (mm)	Thickness (mm)	Span (mm)	Strength (MPa)	Strain @ break (mm/mm)	Flexural Modulus (MPa)
56-E-R	1	12.37	1.15	37.12	2.49E+02	2.39E-02	1.09E+04
	2	12.35	1.17		3.10E+02	2.38E-02	1.32E+04
	3	12.31	1.17		2.83E+02	2.36E-02	1.19E+04
	4	12.26	1.15		2.84E+02	2.65E-02	1.14E+04
	5	12.3	1.17		3.00E+02	3.16E-02	1.16E+04
Average					2.85E+02	2.59E-02	1.18E+04
Standard Deviation					2.34E+01	3.42E-03	8.89E+02

Appendix 7: The initial wetted area measurements (units cm²)

Plaque number	Total initial wetted areas	initial wetted UL (upper left)	initial wetted LL (lower left)	initial wetted LR (lower right)	initial wetted UR (upper right)	initial wetted in Left side	initial wetted in Right side
2	1260	260	439	441	108	699	549
3	1295	284	406	431	118	690	549
4	1202	250	383	434	119	633	553
5	1338	243	364	350	114	607	464
6	1328	255	370	360	120	625	480
7	1501	390	428	442	220	818	662
8	1428	342	471	423	175	813	598
9	1445	290	359	446	142	649	588
10	1457	305	336	412	189	641	601
16	1146	242	335	255	124	577	379
25	1358	330	364	405	160	694	565
26	1214	311	298	383	171	609	554
27	1359	359	331	341	228	690	569
28	1327	300	397	443	141	697	584
31	1183	297	277	314	231	574	545
32	985	263	240	213	92	503	305
34	1057	282	250	254	124	532	378
38	1458	261	358	472	174	619	646
40	1483	314	348	481	164	662	645
41	1142	243	281	338	152	524	490
43	1134	221	287	351	147	508	498
44	1137	237	288	348	143	525	491
45	1099	248	274	317	119	522	436
46	1236	372	244	393	181	616	574
49	1372	310	323	517	157	633	674
54	998	358	243	197	94	601	291
56	1065	248	314	250	97	562	347

Appendix 8: The targeted wetted area measurements (units cm²)

Plaque number	Total targeted wetted area	initial wetted UL (upper left)	initial wetted LL (lower left)	initial wetted LR (lower right)	initial wetted UR (upper right)	initial wetted in Left side	initial wetted in Right side
2	989	294.5	294.5	150.5	150.5	589	301
3	989	294.5	294.5	150.5	150.5	589	301
4	989	294.5	294.5	150.5	150.5	589	301
5	989	294.5	294.5	150.5	150.5	589	301
6	989	294.5	294.5	150.5	150.5	589	301
7	989	294.5	294.5	150.5	150.5	589	301
8	989	294.5	294.5	150.5	150.5	589	301
9	989	294.5	294.5	150.5	150.5	589	301
10	989	294.5	294.5	150.5	150.5	589	301
16	989	294.5	294.5	150.5	150.5	589	301
25	989	294.5	294.5	150.5	150.5	589	301
26	989	294.5	294.5	150.5	150.5	589	301
27	989	294.5	294.5	150.5	150.5	589	301
28	989	294.5	294.5	150.5	150.5	589	301
31	989	294.5	294.5	150.5	150.5	589	301
32	989	294.5	294.5	150.5	150.5	589	301
34	989	294.5	294.5	150.5	150.5	589	301
38	989	294.5	294.5	150.5	150.5	589	301
40	989	294.5	294.5	150.5	150.5	589	301
41	989	294.5	294.5	150.5	150.5	589	301
43	989	294.5	294.5	150.5	150.5	589	301
44	989	294.5	294.5	150.5	150.5	589	301
45	989	294.5	294.5	150.5	150.5	589	301
46	989	294.5	294.5	150.5	150.5	589	301
49	989	294.5	294.5	150.5	150.5	589	301
54	989	294.5	294.5	150.5	150.5	589	301
56	989	294.5	294.5	150.5	150.5	589	301

Curriculum Vitae

Name: Saboora Ayatollahi

Post-secondary Education and Degrees: Babol Noshirvani University of Technology, Babol, Iran
2016-2020 B.A.Sc Chemical Engineering.

The University of Western Ontario
London, Ontario, Canada
2021-2023 M.E.Sc Chemical Engineering

Related Work Experience Teaching Assistant
The University of Western Ontario
2021-2022